POLYTECHNIC UNIVERSITY OF MARCHE
PH.D. SCHOOL IN ENGINEERING SCIENCES
CURRICULUM IN CIVIL, ENVIRONMENTAL AND BUILDING ENGINEERING AND ARCHITECTURE

DISTINCT ELEMENT METHOD FOR ARCHITECTURAL HERITAGE: FROM THE PAST TO FUTURE ADVANCES

Ph.D. Dissertation of:

Mattia Schiavoni

Advisor:

Prof. Stefano Lenci

Co-Advisor:

Prof. Francesco Clementi

Curriculum Supervisor:

Prof. Francesco Fatone

XXXV Cycle – 2019/2022

UNIVERSITÀ POLITECNICA DELLE MARCHE
SCUOLA DI DOTTORATO DI RICERCA IN SCIENZA DELL'INGEGNERIA
CURRICULUM IN INGEGNERIA CIVILE, AMBIENTALE, EDILE E ARCHITETTURA

METODO DEGLI ELEMENTI DISTINTI PER IL PATRIMONIO ARCHITETTONICO: DAL PASSATO AI PROGRESSI FUTURI

Tesi di Dottorato di:

Mattia Schiavoni

Tutor:

Prof. Stefano Lenci

Co-Tutor:

Prof. Francesco Clementi

Coordinatore del corso:

Prof. Francesco Fatone

XXXV Ciclo – 2019/2022

Università Politecnica delle Marche
Dipartimento di Ingegneria Civile, Ambientale Edile e Architettura
Via Brecce Bianche – 60131 - Ancona

Ai miei cari

To my loved ones

ACKNOWLEDGMENTS

Another important stage of my life is about to end. I would like to thank all the people who have been accompanied, encouraged and allowed me to bring this enormous goal to an end.

First of all, my sincere thanks go to my advisor Professor Stefano Lenci.

I would like to thank my co-advisor Professor Francesco Clementi for giving me the opportunity to embark on this adventure, for always being present and for believing in me.

Special thanks also go to Professor Daniel V. Oliveira and Professor Nuno Mendes, who, during my time abroad at the Universidade do Minho, allowed me to address new issues and enrich my personal baggage.

I would like to thank Professor Daniel V. Oliveira and Professor Marius Mosoarca for their support in revising the final draft and for the advice provided to improve the quality of this Dissertation.

I also want to thank the Itasca group for providing me with access and support 3DEC© under IEP program.

To the wonderful guys met on this journey. Angela, Ersilia, Francesca B., Francesca C., Gianluca, Giorgio, Marina, Nico, Valentina and Vitali, thank you for all the happy moments spent together.

To my friends, thank you for the support, for the advice and for the carefree moments spent together.

To M. Pia, Chiara and Matteo, thank you for encouraging me.

To my family, who have always believed in me, helping me in the most difficult moments.

To Chiara, simply thank you for being there.

CONTENTS

LIST OF FIGURES

LIST OF TABLES

ABSTRACT

The aim of the following research work is to present developments on some aspects of discontinuous approaches not yet been fully investigated.

This work focuses on three aspects such as the possibility of comparing continuous approaches with discontinuous one, evaluating the influence of stereotomy to simulate the non-linear dynamic behaviour of masonry structures, giving indications regarding the possibility of carrying out a calibration through the Distinct Element Method (DEM).

The masonry in the continuous approach was first represented as a homogeneous medium and isotropic material where the mechanical properties depend on those of its components (mortar and bricks), in this case the analyses were based on the Concrete Damage Plasticity (CDP).

In the discontinuous approach, the masonry is discretized into blocks (bricks) that include the mortar in their thickness, implicit temporal integration schemes have been used as in the case of the Non-Smooth Contact Dynamic (NSCD) implemented in the LMGC90© code where the sliding movements are governed by the condition of impenetrability of Signorini and by the dry-friction Coulomb law, and explicit integration schemes in the Discrete Element Method implement in the 3DEC© code where sliding between blocks are governed by linear and non-linear law in normal and shear direction.

A set of case studies of real structures have been considered using different types of discretization, starting from the simplest to the most articulated one where the chaotic masonry is represented in a manner faithful to reality.

The numerical results have highlighted the methods of progressive damage under dynamic actions recorded during the seismic events that occurred in the Italian

territory in the last decades. The numerical approaches are able to simulate large displacements and the separation between the elements that constitute the masonry, thus obtaining predictions on the evaluation of the vulnerability of historical buildings. In addition, the results obtained with DEM calibration are a first indication, on which to undertake future studies to obtain more accurate results.

The results discussed are valuable for the preservation of cultural heritage by proposing guidelines for the conservation, strengthening and seismic retrofitting of historical masonry structures.

SOMMARIO

Lo scopo del seguente lavoro di ricerca è quello di presentare sviluppi su alcuni aspetti degli approcci discontinui non ancora approfonditi.

Questo lavoro pone l'attenzione su tre aspetti come la possibilità di confrontare approcci continui con approcci discontinui, valutare l'influenza della stereotomia per simulare il comportamento dinamico non lineare delle strutture in muratura, dare indicazioni riguardanti la possibilità di realizzare una calibrazione tramite il Distinct Element Method (DEM).

La muratura nell'approccio al continuo è stata prima rappresentata come un materiale omogeneo ed isotropico dove le proprietà meccaniche dipendono da quelle delle sue componenenti (malta e mattoni) in questo caso le analisi sono basata sul Concrete Damage Plasticity (CDP). Negli approcci al discontinuo invece, la muratura viene discretizzata in blocchi (mattoni) che comprendono nel loro spessore la malta, sono stati utilizzati schemi di integrazione temporale impliciti come nel caso del metodo Non-Smooth Contact Dynamic (NSCD) implementato nel codice LMGC90© dove i movimenti di scorrimento sono governati dalla condizione di impenetrabilità di Signorini e dalla legge di Coulomb di attrito secco, e schemi di integrazione espliciti nel Discrete Element Method implementato nel codice 3DEC© dove gli scorrimenti tra i blocchi sono governati da leggi lineari e non lineari in direzione normale e di taglio.

Sono stati considerati un insieme di casi studio a partire da strutture reali utilizzando diversi tipi di discretizzazione, partendo da quella più semplice arrivando a quella più articolata dove la muratura caotica viene rappresentata in maniera fedele alla realtà.

I risultati numerici hanno evidenziato le modalità di danneggiamento progressivo sotto azioni dinamiche registrate durante gli eventi sismici che hanno colpito il territorio italiano negli ultimi decenni. Gli approcci numerici sono in grado di simulare grandi spostamenti e la separazione tra gli elementi che vanno a costituire la muratura, ottenendo così previsioni sulla valutazione della vulnerabilità degli edifici di carattere storico. Inoltre, i risultati ottenuti con la calibrazione DEM sono una prima indicazione, sulla base della quale intraprendere studi futuri per ottenere risultati più accurati.

I risultati discussi sono preziosi al fine di preservare il patrimonio culturale proponendo linee guida per la conservazione, il rafforzamento, l'adeguamento sismico delle strutture storiche in muratura.

INTRODUCTION

The historical masonry structures characterize the Italian historical and artistic heritage; their conservation is therefore a fundamental aspect on which research pays close attention.

These structures showed high fragility when subjected to horizontal loads. The recent earthquakes that hit the territory of Central Italy between 2016 and 2017 have highlighted the vulnerability of masonry buildings.

For this reason, the research highlighted the need to assess the vulnerability of existing structures and find techniques to improve the structural behaviour of masonry buildings.

Research in the field of masonry structures, through experimental and mathematical work, returns information on structural behaviour by improving numerical simulations and existing methods. For this purpose, a large number of numerical models of large-scale masonry structures must be validated in order to progress.

This research work moves in this direction. With the use of discrete approaches, several case studies have been investigated in order to fill in some aspects not yet fully investigated. These approaches have been used because, by representing the masonry as a set of blocks capable of translating and rotating, it is possible to grasp both the in-plane and out-of-plane behaviours. This is, therefore, a remarkable capacity.

First, discrete approaches were compared with continuous one in order to assess possible discrepancies.

Subsequently, the focus was on discrete methods as they are able to better grasp the behaviour of the masonry. Two different stereotomies were studied in order to

understand if it is correct to approximate irregular shapes with regular shapes to obtain less burdensome computational burdens.

Finally, a topic was addressed that has been widely developed in the world of continuous, but that in the field of discrete has not yet been investigated, i.e. calibration.

These aspects have been investigated considering as case studies a series of existing historical structures that characterize the Italian historical and artistic heritage.

This research thesis consists of six chapters.

CHAPTER 1| introduces a literature review on historical masonry structures, the criteria for masonry structure vulnerability assessments, and their seismic behaviour.

CHAPTER 2| summarises and explains the different methods employed in this thesis work.

CHAPTER 3| deals the modeling and vulnerability assessment of a first case study, explain the differences between the discontinuous and continuous approaches to evaluate any discrepancies between the two methods.

CHAPTER 4| deals with the modeling and assessment of the vulnerability of a second case study, using the discontinuous approach two models are compared, one with reinforcement interventions and one without using two different stereotomies to evaluate how correct it is to use an approximate stereotomy.

CHAPTER 5| deals with the modeling of a third case study, non-destructive method of investigation and the discontinuous approach are combined in order to obtain an initial indication of the feasibility and possible limits that OMA finds in the DEM world.

CHAPTER 6| outlines the strengths of the research carried out and possible developments for future work.

1 | LITERARY REVIEW: A FRAMING OF THE MASONRY

1.1. THE ITALIAN HERITAGE

The Italian building heritage fully represents, in its richness and variety, the succession of all historical periods ranging from Roman, medieval, Renaissance and nineteenth-century buildings, up to the most recent ones that reach the present day. Despite all this it constitutes a historical heritage of considerable architectural-artistic importance, every time we must intervene in these structures, we are faced with problems due to the uncertainty related to the identification of the type of walls and the mechanical characteristics of the materials that compose it. Technical knowledge, the availability of raw materials and economic and social contexts have determined what is presented today: most of the existing buildings on the Italian territory consist of a masonry structure and are not designed to have a correct seismic response.

The Italian territory is characterized by medium-high seismicity [1], the activity is concentrated in the central part and the southern part of the peninsula. In fact, in recent decades there have been several seismic events of considerable importance (Umbria – Marche 1997/98, Molise 2002, Abruzzo 2009, Emilia-Romagna 2012, Marche – Lazio – Umbria – Abruzzo 2016) which have damaged the Italian heritage causing damage and deaths [2,3]. Among the most important events, the seismic sequence of central Italy in 2016 highlighted the vulnerability of the Italian historical and artistic heritage [4–8]. In October 2016 in the Marche region of central Italy, two major earthquakes caused several damage to historic buildings. The second quake destroyed Amatrice, Accumoli, Norcia, Arquata del Tronto and Visso and caused

severe damage to other neighbouring countries such as Camerino, San Severino Marche and Tolentino.

1.2. THE BEHAVIOUR OF MASONRY BUILDINGS

A masonry structure has at its base a heterogeneous composition, formed by resistant elements (bricks or stone ashlars) and mortar joints [9]. The assembly of such elements, which can be very diverse, has consequences on the building's response to gravitational and seismic loads. The static and dynamic behaviour of masonry buildings, therefore, depends on several factors, including the type of material used, the wall texture, and the adequate connection between the various elements of the building (wall-wall, wall-floor) [10,11].

The material used and the wall texture together constitute the *quality of the masonry*: generally, masonry with a chaotic texture is of poor quality and will tend to disintegrate even for small earthquakes. For this reason, the first step in assessing the response of a masonry building is the definition of the wall quality under consideration. In the case of a good quality of the masonry, the seismic response will depend above all on the organization of the elements as a whole and on the ability of the structure to distribute the loads evenly: this aspect is mainly determined by the adequate connection between vertical walls and between walls and floors. In a building that has a good quality of masonry but whose elements are not well organized, the local (or first mode) mechanisms will arise in the first place, which concerns the overturning out of the plane of walls or portions of them for different causes (Figure 1a). If, on the other hand, the structure is composed of elements well connected together, the off-plan mechanisms will be avoided and a global (or second mode) mechanism will be favoured that concerns the damage in the plane of the wall panel itself [12–14] (**Figure 1b**).

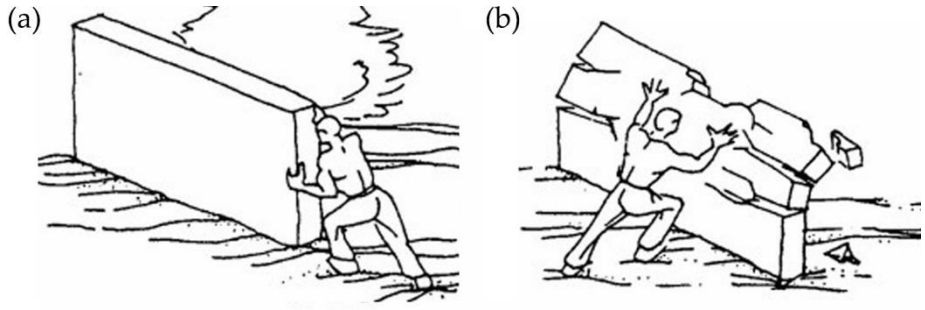

***Figure 1** – Mode I: flexural and overturning behaviour (a), Mode II: shear and bending behaviour (b) (Touliatos, 1996).*

The wall panels of good quality have shown over time good behaviour for actions in their plan, while for actions that invest the wall panel orthogonally to their floor there is very low resistance. Another aspect to consider in the analysis of existing buildings is that the result is greatly influenced by local techniques and uses. A strongly seismic territory will have collected over time a series of constructive measures (or interventions) that have allowed the buildings to be "witnesses" of a construction technique in future centuries. In particular, it is very common to see in a territory that has already faced the seismic problem the use of chains, buttresses and good anchoring. The overall behaviour of a building will be better when all the characteristics described are met. In this case, we are dealing with a structure with box behaviour: each element is closely collaborating and distributes all the stresses in an appropriate way. Particular influence is given by the anchoring and stiffness of the floor and roof floors. A rigid floor allows the distribution of seismic stress on the different walls according to their stiffness, thus limiting damage (**Figure 2**).

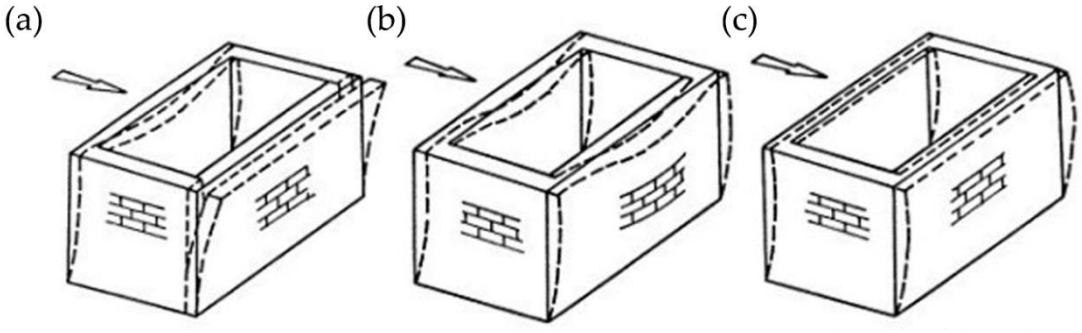

***Figure 2** – Overall behaviour in case of deformable floor and without curb (a), deformable floor with curb (b), rigid floor with curb (c) (Macchi G. Margenes G., 2002).*

1.3. THE MECHANICAL PARAMETERS OF THE MASONRY

The masonry constituting historic buildings is a composite material, formed by blocks (stone or brick) interposed for the most part with mortar. Defining the quality of the masonry means understanding how close you are to an "ideal" situation described by the rules of art, or a series of practical criteria of an empirical nature, deriving from the construction site experience.

The overall response of the masonry depends on the mechanical properties of the block, those of the mortar and the constitutive law. Through experimental tests, it is possible to trace the mechanical properties of the masonry such as compression, shear strength and elasticity [15]. The Italian and European codes indicate the reference parameters of the existing walls, these values have been determined based on surveys aimed at characterizing the most common wall types.

Distinct Element Method (DEM) approaches and micromodeling require the definition of parameters at the unit-mortar or unit-unit interface [16–18]. The required parameters are usually the stiffness and nonlinear properties of the interface in the normal (fracture mode I) and shear (fracture mode II) directions.

Through the Elastic Modulus E (E_u and E_m) and the Shear Modulus G (G_u and G_m) of the unit and the mortar it is possible to define the rigidity of the interface elements in the shear direction, $k_s = G_u G_m / t_m (G_u - G_m)$, and normal direction, $k_n = E_u E_m / t_m (E_u - E_m)$ [19]. In this case t_m is the mortar thickness.

The area below the stress-displacement diagram (in the softening regime) is define fracture energy G_f, is the amount of energy needed to create a unit cracking area (**Figure 3**).

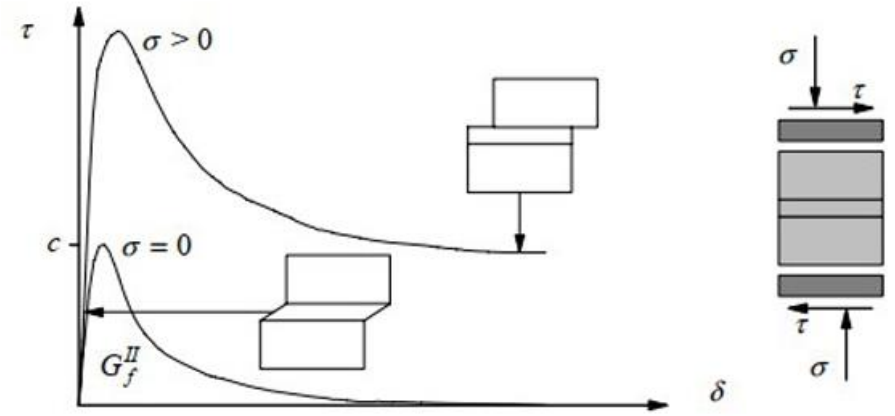

***Figure 3** – Behaviour of masonry under shear and definition of fracture energy* $\boldsymbol{G_f}$ [19].

As for the tensile strength, this depends on the mortar-brick adhesion. This value can be neglected for safety reasons since it has modest values and in some cases equal to zero as in the case of old buildings in stone material and poor mortar or dry joints. In compressive behaviour, unlike traction behaviour, more important values of strength and fracture energy are obtained. Experimental values say that this value is between 10% and 20% of the compressive strength of the masonry.

For the characterization of the shear several tests are available, the mortar-block law is usually weak and resists a cohesive-frictional response in shear where the cohesive contributions depend on the normal stress and a cohesive one in tension (without cohesion in the case of dry joints). The shear strength value is given by $f_{vk} = f_{vk0} + 0.4\sigma_d$ where f_{vk0} is the cohesion of the masonry or the initial shear strength that assumes a value of 0.05 – 0.1 MPa for old masonry with weak mortars, 0.4 is the tangent value of the friction angle suggested by the Italian and European codes, σ_d is the compressive stress of the masonry. As for the value of the tangent of the friction

angle, it is recommended to use 0.2 for the rubble of old masonry structures and 0.3 for the case of stones with an irregular course [20].

1.4. RETROFITTING INTERVENTIONS IN MASONRY BUILDINGS

Masonry buildings that have limitations under seismic loads are classified as unsafe and require interventions to limit their vulnerability and allow safe use. Over the years, various information and techniques have been collected to improve the structural behaviour of existing buildings [21–23]. These techniques are based on different principles such as the improvement of connections to have better overall behaviour, the consolidation of vertical structural elements, the stiffening of horizons, the construction of additional structural elements to improve the strength of buildings when they are subject to horizontal loads and the use of structural elements that act as a reserve to those already existing in case of partial failures.

Depending on the need, different techniques can be used [23], the most common are the following:

- *Ring beams* are built using a pair of longitudinal axes joined together by transverse elements. They favour the box behaviour of the building favouring the wall-roof connection.
- *Buttresses*, are masonry massive elements of typically triangular shape and contrast possible mechanisms outside the plane (**Figure 4a**).
- *Steel chains* (**Figure 4b**) connect the walls. They are used to ensure global behaviour and to avoid the possibility of triggering out-of-plane mechanisms.
- *Strengthening of the connections between the wooden floors and the roof with the walls*. The connection when allowed is made with wooden wedges otherwise with metal elements.
- *Stiffening of horizons with bracing placed diagonally*. With this technique, the diaphragmatic behaviour is improved and consequently the box behaviour.

- *Consolidation of multi-leaves masonry*. The walls composed of several layers as a result of horizontal actions tend to behave independently and consequently overturn out of the plane. To deal with this problem, elements of length equal to the thickness of the wall are inserted that act as a connection, these are fixed by mortar injections or with an anchoring system (**Figure 4c**).
- *Repointing*, this technique is used to consolidate the masonry and consists in replacing the mortar with a better quality one. In some cases, reinforcement reinforcements are also inserted into the mortar joint to cope with damage due to sliding.

(a) 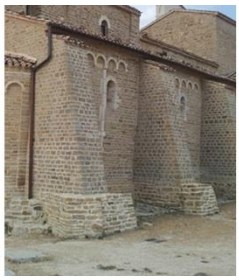 (b)  (c) 

***Figure 4** – Buttresses (a), steel chain (b) and consolidation of multi-leaves masonry (c).*

Innovative seismic retrofitting techniques have introduced other principles such as improving the mechanical properties of walls and reducing the dynamic effects induced by the earthquake [24–26]. Among the most used ones it is good to mention:

- *Injections of mortar inside the masonry*. This technique aims to increase the overall strength of the multi-leave walls as the mortar fills the voids present (**Figure 5a**). This technique will have disadvantages such as the irreversibility and unpredictability of the volume of mortar required to perform the injection.
- *External bonded composites*. On the market, there are several composites, Fibre-Reinforced polymers (FRP) (**Figure 5b**), Steel-Reinforced Ground (SRG), Fibre-Reinforced Cementitius Matrix (FRCM) and Texile-

Reinforced Mortar (TRM). All of them are aimed at reducing the seismic vulnerability of masonry buildings.

- *Base isolation*, this type of intervention aims to isolate the structure from the vibrations induced by the earthquake thanks to the use of an interface with low horizontal rigidity and a good ability to withstand vertical loads. This technique allows to reduce the accelerations of the structure and increase the total displacements (at the base of the system), thus reducing the relative displacements of the structure which works as a rigid body.
- *Passive dampers*, there are various types of dampers, i.e., viscous, viscoelastic, hysteretic metallic and friction dampers. They are intended to dissipate the energy coming from the earthquake, in this way there is a reduction in damage and an increase in seismic performance. Unlike the insulators at the base, they are a less expensive type of intervention and can also be applied only to specific structural elements.

(a)  (b) 

***Figure 5** – Mortar injections (a) and FRP installation (b).*

1.5. MASONRY MODELLING

The modelling of masonry is a difficult issue because the complexity of the real material, with its peculiarities, such as anisotropy, heterogeneity, nonlinearity, and many others, require very high effort to implement an accurate representation. Even

though, it isn't always necessary in every application to use models with such precision . In general, it is possible to affirm that several ways of modelling strategies are present (**Figure 6**), and each one has a specific field of application. The most common are:

- *Detailed micro-modelling*, each component (units and mortar) is represented separately, modelled with its mechanical properties (Young's modulus, Poisson's ratio and, optionally, even the inelastic properties are considered), as a continuous media, while the interfaces between units and mortar are represented by discontinuous elements. This method allows the correct representation of the mortar joints that act as planes of weakness, so giving the possibility to have cracking or slipping along the interfaces.
- *Simplified micro-modelling*, units are represented by continuous elements, while the behaviour of both mortar and the interfaces is lumped in a single discontinuous entity. So, in each mortar joint, the thickness of the mortar and the two mortar-unit interfaces collapse into a single average interface in this modelling strategy, and the unit is represented as an expanded element because it also embeds half of the mortar joint around itself. Also in this case the presence of potential fracture/slip lines is ensured by the presence of the interfaces, but accuracy is lost since Poisson's effect of the mortar is not included.
- *Macro-modeling*, units, mortar, and interfaces are all represented as a homogeneous anisotropic continuous. This is the most common type of modelling masonry because it provides a good compromise between accuracy and efficiency. But should be based on a homogenization technique that, given the initial properties of units, mortar and interfaces, can end up with the homogenised media characteristic.

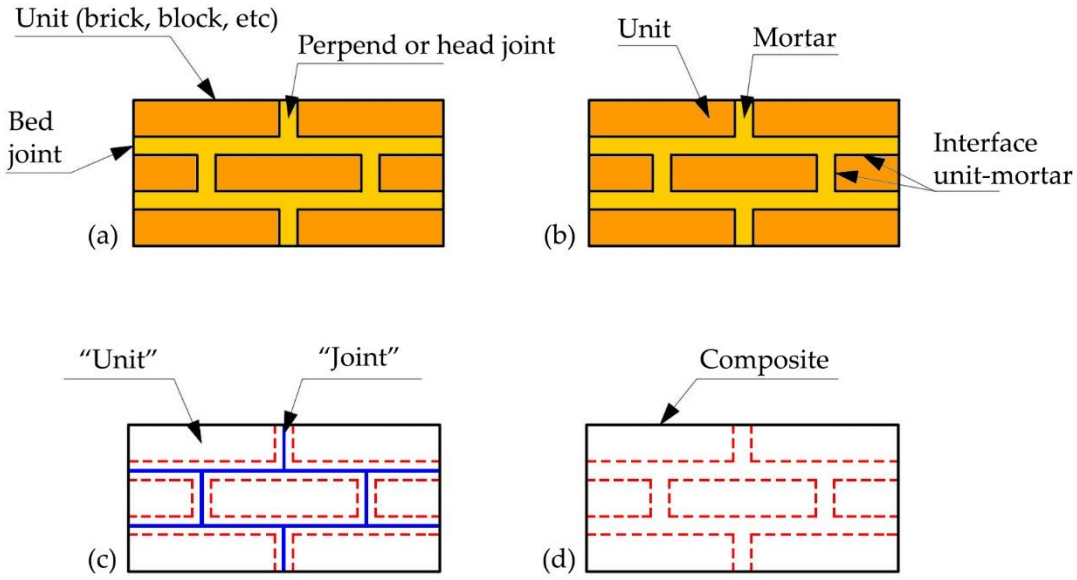

Figure 6 *– Masonry sample (a), detailed micro-modelling (b), simplified micro-modelling (c), macro-modelling (d)* [19].

Numerical models can be divided into two large categories:

- In the *Continuous methods*, the domain of the system is represented through elementary units of simple shape (generally triangles or quadrilaterals) that can be deformed but always remain in contact with each other at their separation surfaces. In this case, all individual units retain the same system properties. The homogenization techniques follow a macroscopic approach in which no distinction is made between the elements that make up the masonry but a single finite element is introduced that has the task of simulating the overall behaviour of the "masonry" material.
- In the *Discontinuous methods*, the system domain is represented as a set of distinct and separate elements that interact with each other only when they come into contact. The bodies transmit forces to each other at the points of contact and, because of them, move in space describing the mechanical behaviour of the system. In discontinuous models it is, therefore necessary, at each iteration, to update the contacts depending on the position and

movement of the individual bodies; this does not happen for continuous models that, instead, keep the contact surfaces between the various elementary units unchanged.

The continuous method allows to study the system in a stable equilibrium condition or at most in limit conditions, those to the discontinuous instead, allow a more in-depth analysis in the event that the rupture of the system is studied, following a detachment if there is a contact the blocks continue to interact with each other.

The continuous methods include the *Finite Difference Method* (FDM), the *Finite Element Method* (FEM) and the *Boundary Element Method* (BEM).

The FDM is the most direct approach to discretizing Partial Differential Equations (PDEs) [27]. Consider a point in space where take the continuum representation of the equations and replace it with a set of discrete equations, called finite-difference equations. The FDM is typically defined on a regular grid and this fact can be used for very efficient solution methods. The solution is obtained by imposing the initial boundary conditions.

The Finite Element Method (FEM), proposed for the first time by Clough in 1960 [28], is one of the most popular numerical procedures in engineering. The discretization of the domain: consists in the subdivision of the domain in a finite number of continuous elements, of regular shape (triangles, quadrilaterals, etc.), defined by a fixed number of nodes. The displacements of the internal points are a function of the nodal displacements. The exact formulation of the elastic problem of the continuum leads to systems of PDEs defined by boundary conditions, in this way it is discretized and refers to a solution of a system of linear equations. Being a continuous method, it does not allow the possibility of separation between the elements and the main disadvantage is the low ability to represent the stress-deformation behaviour of systems subject to failure. The efficiency of the FDM and FEM, decreases as the number of degrees of freedom increases.

The BEM consists of discretizing the contour of the structural element, thereby reducing the size of the problem and simplifying the input data required. The BEM generally involves a reduction in the size of the computational model compared to the FEM, as it requires a discretization only on the contour of the domain and not on its entire extension. In general, however, BEM is not as efficient as the FEM in taking into account the heterogeneity of materials while maintaining the same difficulty in simulating the tenso-deformation behaviour of systems subject to breakage.

The discontinuous methods include the *Discrete Element Method* (DEM), is a relatively recent approach, compared to those mentioned above. Its origins date back to 1971 when Cundall applied it to a rock mechanics problem [29] and 1979 when Cundall and Strack applied it to soil analysis [30]. The theoretical foundation of the method is the formulation and solution of equations of motion of rigid or deformable bodies using implicit and explicit formulations. The key concept of DEM is that the domain of interest is treated as an assemblage of rigid or deformable bodies and the contacts among them need to be identified and continuously updated during the entire motion process and represented by proper constitutive models. In general, contiguous blocks usually interact with each other through unilateral-type contact constraints, having no-tension behaviour and an elastic or elasto-plastic constitutive law in case of compression, and a frictional-type behaviour in case of sliding. The number of degrees of freedom of the model, considering rigid blocks, will be equal to 3N in the case of two-dimensional models and 6N in the case of three-dimensional models, where N indicates the total number of elements. The models that are set up for this kind of method are often characterized by a large number of elements, especially for detailed modelling, for this reason, they require significant processing times, not comparable with the computational burden of a continuous model. The definition of the mesh and the constitutive models of the materials are replaced by the determination of the distribution and the dimensions of the elements that compose the system and the description of the behaviour of the contacts.

Unlike the continuous method in the discontinuous one the blocks are rigid (today there are also formulations with deformable blocks) and the deformabilities are concentrated in the joints, the iterations between the blocks are represented by contact points or edge-to-edge contacts, and complete separation of blocks is allowed and uses time-step algorithms to solve almost static problems.

1.6. REVIEW OF LITERATURE AND OBJECT OF RESEARCH WORK

The Italian historical heritage consists of different structures that differ from each other for complexity showing different damage mechanisms depending on the case. The towers and bell towers, for example, develop mainly in height showing simple architectural forms, although they can have different geometries, holes, wall thicknesses and slenderness are built with construction techniques and similar materials. Churches, on the other hand, unlike towers and bell towers, are characterized by complex geometries, large lights, the lack of horizons, irregularities in plan and different materials. All these characteristics therefore make them particularly vulnerable to the horizontal loads produced by a seismic event. Thanks to a detailed development of numerical analysis it is possible to effectively and reliably predict the behaviour of these structures.

The knowledge of the materials for this type of structures is not always easily identifiable and consequently the development of numerical models is sometimes uncertain [19].

The results identify the most vulnerable elements of these structures, in the case of towers and bell towers, these can also be easily determined starting from the characteristics of the structure using simplified methods that do not take into account the possibility of irregularities in shape [31]. As regards the churches, however, the question is more articulated and several studies are moving in this direction. [32]. Conventional approaches, in some cases, do not take into account the vertical component (z-direction) of the dynamic input, thus neglecting the vertical

displacement of the structure, which, however, cannot be neglected to obtain a realistic prediction of the behaviour of the structure.

It is necessary to take into account the wealth of technical-scientific knowledge that has accumulated over the centuries on the mechanics of materials and on the type of structures, in this way it is possible to adequately evaluate the safety of the structures. Depending on the case study it is possible to use different approaches, among those proposed [19,33] we find:

- Detailed micro-modeling;
- Simplified micro-modeling;
- Macro-modeling.

There are also several methods that study the dynamic response of large-scale masonry structures [34,35].

The continuous approach is certainly among the most used, in the Finite Element Method (FEM) [12,20] the masonry material is seen as a homogeneous medium, with this method it is possible to reproduce the overall behaviour of the structure [36], but not grasping local behaviours.

The discontinuous approach involving the Discrete Element Method (DEM), unlike the FEM, allows to reproduce both the global behaviour and the possible activation of local mechanisms [37–40]. DEM methods are happily used for simple structural elements such as columns and vaults [41,42] and in recent years they have also been used for non-linear dynamic analysis of more complex structures such as churches [43], towers [44,45] and so on [46,47]. In fact, these ancient masonry structures can be represented as a discontinuous structural system consisting of individual units (i.e. blocks, bricks, stones, etc.) which interact with each other. For this purpose, in recent years several calculation codes have been developed that allow to investigate the behaviour of these structures through the discontinuous approach such as the DEM code [48], the Non-Smooth Contact Dynamics method (NSCD) [49–51] and the Cohesive Zone Model (CZM) [49].

The peculiar aspects on which the structural response of a structure is based are the mechanical behaviour, the structural details and the geometric characteristics, these factors are fundamental aspects to obtain a reliable simulation.

Various problems related to the modeling of masonry buildings were addressed, such as the realization of complex geometries, the difficulty of numerical convergence, high computational burdens due to a large number of elements and consequently contacts, etc.

With the aim of validating the numerical results these were compared with the damage actually suffered by the structures [52,53] following several earthquakes that have hit the Italian territory in the last decade.

It is precisely from these works that ideas have emerged to investigate further aspects related to discrete approaches and improve research work. The priority was to reproduce a faithful geometry and wall texture in order to obtain a correct structural response and reduce the differences between numerical model and reality.

In [52] through the NSCD method, two advanced numerical models were compared in order to evaluate the influence of the intervention of hydraulic lime placed on the top of the structure. The study allowed to define the average geometric properties that affect the dynamic behaviour of the façade and to recognize the most common forms of degradation, to support the monitoring of the state of conservation and the elaboration of an intervention plan or replacement of those already presented.

In [53] through discrete approaches, four different models were created that took into account the stereotomy of the structure. Four different levels of discretization were used: a multileaf model, a double-leaf model, a single-leaf model and a single-leaf model with large blocks. All this has been set with the final goal of studying how, as the degree of detail of the structure decreases, more or less important information is lost to the advantage of a greater speed of calculation, a fundamental aspect in professional practice.

The reliability of these models is tested by comparing the solution with experimental data, these especially in the case of complex historical structures are not

easy to determine and, in most cases, refer to a limited number of parameters (as in the case of operational modal analysis). If experimental results were available for all parameters the sense of using a numerical model would be lost, the purpose of which is to provide predictions about the behaviour of the system when a limited amount of information is available. A methodology to evaluate the reliability of the model consists in using two different approximate solutions, from the comparison of the two different solutions it can be said that the solution is correct only in the case in which we are close to the exact solution, vice versa it is unlikely that we will arrive at the same solution in the case of an incorrect solution as the techniques used are different from each other.

Due to the complexities and uncertainties that characterize the geometry and non-linear response of historic masonry buildings, it is still challenging to create a reliable numerical model. Mechanical parameters such as strength and stiffness are not used in common practices that are not in line with current national and international regulations. In addition, in the literature we find different thoughts that make it difficult to determine which method is more correct than the others.

The following research work aims to contribute to the main problems related to the application of discrete models for the assessment of the vulnerability of masonry structures of a historical-monumental nature. In the literature there is the total or partial absence of some aspects that characterize this research work.

In this thesis work a comparison was first carried out between the discontinuous and continuous approaches to evaluate any discrepancies between the two methods. The scope is to examine how structural components interact with each other and influence how buildings react to earthquakes [54–56]. To evaluated this aspect two different models are created.

Subsequently, in a recent thesis work the chaotic masonry has been regularized and it has been studied how different regularizations could affect the structural behaviour, hence the question of whether regularization is too important a hypothesis for the purposes of the structural response. To answer this question in this thesis work

it was decided to use a chaotic discretization of the walls characterized by erratic stones arranged irregularly (typical in the rubble masonry in multi-leaf walls), usually present in Italian historical structures. In previous works [52,53] this aspect has always been neglected by choosing a simplified modeling in favor of lower computational burdens. Two models were used that differ in the discretization of the facing composed of irregular erratic stones. The purpose of the following research work is to understand whether it is right to neglect the irregularity of the stones in favor of lower computational burdens. A quantitative and qualitative evaluation of the models was then carried out, the main constitutive laws were compared, and finally the contribution of seismic improvement interventions on the dynamic response of the structure was evaluated.

Another aspect widely opened in the DEM world is that concerning the impossibility, at least now, of using non-destructive methods of investigation such as the Operation Modal Analysis (OMA) to know quantitatively the state of the structure through the calibration of mechanical, elasto-geometric and boundary condition parameters.

The OMA is widely used and developed in the FEM world [57–60] where it has even come to an automatic calibration using genetic algorithms [61]. In the DEM, on the other hand, this practice finds little development, in fact, given the complexity of realization in the literature there are works concerning only simple structural elements [62]. The following thesis work aims to give a first indication of the feasibility of this procedure and indicate the possible limitations that the OMA finds in the DEM world.

As for the continuous approach, in the Finite Element Method (FEM) implemented in the MIDAS FEA NX© calculation software, the wall structure is modeled continuously, without the need for schematization or excessive geometric simplifications, through the use of solid finite elements. The masonry material is approximated as homogeneous and isotropic, endowed with a good compressive strength and a poor (but not nothing) tensile strength. Nonlinear constitutive laws are

equipped with softening and damage and require resistant parameters that can be easily obtained.

As for the linear numerical analyses, they were carried out with the Discrete Elements Method (DEM) [48,63] implemented in the 3DEC© code issued by the Itasca Group [64] meanwhile nonlinear numerical analyses were performed with both DEM and the Non-Smooth Contact Dynamics (NSCD) method [65] implemented in the open-source code LMGC90© developed by the LMGC (Laboratory of Mechanical and Civil Engineering) developed by the research laboratory of the University of Montpellier and the CNRS.

In both calculation software, the masonry was represented as a set composed of distinct rigid blocks which maintain their initial geometry even after the application of the loads. In this way, the deformations take place only in correspondence of the mortar joints which are represented by the interfaces (of zero thickness) that are between the blocks. During the calculation, large displacements, rotations between blocks, sliding, the formation of openings and even complete detachment between blocks are allowed, in addition, there is automatic detection of new contacts. Rigid blocks in the NSCD method are subject to Coulomb friction laws and impact laws, due to the non-smooth nature of the contact laws and geometric nonlinearity the structure exhibits a complex dynamic behaviour with particular attention to the possible non-uniform nature of the dynamic response which occurs immediately before or during the collapse with discontinuous velocity.

DEM models, on the other hand, use smooth functions to describe the interactions between blocks with continuous velocities, interfaces are assigned the nonlinear behaviour of the mortar with a Mohr-Coulomb constituent model that involves parameters such as friction angle, cohesion and tensile strength. The stiffness near the interfaces is regulated by two springs in the normal and shear direction, connecting the contact stresses with the relative displacements of the blocks.

2 | CONTINUOUS AND DISCONTINUOUS APPROACHES FOR MASONRY STRUCTURES

In this thesis work, two different approaches were initially used, the continuous one, based on Finite Element Method (FEM) and two discontinuous approaches. The first discontinuous approach is implemented on the open-source calculation code LMGC90©, while the second one in the commercial calculation software 3DEC© code. Subsequently, attention was focused on discontinuous approaches as in this field there are still aspects not completely deepened.

2.1. CONTINUOUS APPROACH

In the continuous approach, the domain of the system is discretized through unit elements made of basic shapes (tetrahedral elements) that can deform but always remain in contact with each other in correspondence of their separation surfaces.

Masonry is considered as a homogeneous and isotropic material where the mechanical properties depend on those of its components (mortar and bricks).
The analyses were based on the Concrete Damage Plasticity (CDP) model presented by J. Lubliner et al. [66] and then modified by Lee et al. [67], and available within the MIDAS FEA NX© software . Although originally conceived to describe the nonlinear behaviour of concrete, the model can be used for masonry through an appropriate adaptation of the main parameters [68].

2.1.1. CONCRETE DAMAGE PLASTICITY (CDP)

The Concrete Damage Plasticity (CDP) model is based on the assumption of isotropic scalar damage with distinct tensile and compression parameters, thus being

able to consider a different elasto-plastic behaviour as the sign of the stress state changes (**Figure 7**), and is suitable for both static and dynamic analysis. In traction, the stress-strain constitutive law follows a linear-elastic relationship until the peak tension $\sigma_{\tau 0}$ is reached. Subsequently, micro-cracks begin to propagate in the material, a phenomenon macroscopically represented with a clear non-linear softening trend. In compression, the response is almost linear up to the value of the yield strength after which, the response is typically hardening, up to the tension σ_{Cu} where there is crushing by compression, represented by a non-linear softening branch beyond the peak tension.

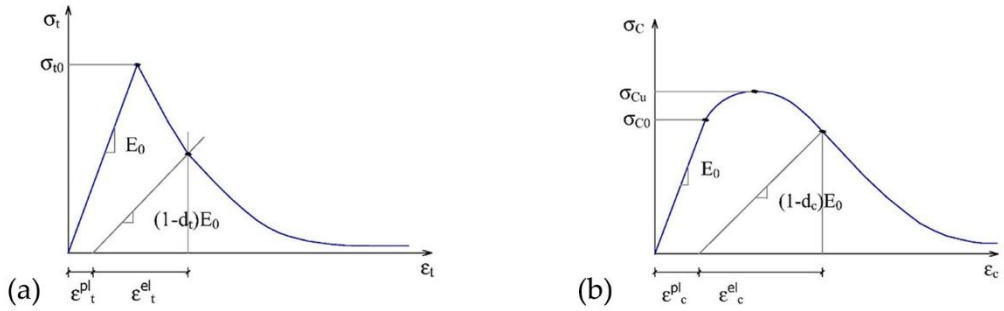

***Figure 7** – Uniaxial constitutive tensile (a) and compression (b) laws adopted in numerical simulations.*

The two constitutive traction (σ_t) and compression (σ_c) laws are defined as:

$$\sigma_t = (1 - d_t)E_o(\varepsilon_t - \varepsilon_t^{pl}), \tag{2.1.1.1}$$

$$\sigma_c = (1 - d_c)E_o(\varepsilon_c - \varepsilon_c^{pl}), \tag{2.1.1.2}$$

where E_o is the initial elastic modulus, while ε_t and ε_c is the total deformation, and ε_t^{pl} and ε_c^{pl} the plastic deformation equivalent to traction and compression respectively. The elastic modulus gradually degrades each time the deformation reaches a critical value through the tensile damage parameters (d_t) and compression (d_c) that are assumed to vary linearly: the values range from zero, for the deformation

corresponding to the peak of stress, to 0.90, for the last deformation value in the softening section.

To describe the real behaviour, therefore multi-dimensional in the plastic range, it is assumed that the masonry obeys the Drucker-Prager resistance criterion with an unassociated flow law (**Figure 8**).

Through a parameter, Kc = 0.667 applied to the analytical expression of the Drucker-Prager surface, in the space of the main tensions, it is possible to distort the surface making it more like that of the Mohr-Coulomb criterion.

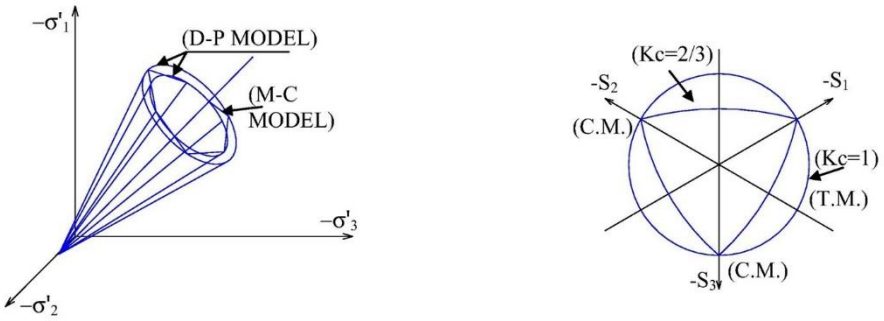

***Figure 8** – 3D resistance domain adopted in MIDAS FEA NX© for the CDP model and meaning of the Kc parameter. It is indicated by D-P: Drucker Prager resistance criterion; M-C: Mohr-Coulomb resistance criterion; C.M.: compression meridian; T.M.: meridian of traction.*

To avoid problems of numerical convergence, the apex of the conical domain of the Drucker-Prager criterion is "approximated" with a hyperbolic function. The MIDAS FEA NX© code allows to adjust this "approximation" using the so-called eccentricity parameter, here taken equal to 0.2, which represents the length of the segment between the points of intersection of the cone and hyperbola with the p-axis in the p-q space (total average tension-average deviatory tension) (**Figure 9**). Smaller values can cause convergence problems when the material is subjected to low confinement pressures due to the "close" curvature.

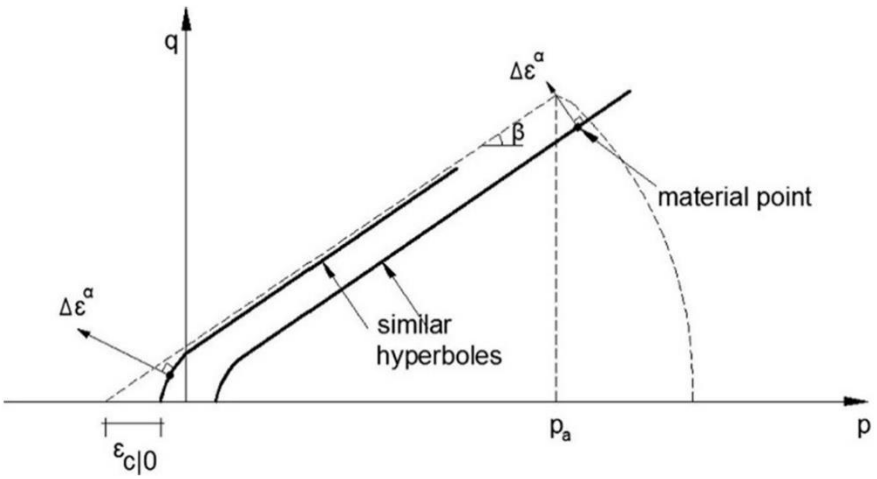

Figure 9 *– Drucker-Prager breaking criterion "approximated" and adopted in numerical simulations, p-q plan.*

For the angle of expansion, a value of 13° is assumed, according to experimental evidence available in the literature [9]. A suitable model should take into account the ratio of the ultimate compressive strength in biaxial stress states and uniaxial conditions. This f_{b0}/f_{c0} ratio, which has some similarities between concrete and masonry, is reasonably placed at 1.16.

Some convergence difficulties may arise for numerical analysis when constitutive laws with softening behaviour and stiffness degradation are used. For this reason, a viscosity parameter ($\lambda = 0.002$) is introduced in the model to obtain a visco-plastic regularization of the constituent equations, allowing to overcome the convergence difficulties. In fact, small values of the viscosity parameter help to improve the rate of convergence in the softening branch without significantly compromising the results.

2.2. DISCONTINUOUS APPROACHES

The behaviour of masonry structures through discrete approaches aims to represent the masonry consisting of a set of distinct elements that interact with each other. In this way, the global behaviour of the structure is studied starting from the

local one through the points of contact present in the interface between the various blocks. The interfaces represent the joints and are governed by various contact laws.

In this thesis work, two different methods were used and implemented in two different calculation software: the open-source code LMGC90© and the commercial code 3DEC©.

The first implements the Non-Smooth Contact Dynamics (NSCD) method, is based on a non-smooth formulation of body dynamics, i.e., laws of contact and friction with speed jumps (shock), uses implicit time integration and contact solvers. In the Distinct Element Method (DEM) implement in the 3DEC© instead, unlike the NSCD method, we find smooth contact laws (continuous and sufficiently differentiable) and interactions at the points of contact involving relative velocities, using explicit solution algorithms for the dynamic equation.

In the NSCD method, there are inelastic shock laws with a return coefficient of zero, in the DEM there are damping terms with a return coefficient to guarantee the numerical stability of the explicit scheme used.

In both methods, models are made as a set of polyhedral bodies, which interact with each other through interfaces (representing mortar joints) of zero thickness. Blocks must necessarily be modeled as non-convex elements, if necessary, it is possible to combine several elements to obtain convex geometries. In correspondence of the interfaces, regulated by special constitutive laws, the mechanical interaction between the blocks is allowed. At each step of time, integrating the Newtonian equations of motion, the motion of the masonry units is calculated.

In this thesis work, the blocks were modeled as rigid bodies with six degrees of freedom (three translational and three rotational) assigning mass density as the only parameter. This property consists of mass divided by volume and does not consider gravitational acceleration.

2.2.1. THE NON-SMOOTH CONTACT DYNAMIC METHOD

The NSCD method is part of the discrete element method family introduced by P. Cundall [29], it was introduced and developed by Jean [69] and Moreau [70] and implemented in LMGC90© [49] open-source code. The NSCD method differs from the original DEM for the implicit integration scheme and the non-regularized interactions laws of Signorini unilateral contact and Coulomb dry-friction. Moreover, other features of the method are the simplification of the contacts between blocks, which are assumed punctual and the hypothesis of rigid bodies, having the strain applied to the contact points. In the following section, all the components of this particular discrete element method will be presented, especially for what concerns the space discretization of the bodies, the dynamical behaviour, the time integration of bodies movement, contact detection, interaction laws (impact laws, behaviour laws, etc.)

2.2.1.1. Treatment of the dynamics equation in the NSCD method

Let's define $q = (q_1, \dots, q_n) \in R^N$ as the vector of generalized coordinates of a set of n_b rigid bodies, with $N = 6n_b$ as the total number of degrees of freedom of the system. For simplicity, we assume that any bilateral constrain, eventually imposed on the system, has been taken into account through the reduction of the size of the vector q. Let's consider the contact α between a candidate body and an antagonist body. The unilateral contacts of impenetrability are expressed through the following inequality:

$$f_a(t, q) \geq 0, \qquad \alpha \in \{1, \dots, n_c\} \tag{2.2.1.1}$$

Where f_a is a function depending on both time and configuration of the q vector and α indicate the generic contact. This double dependence implies a geometrical constraint between the bodies, that can't overlap each other (due to the q dependence) and a temporal constraint (due to the t dependence). When $f_a = 0$, this

means that the candidate body is in contact with the antagonist one. The result of the interaction (**Figure 10**) of the antagonist body (AB) on the candidate body (CB) can be described by a force $r_a \in R^3$, acting in a contact point I_a.

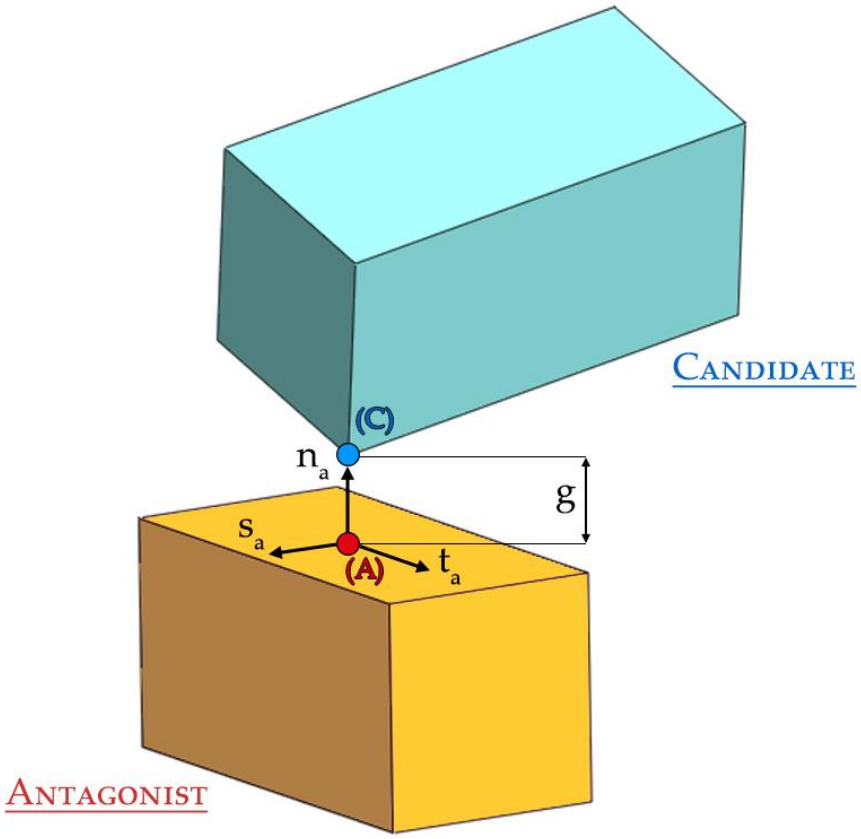

***Figure 10** – Relation between candidate an antagonist in 3D space.*

Let's define, then, a local reference system F_a, having as base three vectors: a normal vector n_a, oriented toward the AB, and two tangent vectors s_a and t_a, defining the tangential plane, such that:

$$n_a = s_a \otimes t_a \qquad (2.2.1.2)$$

Let's call ga the distance between the bodies in the normal direction ($g_a < 0$ when the bodies are overlapped). The local forces r_a expressed in the local reference system,

can be expressed in function of the global reference system through the following linear relation:

$$R_\alpha = H_\alpha(q) r_\alpha \tag{2.2.1.3}$$

Where:

- $H_\alpha(q) : R^N \rightarrow R^{3N}$ is a mapping that contains the information that makes it possible to link the local forces (r_α), to the global ones (R_α).
- q is the vector containing the generalised motion coordinates (displacements and rotations of the centroid of the rigid body).

Each R_α component represents the contribution, of the contact α, to the global forces, and can be decomposed in $(n_b - 2)$ null vectors ($\in R^6$), and two vectors ($R_{\alpha,C}$ and $R_{\alpha,A}$), corresponding respectively to the candidate and antagonist bodies. The resultant vector of the global contact forces can be built through the following relationship:

$$R = \sum_\alpha R_\alpha \tag{2.2.1.4}$$

In the same way, the velocity of the bodies can be expressed through the local reference system F_α.

Let's define the relative velocity u_α in the contact point between the bodies AB and CB, through the following relationship:

$$u_\alpha = H_\alpha^T(q) dq \tag{2.2.1.5}$$

Where:

- $H_\alpha^T(q)$ is the transponse of $H_\alpha(q)$.
- dq is the derivative of the vector q.

The relative velocity vector u_α can be decomposed in a normal component $u_{\alpha,N}$ and in two tangential components $u_{\alpha,T} = \left(u_{\alpha,s};\ u_{\alpha,t}\right)$. The last two relations give the possibility to move from the global to the local reference system. So, it is possible to change the reference system through the $H_\alpha(q)$ and $H_\alpha^T(q)$ linear operators, as schematized in the following figure:

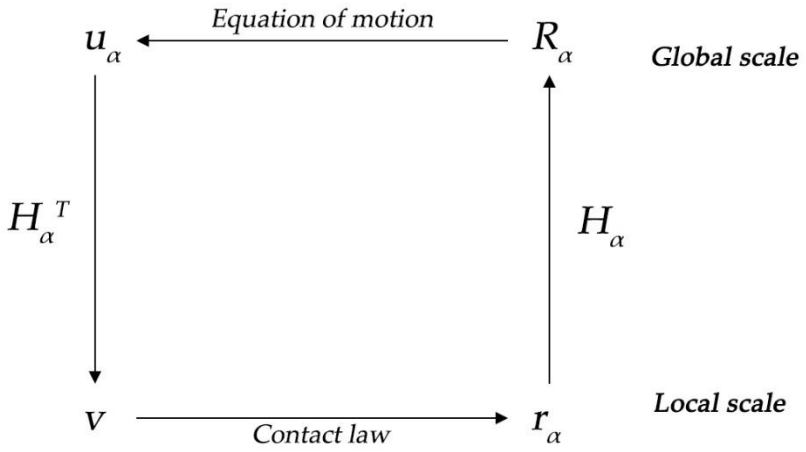

Figure 11 *– Relationship between local and global parameters in the NSCD framework.*

2.2.1.2. Contact laws

The kinematic relationships that have been adopted, to link relative velocities to local forces are Signorini's contact law (impenetrability law) and dry friction Coulomb's law [70]. Specifically, Signorini's law (**Figure 12b**) governs the impenetrability between the blocks:

$$g \geq 0, \qquad r_n \geq 0, \qquad g r_n = 0 \tag{2.2.1.6}$$

$$\text{if } If \quad g = 0 \ \rightarrow\ \dot{u}_n \geq 0 \ \rightarrow\ r_n \geq 0 \ \rightarrow\ \dot{u}_n r_n = 0 \tag{2.2.1.7}$$

This law indicates a perfectly plastic impact, i.e. Newton's law returns a coefficient equal to zero. As a result of the impact, there are no bounces, in the case of stones and bricks there is a low coefficient of return, and for this reason, it can be neglected.

The dry-friction Coulomb's law (**Figure 12c**):

$$|r_n| \leq \mu r_n; \begin{cases} r_t < \mu r_n \rightarrow \dot{u}_t = 0 \\ |r_t| = \mu r_n \rightarrow \dot{u}_t = -\lambda \dfrac{r_t}{|r_t|} \end{cases} \tag{2.2.1.8}$$

The friction coefficient is μ, λ is a positive real arbitrary number.

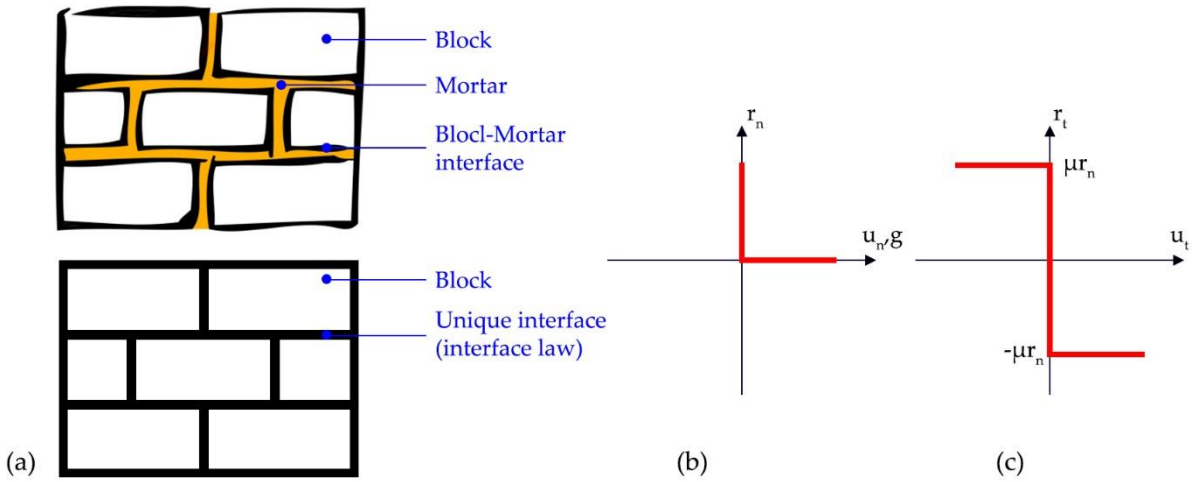

Figure 12 *– Contact at the interface between blocks (a), Signorini's impenetrability condition (b), and friction Coulomb's law (c).*

2.2.1.3. Discrete formulation of the dynamical equation of motion

The dynamic equation of motion of a body that undergoes contact can be synthesized in the following relation:

$$Md(dq) = F(t, q, dq)dt + dR \tag{2.2.1.9}$$

Where dt is the temporal increment, $d(dq)$ is a differential measure that indicates the increment of generalised velocities, dR is a real non-negative measure (representing the impulses), M is the mass matrix and $F(t, q, dq)$ is a vector that embeds all the internal and external forces acting on the system.

Let's use the temporal integration technique (time-stepping), through which the contact events aren't treated explicitly. This method practically consists in a temporal discretization through time-ranges $[t_i, t_{i+1}]$ having length h, such that the contact problem is solved during the interval. To obtain this feature, the dynamic equation of motion is integrated into each time-step, and can be rewritten as follows:

$$\begin{cases} M(dq_{i+1} - dq_i) = \int_{t_i}^{t_{i+1}} F(t, q, dq)dt + dR_{i+1} \\ q_{i+1} = q_i + \int_{t_i}^{t_{i+1}} dq(t)dt \end{cases} \tag{2.2.1.10}$$

Where dq_{i+1} is the variable that represents the approximation of the right limit of the velocity, at the time t_{i+1} and $q_{i+1} \sim q(t_{i+1})$.

For the action dR, it is possible to approximate the measure in the time range $[t_i, t_{i+1}]$:

$$dR([t_i, t_{i+1}]) = \int dR \sim R_{i+1} \tag{2.2.1.11}$$

To solve (2.2.1.10) the θ method is used (implicit time integration). The stability condition of the method is reached when $\theta \in (0.5; 1)$. The system of integrals can be rewritten in this way:

$$\begin{cases} \int_{t_i}^{t_{i+1}} F(t,q,dq)dt = h\theta F(t_{i+1},q_{i+1},dq_{i+1}) + h(1-\theta)F(t_i,q_i,dq_i) \\ \int_{t_i}^{t_{i+1}} dq(t) = h\theta dq_{i+1} + h(1-\theta)d_i \end{cases} \quad (2.2.1.12)$$

This approach leads to the following format:

$$\begin{cases} M(dq_{i+1} - dq_i) = h\theta F(t_{i+1},q_{i+1},dq_{i+1}) + R_i + 1 \\ q_{i+1} = q_i + h\theta d_{i+1} + h(1-\theta)d_i \end{cases} \quad (2.2.1.13)$$

It is important to highlight that the work done by the contact impulse to time t_i represents the energy dissipated in case of non-smooth motion with impact. The impacts are considered completely inelastic and as a result of them there is a loss of energy in the system.

The NSCD method is therefore characterized by three main factors

(i) Non-smooth contact laws are directly integrated into it,

(ii) Use an implicit integration scheme

(iii) Damping is not considered.

The development of the model requires some simplifications, it is assumed that the bodies are perfectly rigid and that the contact between them is governed by laws of impenetrability (Signorini's law) and friction (Coulomb's law). These laws lead to perfectly plastic impacts, without bounces (zero value of Newton's restitution coefficient) favoring the computational burden. An additional advantage due to the perfectly plastic impact is related to the dissipation of energy, explains the damage to the material and the microcracks that form on the stones after the impact. The energy dissipated by these models does not take into account damping but is determined by friction.

2.2.2. DISCRETE ELEMENT METHOD

The displacement of the blocks, in the Discrete Element Method (DEM) implemented by Cundall et al. [29,30,71] is calculated in finite and small time steps through the explicit numerical integration of the equations of motion. Following contact, the contact algorithm recognizes it and returns a unit normal vector (contact normal) and defines the plane along which the sliding takes place. As the blocks keep moving, the normal unit changes all the time. When a face of a rigid block is in contact with the plane in common, this is automatically discretized into sub-contacts (triangular faces). The basis of the calculations is the relative velocity v_i of the sub-contacts, defined as:

$$v_i = v_i^V + v_i^F \tag{2.2.2.1}$$

Where v_i^V is the velocity of the analysed node and v_i^F is the velocity of the corresponding point of the opposite face on the other block, this is calculated with linear interpolation. The translation vector Δ_{u_i} belonging to the sub-contact is defined as:

$$\Delta_{u_i} = v_i \Delta t \tag{2.2.2.2}$$

Where Δt is the length of the time step.

The normal forces and the shear forces belonging to the sub-contact is defined from the equations:

$$\Delta F_n = -K_n \Delta_{u_n} A_c \tag{2.2.2.3}$$

$$\Delta F_{s.i} = -K_s \Delta_{u_{s,i}} A_c \tag{2.2.2.4}$$

Where K_n is the normal stiffness and K_s is the shear stiffness of the contact, instead A_c is the area of the sub-contact. When two blocks come together, it is equivalent to two sets of sub-contacts in parallel, each of which has sub-contact forces. The behaviour of the interface will be given by the average of the two sets.

2.2.2.1. Constitutive model for contacts

Parameters such as friction angle, cohesion, finite tensile strength and stiffness defined in normal and shear direction define the mechanical behaviour of contacts in DEM models (**Figure 13**).

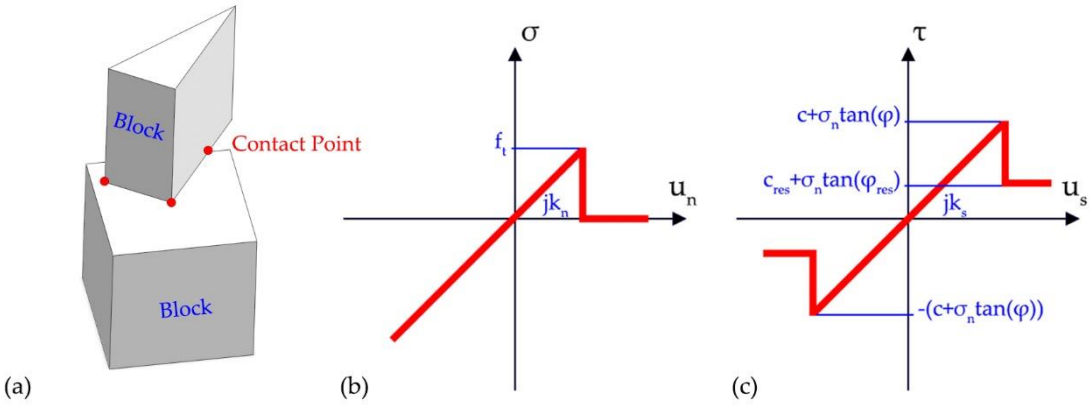

***Figure 13** – Mechanical representation of contact point between blocks (a), contact constitutive law in tension (b), and in shear (c).*

The deformability of the blocks is represented by the contact stiffness [48]. In the normal direction, in the case of mortar joints, the rigidity can be directly related to the thickness of the mortar or depend on the rough and irregular surfaces in the case of

dry joints. Shear stiffness plays a similar role, and Coulomb friction dictates a limit to the shear stress of the sub-contact.

When we are in the elastic range there is no sliding and separation between the blocks and the behaviour is regulated by the normal K_n and shear K_s stiffness of the joints:

$$\Delta\sigma_n = K_n \Delta_{u_n} \tag{2.2.2.5}$$

$$\Delta\tau_s = K_s \Delta_{u_s} \tag{2.2.2.6}$$

Where:

- $\Delta\sigma_n$ is the normal force (resultant for the sub-contact),
- $\Delta\sigma_s$ is the shear force (resultant for the sub-contact)
- K_n is the normal stiffness of the joint,
- K_s is the shear stiffness of the joint,
- Δ_{u_n} is the normal displacement increments belonging to the sub-contact
- Δ_{u_s} is the shear displacement increments belonging to the sub-contact.

In the joints, the constitutive model of Coulomb friction with breakage by shear and traction is used. The force of the joint is controlled by the tensile strength f_t and the maximum shear force τ_{max}:

$$\sigma_n \leq f_t \tag{2.2.2.7}$$

$$\tau_s \leq c + \tan(\varphi) = \tau_{max} \tag{2.2.2.8}$$

Where φ is the friction angle.

2.2.2.2. Solution algorithm

An explicit time-step algorithm is used, for each node of rigid block the equations of motion are:

$$m\frac{\dot{u}_i}{dt} + \alpha m\dot{u}_i = \sum f_i \tag{2.2.2.9}$$

Where:

- u_i is the nodal displacement vector of a node,
- m is the nodal mass,
- α is the mass-proportional viscous damping constant,
- $\sum f_i$ is the total nodal force given by a sum of contact forces, nodal forces and external loads (including gravity).

The **Figure 14** represents the dynamic calculation scheme for rigid blocks. To avoid numerical instabilities, for each node a limit time step is evaluated by analogy with a simple system of degrees of freedom in the form:

$$\Delta t = 2f_R\sqrt{\frac{m}{K_n}} \tag{2.2.2.10}$$

Where K_n is obtained by adding all the rigidities of all the elements and contacts that are connected to the node. Using the fraction of the critical time-step f_R it is possible to reduce the duration of the time-step.

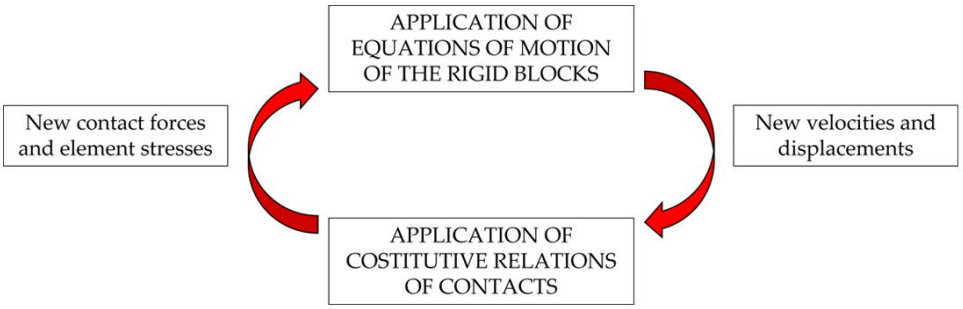

Figure 14 *– Cycle of mechanical calculation.*

2.2.2.3.Damping and numerical stability

To perform the dynamic analysis, it is usually necessary to account for energy dissipations that take place in the real physical system, due to heat or hysteresis phenomena, but that are not represented in the numerical algorithm. In 3DEC© code damping is applied also to limit the false oscillations of the mechanical system that comes from the explicit nature of the time-integration scheme implemented, and as a tool to reach the equilibrium state for each step in less time possible. Between the different possibilities that are available to model damping [72], using the global damping technique is possible. to obtain a shorter computational effort to find the equilibrium state. More in detail, adaptive global damping can be implemented, based on the use of viscous forces, in which viscosity is continuously updated to maintain constant the ratio of the power dissipated by damping with respect to the rate of change of kinetic energy in the system. For those reasons, adaptive global damping was used.

3 | COMPARISON BETWEEN CONTINUOUS AND DISCONTINUOUS APPROACHES ON THE ACCUMOLI CIVIC TOWER AND THE PALACE OF PODESTÀ

3.1. INTRODUCTION

In this chapter, advanced numerical models are used to study the progressive damage of a historic building, namely the Palace of Podestà and the Civic Tower of Accumoli located in Rieti province, Lazio region. The dynamic behaviour of the structure is analyzed following important seismic events such as those that occurred in 2016-2017 [73,74]. The Palace and the Civic Tower are placed in Seismic Zone 1 (ref. PCM Ordinance No.3274/2003), this area is catalogued as a high seismicity zone as represented in **Figure 15**.

The primary goal of this thesis is to assess how structural units interacting with each other affect the buildings' response during an earthquake. For this purpose, to investigate the interactions, two different models are created, one for the entire structure and the other for just the tower.

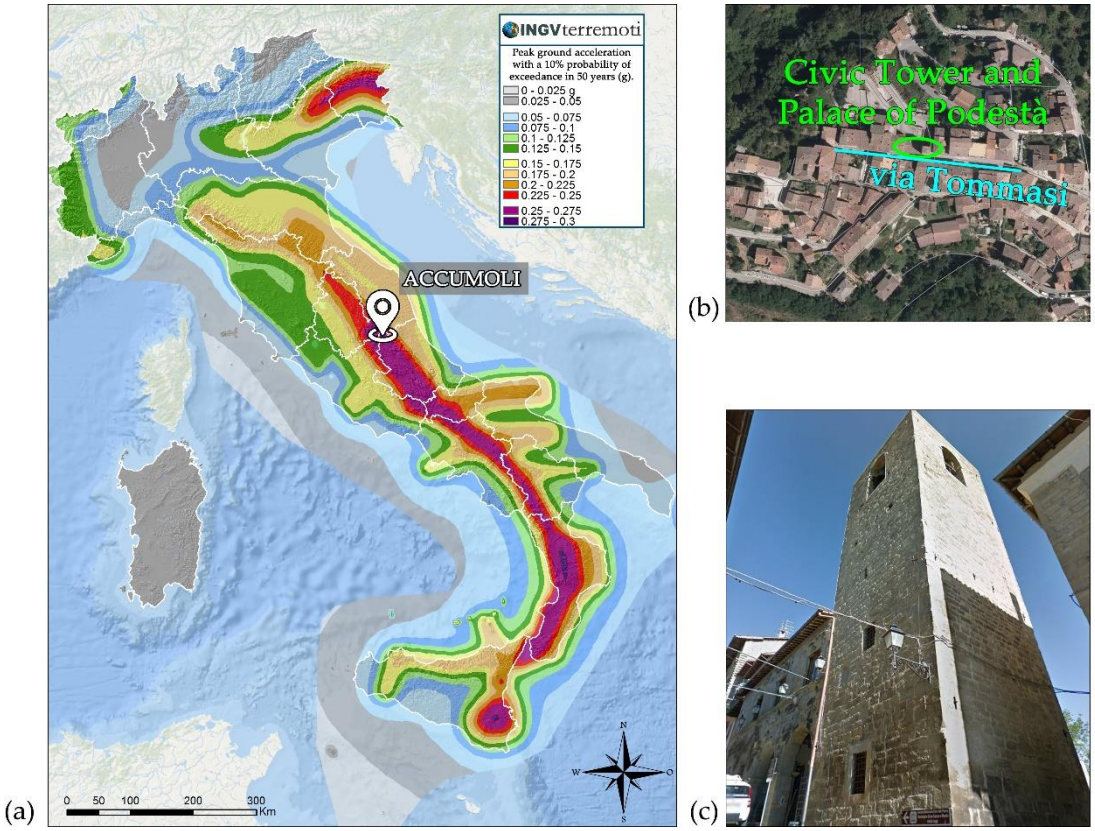

Figure 15 *– Geographical location of the Civic Tower and the Palace of Podestà (Accumoli, Rieti, Italy) (a,b) on the seismic hazard map (http://www.ingv.it/it/) and a view of the Civic Tower and the Palace of Podestà (c).*

3.2. CHARACTERISTICS OF THE CIVIC TOWER AND THE PALACE

Accumoli dates back to 1211, the territory was initially much larger than the current ones it included several municipalities. During the early years, the territory had been under the dominion of the Kingdom of Naples but, at the same time, it was very close to the State of the Church. Over the years it had to defend itself from different tyrants and its territory was reduced.

In the mid-600s it became a possession of the Medici dynasty but quickly returned to the Kingdom of Naples. The troubling events were followed by periods of prosperity during which the noble families of the time built great-value constructions.

At the heart of this small village, there is the case study of this work, i.e. the Civic Tower of Accumoli and the adjacent Podestà Palace. The Tower dates to the twelfth century, and it is unique in the entire Tronto's valley. It is located in via Tommasi, featuring a square plan measuring 6.15x6.15 m with walls of 1.20 m thickness at the base and 1.00 m at the top. In elevation, the maximum height exceeds 20 m (**Figure 16**). It shows four single-arch windows in correspondence od the bell-cell, and three embrasures along the height. Inside there is one cross vault in masonry, instead, the roof is realized in reinforced concrete. The bearing structure consists of multi-leaf walls [75,76], the perimeter curtains are in cut stones and the inner core is in irregular stones.

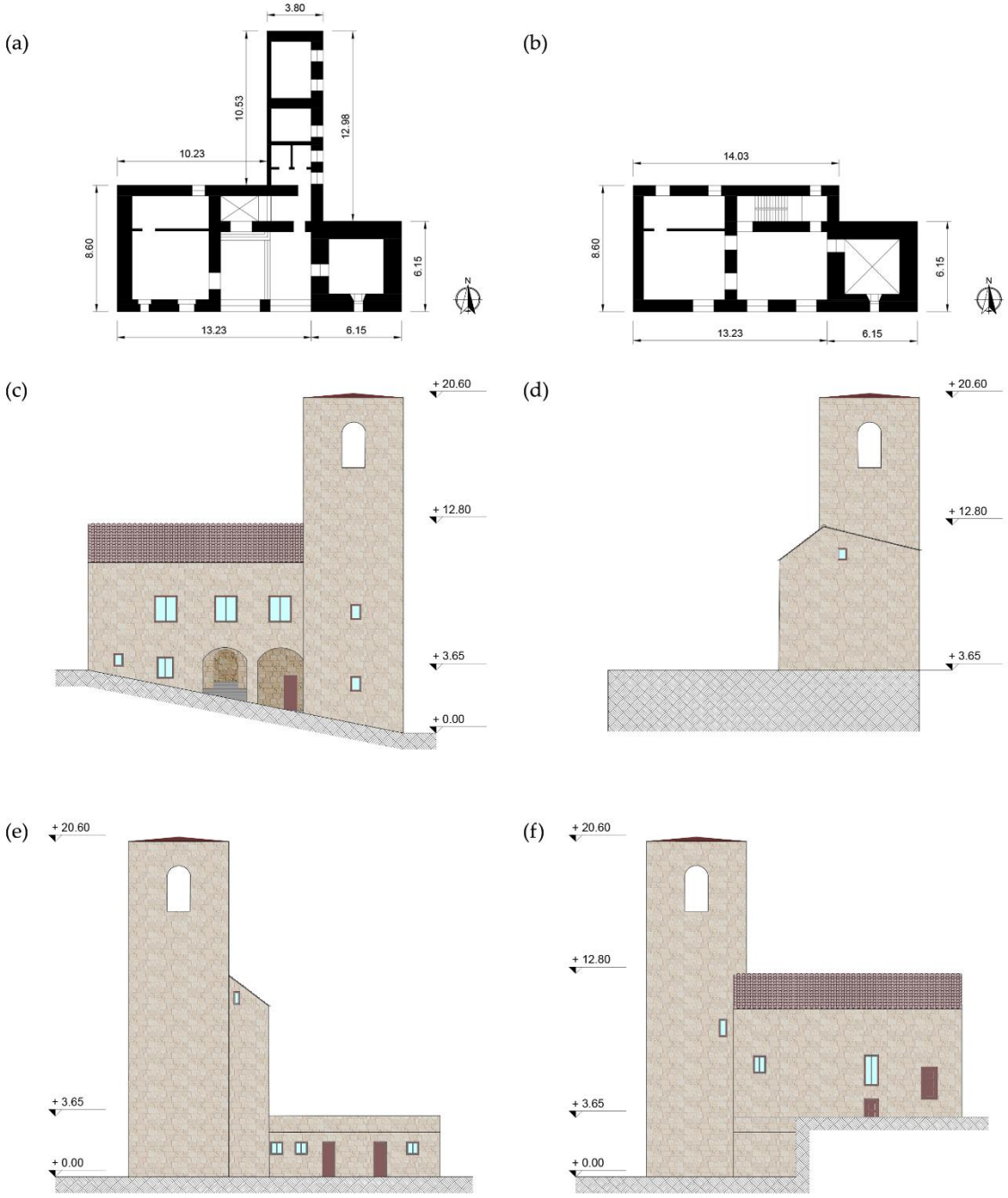

Figure 16 – *Ground floor (a), First floor (b), North façade (c), West façade (d), East façade (e) and South façade (d). (All dimensions are in meters).*

Next to the tower, there is the Palace of Podestà. It dates to the thirteenth century and it is the oldest structure in Accumoli village. The palace has a rectangular plan of

8.6x16 m dimensions and a maximum height of 12.00 m. It consists of ground and noble floors. In the latter, there are architrave windows, instead in the ground floor there are two arched openings, typical of medieval public buildings. The bearing structure is made of square and smooth sandstone ashlars. (**Figure 17**). Except for a masonry cross-vault on the stairwell, all the slabs are realized with wood. On the north side of the palace, there is a little annexe of one floor. It has a rectangular plant of 10x3.8 m.

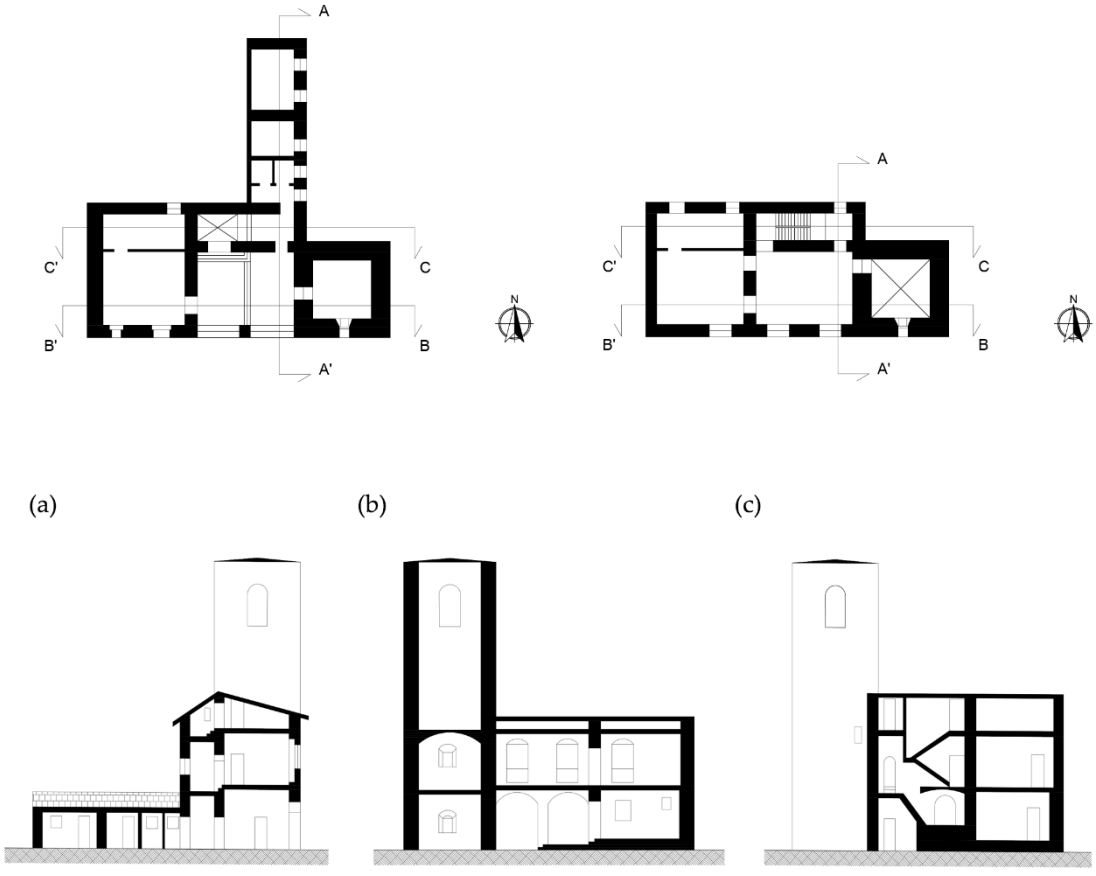

***Figure 17** – Section A-A'(a), section B-B'(b), section C-C'(c) of the Civic Tower and the Palace.*

3.3. DAMAGE SUFFERED FOLLOWING THE CENTRAL ITALY EARTHQUAKE

The structure showed deep cracks following the earthquake, the part more involved in the damage was the tower, as seen in **Figure 18**.

It showed a torsion-flexural deformation on its upper part, sub-horizontal cracks, masonry disaggregation on the roof's support surface and spread diagonal cracks in each bell-cell corner.

Before the last strong quake occurred the 30th of October, the firefighter secured it, they enclosed the tower with a system of ties and wood elements to avoid its collapse (**Figure 18f**).

The Palace, on the other hand, is less damaged, the part most affected by the seismic sequence is the one in correspondence with the main façade where there are cracks near the openings as shown in **Figure 18e**.

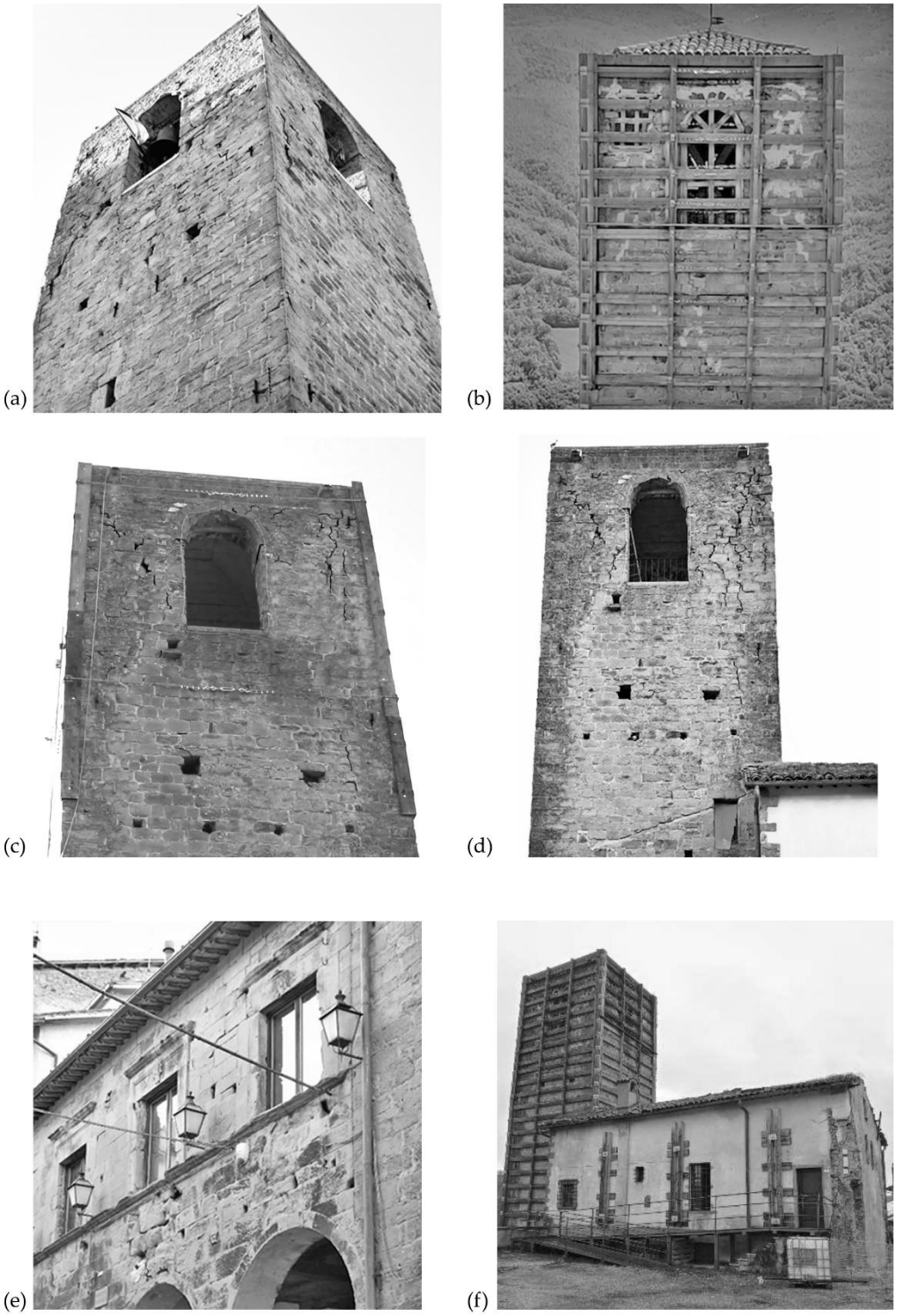

***Figure 18** – Damage suffered by the structure following the Central Italy Earthquakes. Bell-cell North (a), West (b), East (c) and South (d) façade; Podestà Palace North façade (e) and securing by fire fighters (f).*

3.4. NUMERICAL MODEL

To better study the behaviour of the Tower and the Palace and investigate different possible scenarios, two different numerical models were used. The first model represents the Palace and the Tower (Model 1), while in the second only the Civic Tower (Model 2) is modeled.

In the Continuous Model (CM), the structure's geometry, which reported each structural element and the main openings, was meshed with 3D 4-nodes solid brick elements with 0.4 m of average dimension (**Figure 19a**). The Model 1 (CM) had 92986 elements, 23091 nodes and 69276 degrees of freedom , meanwhile, Model 2 (CM) had 57780 elements, 13123 nodes and 39372 degrees of freedom. It was realized with the commercial software MIDAS FEA NX© employed the Concrete Damage Plasticity Model to define the masonry response.

In the Discontinuous Models (DMs), it is not possible to represent the texture automatically using e.g. tools present in the CAD codes, for this reason, the first step was to represent the arrangement of the blocks in 2D and subsequently extrude the 2D lines the 3D numerical model was obtained.

Both models use blocks of regular convex shapes and different sizes, the size of the blocks has been approximated to obtain a fair compromise between a good degree of detail and a not too expensive computational burden. The joints placed between the bricks have zero thickness, the blocks in fact represent both the mortar and the brick as a single element.

In addition, as regards the tower, as shown in **Figure 19e** in both models we chose to consider three layers, two external ones characterized by regular stones and an internal rubble masonry one (**Figure 19g**). This layer has also been built to such a size as to obtain acceptable computational burdens.

Model 1 (DM) had 6800 blocks, meanwhile, Model 2 (DM) had 4025 blocks. In Both models, the dynamics response of the structure is studied with the open-source software LMGC90©, considering the Non-Smoot Contact Dynamic (NSCD)

implemented on it and with the Distinct Element Method (DEM) implemented in 3DEC© code.

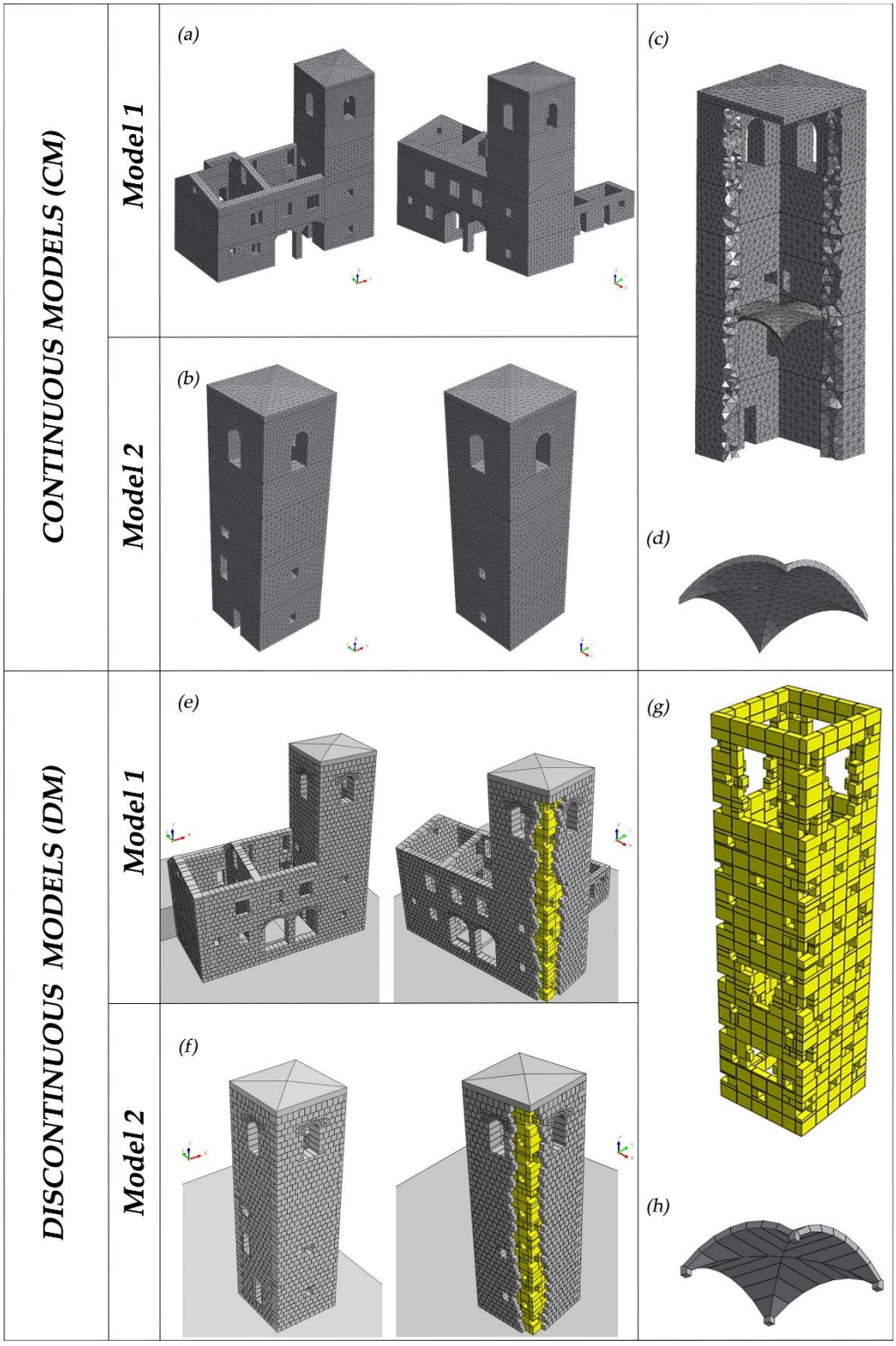

Figure 19 *– Continuous models (a-d) and dicontinuous models (e-h).*

3.5. MATERIAL PROPERTIES

The mechanical parameters adopted are in line with the Italian code [77,78] it should be specified that it was not possible to carry out tests on materials, nor a dynamic identification to identify in a non-invasive way some parameters of the structure such as the elastic modulus.

As for the continuous models, the mechanical parameters are shown in **Table 1**.

Two materials were defined: one for the complex and tower body and one for the bell cell. Observing the structures and the cracks that occurred, it was evident that the quality of the masonry was good in the Podestà Palace and annex, but also in the tower body, although the latter had an inner core. For these reasons, they were assigned the material "Good Masonry" (**Table 1**). Instead, the bell cell, due to its exposition to the atmospheric agents, showed a reduction of the mortar in the joints, which was simulated by lowering its non-linear parameters "Bad Masonry" (**Table 1**). Finally, the roof was assigned the elastic parameters of the concrete. The non-linear parameters of the concrete were not defined since no damage was observed on the roof during the earthquakes. The mono-axial tensile and compressive laws are shown in **Figure 7**. The yield surface parameters employed are shown in **Table 1**.

Table 1 – *Characteristic of the mechanical parameters used for the numerical analyses of the continuous approach in both configurations.*

MODEL 1 (CM), MODEL 2(CM)		***Good Masonry***	***Bad Masonry***
Young's Module	*[MPa]*	*2800*	*2800*
Poisson's Module	*-*	*0.25*	*0.25*
Mass	*[kN/m³]*	*22*	*22*
Strength in Compression	*[MPa]*	*8.0*	*5.6*
Strength in Tension	*[MPa]*	*1.6*	*0.46*
Dilation angle ψ	*-*	*10°*	*10°*
Correction Parameter k_c	*-*	*0.666*	*0.666*
Eccentricity ε_{eccen}	*-*	*0.1*	*0.1*
Biaxial strength ratio f_{b0}/f_{c0}	*-*	*1.16*	*1.16*
Viscosity	*-*	*0.1*	*0.1*

As regards discrete approaches, the parameters shown in **Table 2** were used in both methods.

Table 2 – *Characteristic of the mechanical parameters used for the numerical analyses of the discontinuous approach in both configurations.*

MODEL 1 (DM), MODEL 2(DM)		***NSCD***	***DEM***
Density ρ	*[kg/m³]*	*2200, 1900*	*2200, 1900*
Joint friction μ	*-*	*0.3, 0.5, 0.9*	*17°, 27°, 42°*
Joint normal stiffness Jk_n	*[Pa/m]*	*-*	*7.67e9, 2.67e10*
Joint shear stiffness Jk_s	*[Pa/m]*	*-*	*3.07e9, 1.07e10*
Joint cohesion Jcoh	*[Pa]*	*-*	*0.1e6*
Joint tensile strength Jten	*[Pa]*	*-*	*0.1e6*

The blocks were considered as rigid, a density of 2200 kg/m^3 was assigned to the blocks of the external layers of the tower and to those of the building, only the blocks of the internal filling of the tower instead were assigned a density of 1900 kg/m^3, furthermore for the roof a density of 2500 kg/m^3 was used.

Given the regular texture of the arrangement and the blocks, in accordance with [53] and with the Italian code [80] a value of friction coefficient between the blocks equal to:

- 0.5 between the contacts of the blocks of the external layers of the tower and between the contacts of the tower and the palace,
- 0.3 between the contacts of the blocks of the internal layer of the tower and between the contacts of the internal layer with the external ones,
- 0.9 between the contacts of the blocks of the tower and the palace with the foundation.

In particular, a coefficient of friction value of 0.3 was used to characterize the rubble masonry and thus reproduce a mortar of poor quality.

The Mohr-Coulomb policy implemented in the 3DEC© calculation code requires other parameters at the interfaces. To the values of the coefficient of friction described above must be added other parameters, about the value of Joint normal stiffness values equal to:

- 2.67e10 Pa/m between the contacts of the blocks of the outer layers of the tower and between the contacts of the tower and the palace,
- 7.67e9 Pa/m between the contacts of the blocks of the internal layer of the tower and between the contacts of the internal layer with the external ones.

While about Joint shear stiffness values equal to:

- 1.07e10 Pa/m between the contacts of the blocks of the outer layers of the tower and between the contacts of the tower and the palace,
- 3.07e9 Pa/m between the contacts of the blocks of the internal layer of the tower and between the contacts of the internal layer with the external ones.

Finally, to the joint cohesion and the joint tensile strength a value of 0.1e6 Pa, although these assume small values, it has been seen that they can influence the displacement capacity.

3.6. APPLICATION LOADS

First of all, the behaviour of the structure subjected only to gravitational loads was studied, subsequently, to study the dynamic behaviour, a set of accelerations (continuous model) and velocity (discontinuous model) was applied to the base of the structure.

These were applied in the three main directions, i.e. two horizontal and one vertical (z-direction). Both speeds and accelerations were recorded by the reference stations of Amatrice (AMT) and Accumoli (ACC) during the 2016 Central Italy seismic sequence. For the first two events the choice fell on the nearby Amatrice station as in that of Accumoli the recordings were of poor quality.

In this work, the three most important events were considered:

- **24th August 2016 in Amatrice** with $M_L = 6.0$ and $M_W = 6.0$ (AMT station in Italian Accelerometric Archive (ITACA)),
- **26th October 2016 in Amatrice** with $M_L = 5.9$ and $M_W = 5.9$ (AMT station in Italian Accelerometric Archive (ITACA)),
- **30th October 2016 in Accumoli** with $M_L = 6.1$ and $M_W = 6.1$ (ACC station in Italian Accelerometric Archive (ITACA)).

The base of the structure was exited by a seismic action with a total duration of 34 seconds. For each event, we considered the 10 seconds of strong motion and 2 seconds of zero speed between one event and another. The speeds and accelerations applied to the base of the structures are shown in **Figure 20**.

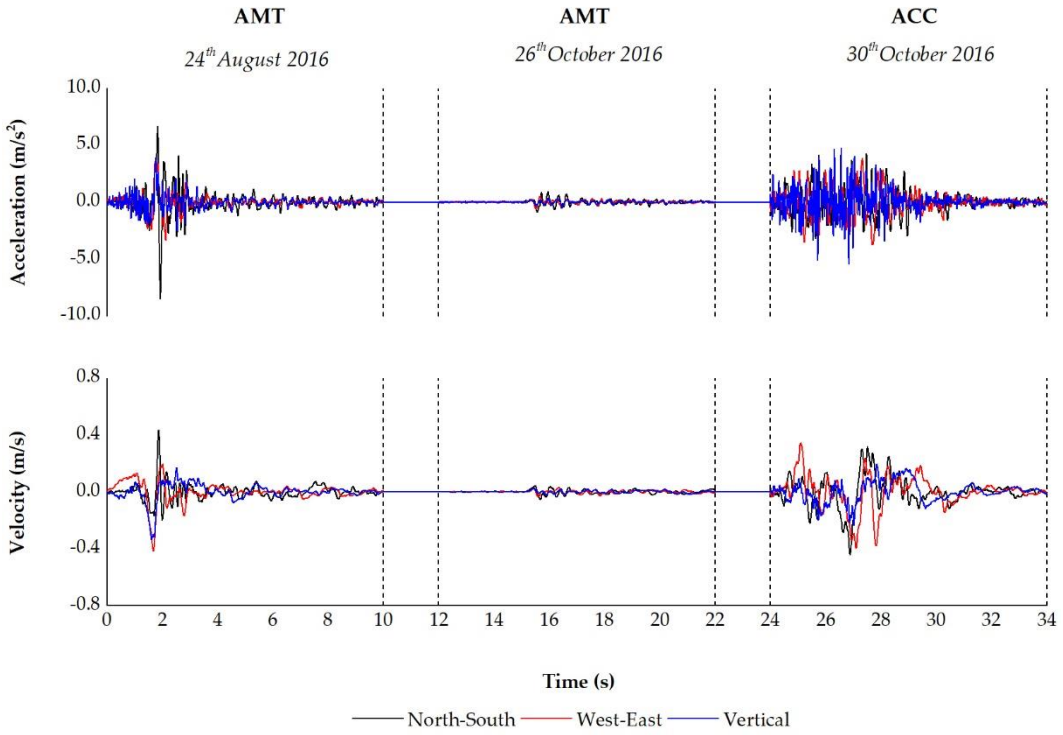

Figure 20 – *Acceleration and velocity of strong motion recorded by the Amatrice (AMT) and Accumoli (ACC) stations.*

Table 3 shows the characteristics of the main seismic events of the last few decades in Italy recorded in Amatrice (AMT) and Accumoli (ACC) stations.

***Table 3** – Characteristic of main earthquakes recorded in Amatrice (AMT) and Accumoli (ACC) stations during the Central Italy earthquake in 2016, where (*) indicates that site classification is not based on a direct $V_{s,30}$ measurements.*

Seismic Event		M_L	*Depth*	*Station*	*Class EC8*	R_{jb}	R_{rup}	R_{epi}	*Channel NS PGA*	*Channel EW PGA*	*Channel UD PGA*
[-]		*[-]*	*[km]*	*[-]*	*[-]*	*[km]*	*[km]*	*[km]*	*[cm/s²]*	*[cm/s²]*	*[cm/s²]*
1st	***24/08/2016***	*6*	*8.1*	*AMT*	*B**	*1.38*	*4.62*	*8.5*	*368.39*	*-850.8*	*391.37*
2nd	***26/10/2016***	*5.9*	*7.5*	*AMT*	*B**	*25.93*	*26.09*	*33.3*	*-58.55*	*90.74*	*-49.11*
3rd	***30/10/2016***	*6.1*	*9.2*	*ACC*	*B**	*35.33*	*35.32*	*47.1*	*-122.44*	*75.95*	*-44.07*

where [79–81]:

- R_{jb}, is the Joyner-Boore distance, known as the smallest spacing from the site to the surface projection of the rupture surface,
- R_{rup}, is the shortest distance between the site and the rupture surface,
- R_{epi}, is the distance estimated by the geometric swap.

3.7. NUMERICAL RESULTS

The numerical models' results are compared in terms of displacements (**Figure 22** and **Figure 23**) and damages (**Figure 24** and **Figure 25**). For this purpose, four control points along the external roof's perimeter were considered: two on the tower (P_1 and P_2), and two on the palace (P_3 and P_4), as shown in **Figure 21**.

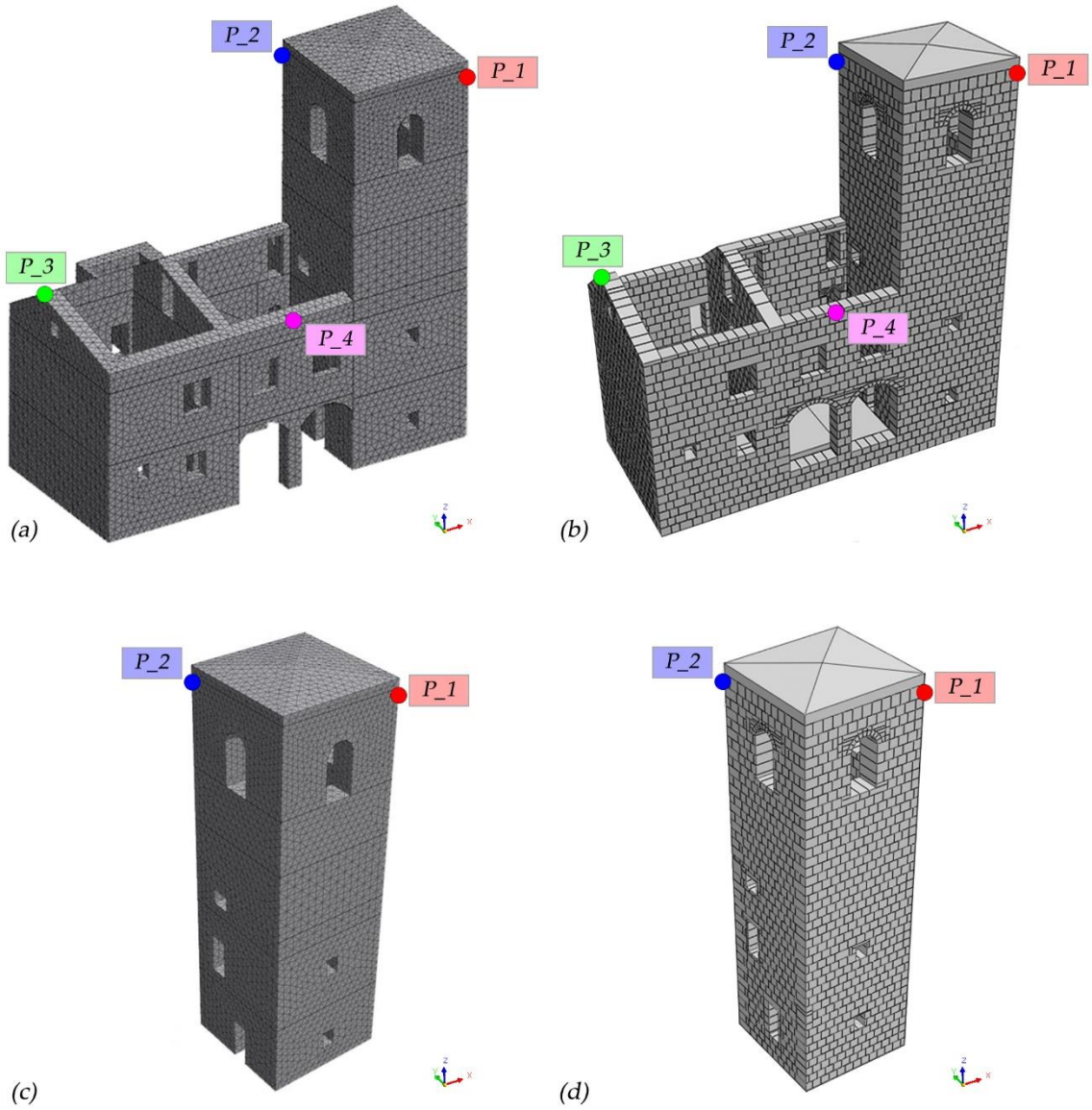

Figure 21 *– Control points in the continuous (a,c) and discontinuous (b,d) approach.*

The time histories of the Model 1 (actual configuration) have similar trends for each software utilized (**Figure 22** and **Figure 23**).

The points that record the major displacements are those on the tower, P_1, and P_2, especially in the X and Y directions. At the end of the first event of 24th August, the X and Y residual displacements of P_1 are equal to 0.05 m/0.02 m in CM, 0.07 m/-0.1 m with DEM and 0.04 m/-0.07 m with NSCD. Moreover, P_2 values are 0.05 m/0.01

m in CM,-0.07 m/0.02 m with DEM and -0.08 m/0.01 m with NSCD. Contrary to the second event, which didn't worsen the situation, the earthquake of 30th October increased the structure's damage. At the end of the sequence, the residual displacements of the P_1 are 0.05 m/0.08 m in CM, 0.21 m/-0.20 m with DEM and 0.15 m/-0.13 m with NSCD. Instead, the ones measured in P_2 are 0.05 m/0.06 m in CM,-0.17 m/0.06 m with DEM and-0.20 m/0.10 m with NSCD.

For what concern the Podestà Palace, the displacements were smaller than the tower ones. Their plastic displacements are close to zero in the CM and in a range of 0.003 m and 0.01 m, considering the values in modulus, in the DMs and at 34 seconds.

The residual displacements of the Model 2 (**Figure 22** and **Figure 23**) in the CM are lower than those of the entire structure. Indeed, the percentage of completely damaged volume in the tower is 4.5% when it is isolated, and 10.4% when the palace is considered. In the DMs, observing the graphs, a fast evaluation of that is impossible. In the X-Direction, the plastic deformations of P_1 are reduced while those of P_2 are comparable with those of the Model 1. Otherwise, along the Y-direction, both points measure larger displacements than in previous analyses, with the only exception of that of P_1 obtained with NSCD, which is slightly lower. To analyze if the tower reported major or minor plastic displacements at the end of the sequence, compared to the previous model, the resultant displacements, considering the X and Y values, are calculated. In the Model 1, these were measured in P_1 0.29 m and 0.20 m using DEM and NSCD, respectively, and the P_2 0.18 m and 0.22 m. Instead, in the Model 2 these are in P_1 of 0.24 m and 0.22 m, and in P_2 0.25 m and 0.26 m. The resultant displacements show that if the tower were isolated, the angles would suffer from greater displacements, especially the P_2.

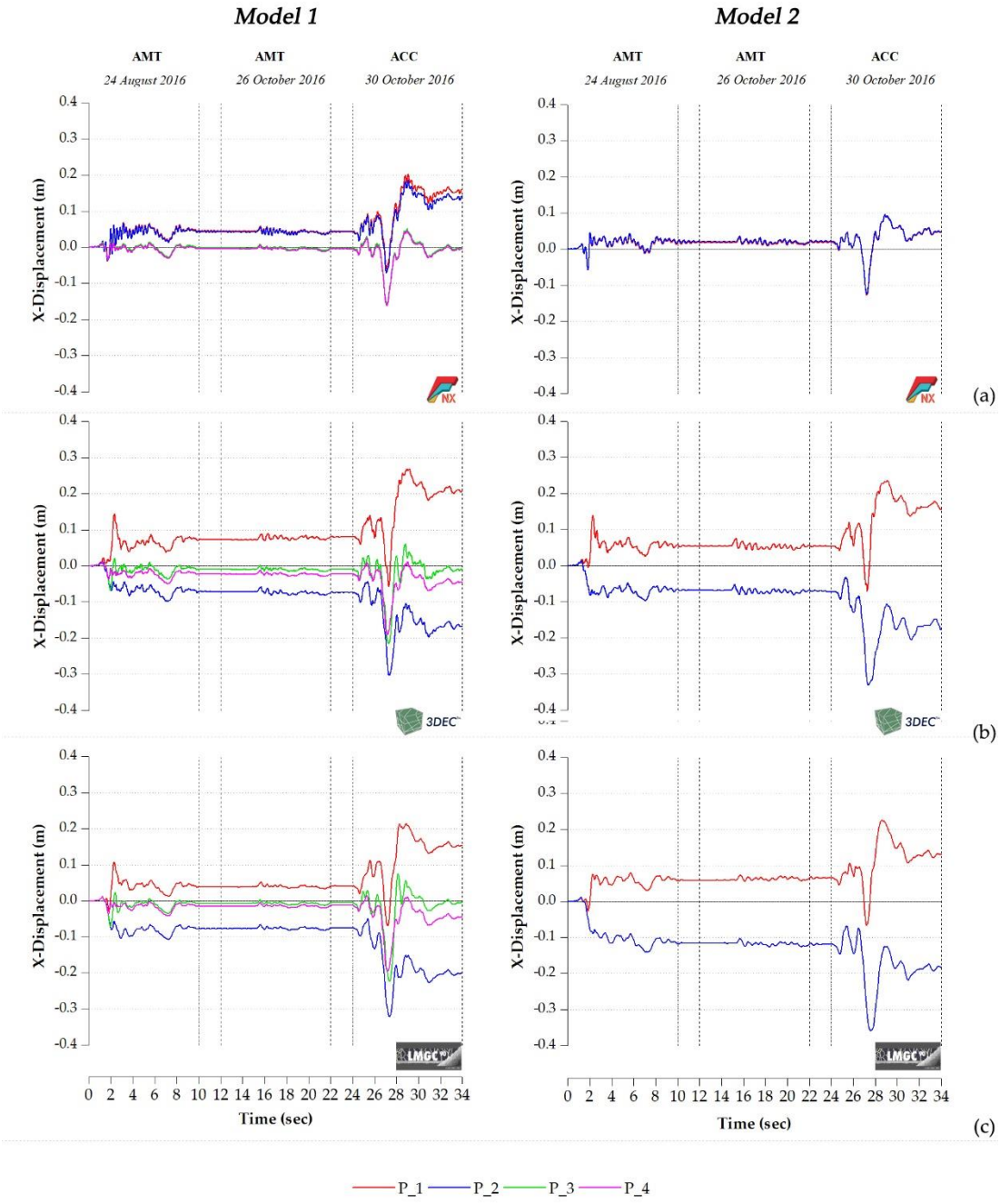

Figure 22 – *Comparison between Model 1 and Model 2 X-displacement's time histories, obtained with CM (a) and DMs (b, c).*

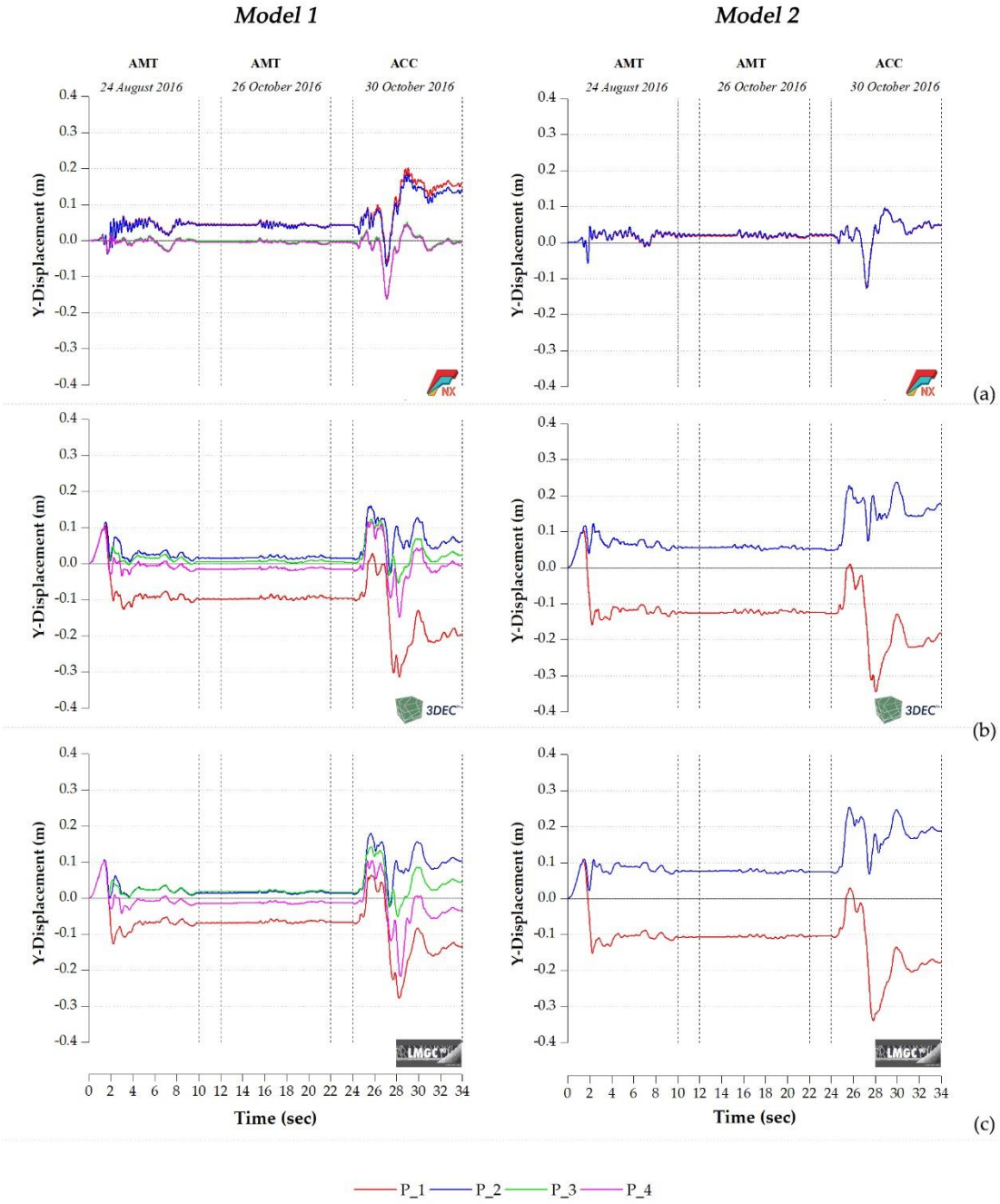

Figure 23 – *Comparison between Model 1 and Model 2 Y-displacement's time histories, obtained with CM (a) and DMs (b, c).*

The results in terms of damages for the Model 1 are plotted at the end of the each event (**Figure 24**). The DMs' results are very similar to each other, while there are differences between them and the CM. The discontinuous formulations allow the blocks to move in opposite directions, in contrast to the CM formulation. This is reflected in the numerical damage that shows in the CM the occurrence of horizontal cracks that go from the arched windows to the corners and in the DMs the starting of the out-of-plane mechanisms of the tower's angles.

For what concern the Podestà Palace, , the damages showed by CM and DMs are comparable.

In the case of the Model 2 (isolated Tower), the palace's presence reduces the walls' opening since the hinges' formation, of the corners' out-of-the-plane mechanisms, in Model 1 is higher than in the Model 2, see **Figure 24** and **Figure 25**. The CM, instead, shows the development of cracks at the base, as visible in **Figure 25**.

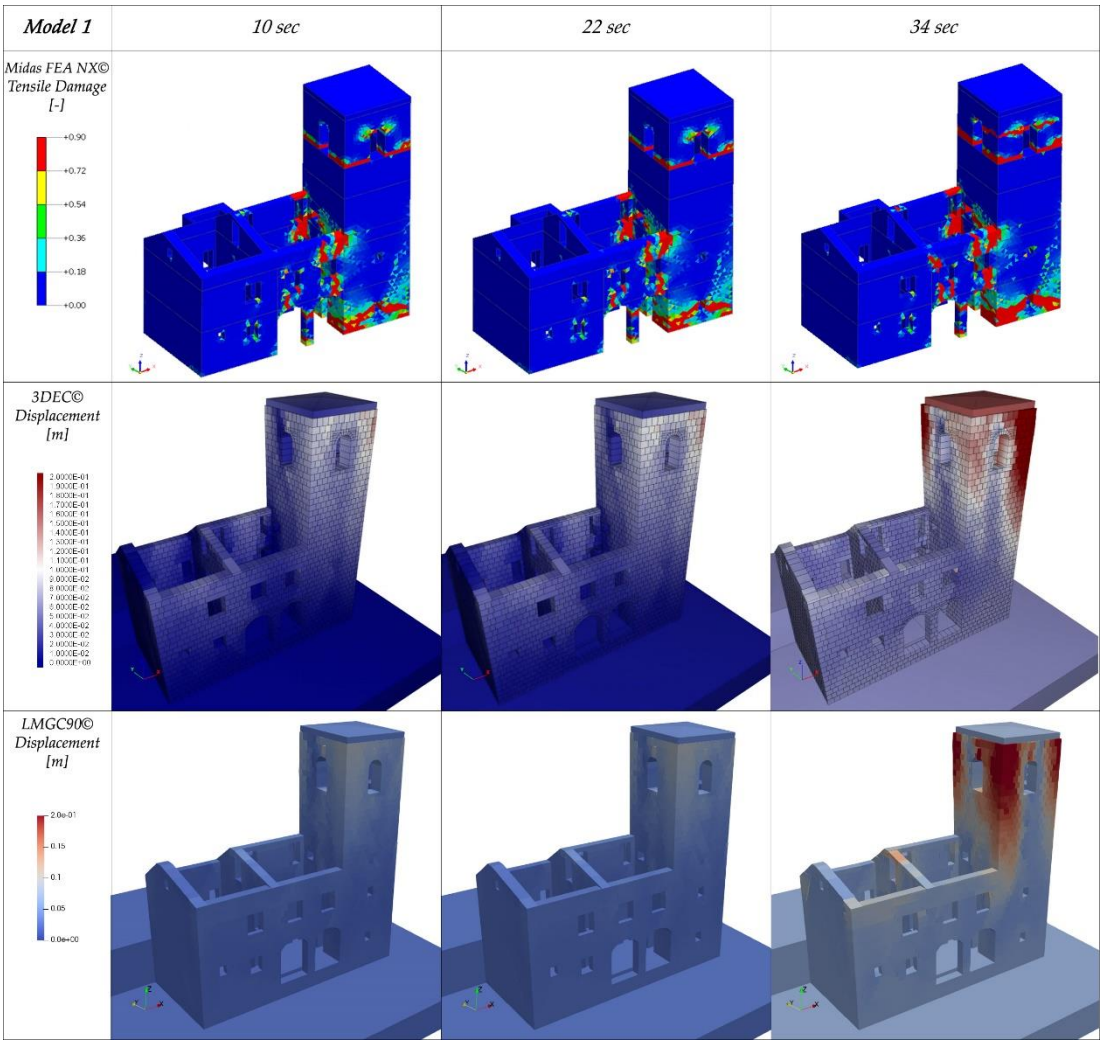

Figure 24 – *Damage at the end of each event obtained with the CM and DMs analyzing the whole structure (Model 1).*

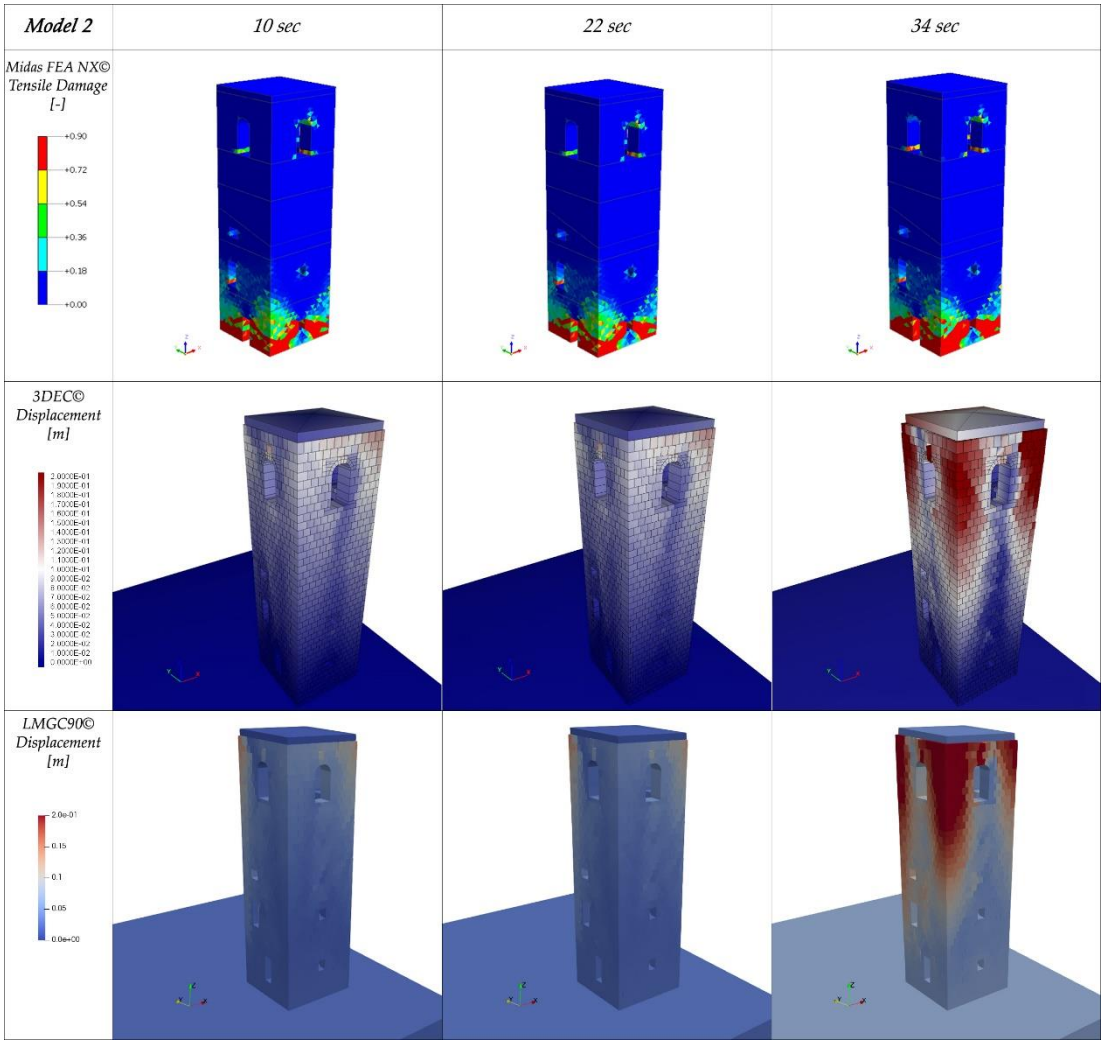

Figure 25 - *Damage at the end of each event obtained with the CM and DMs analyzing only the Civic Tower (Model 2).*

Comparing the damage obtained with the numerical models with those actually present on the building we observe that cracks are between the entrance openings and in the tower-palace connection like the actual ones (**Figure 26**). As a result, the cracks on the bell cell are fewer than those seen with the total model and are inconsistent with reality, as shown in **Figure 27**.

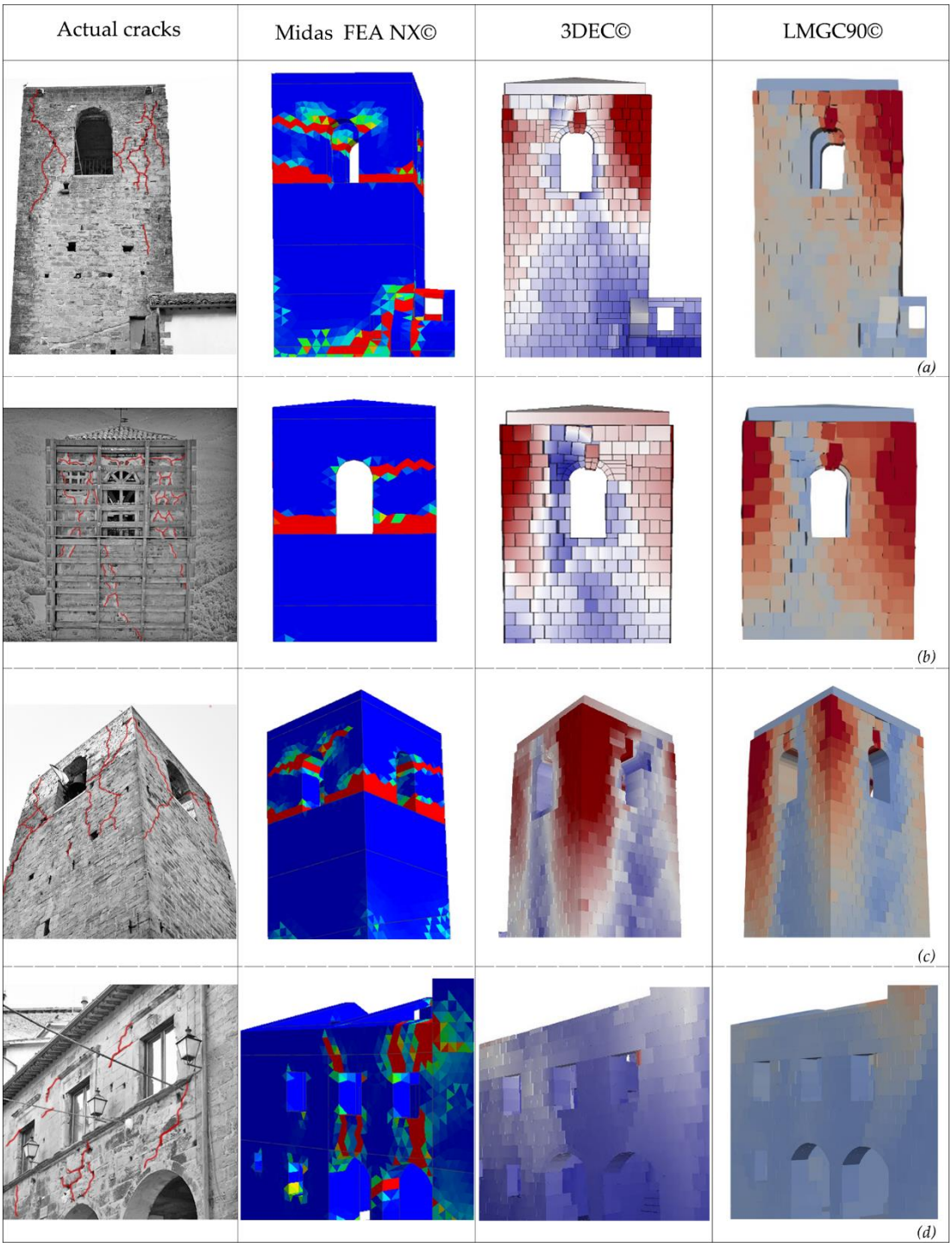

Figure 26 – *Comparison of the actual cracks and the numerical damage, obtained in Model 1 with CM and DMs. Bell-tower North façade (a), West-façade (b), South-East corner (c) and Podestà Palace South façade (d).*

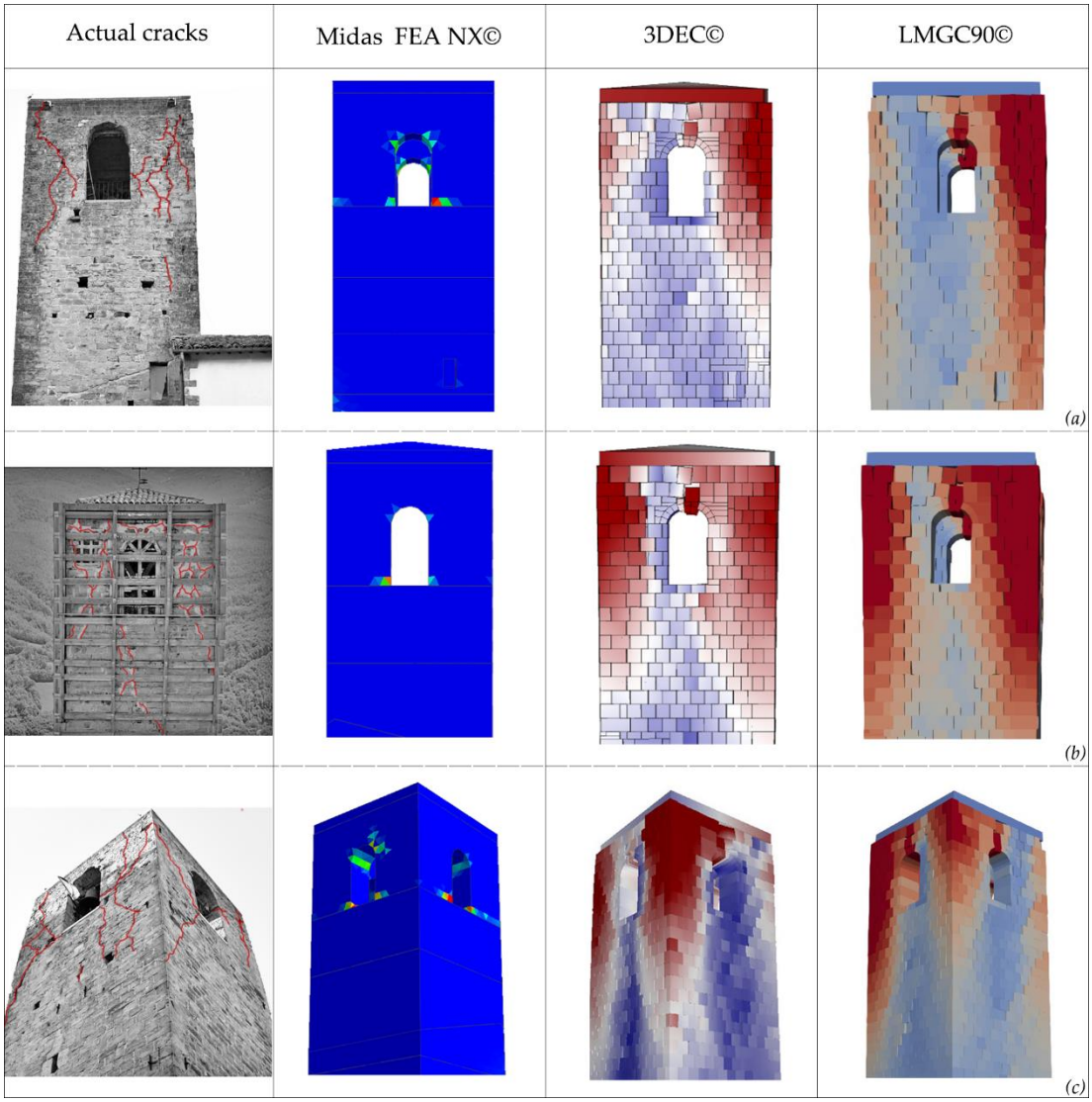

Figure 27 *– Comparison of the actual cracks and the numerical damage, obtained in Model 2 with CM and DMs. Bell-tower North façade (a), West-façade (b), South-East corner (c).*

4 | INFLUENCE OF THE STEREOTOMY IN THE ICONIC CASE OF THE AMATRICE CIVIC TOWER DURING CENTRAL ITALY SEISMIC SEQUENCE

4.1. INTRODUCTION

This chapter aims to investigate an aspect not yet very in-depth in the field of research, i.e., the role of erratic and rubble masonry.

Chaotic masonry has always been simplified with regular shapes [82,83], for this purpose, two different stereotomies of the stones present in the inner sack (rubble masonry) and some portions of the facades of the Tower (erratic masonry) have been reproduced of the iconic Civic Tower of Amatrice (Lazio Region, Italy).

At the same time, the role of retrofitting interventions on the dynamic behaviour of the Civic Tower was also evaluated, which following one of the most catastrophic events in Central Italy has not lost its load-bearing capabilities. In fact, it is one of the few structures in the municipality of Amatrice that has managed to cope with the tragic seismic sequence of Central Italy in 2016 thus becoming an iconic case (**Figure 28**).

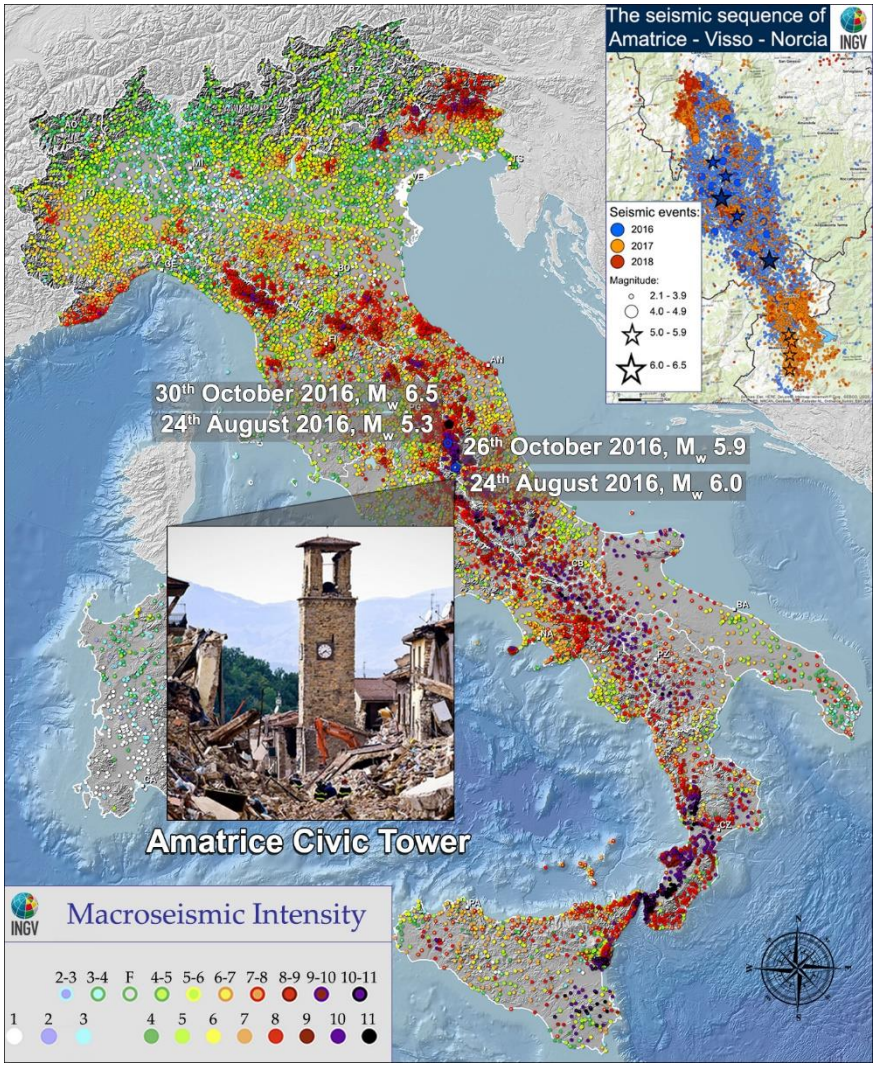

***Figure 28** – Position of the Amatrice Civic Tower in Lazio Region (Italy) in the Italian Macroseismic intensity map (http://www.ingv.it/it) with the position of the seismic events considered for the non-linear analyses.*

In addition to Norcia and Visso, Amatrice was the site of one of the epicenters that characterized the seismic sequence (**Figure 28**), this area is characterized by high seismicity falling into Seismic Zone 1 (ref. PCM Ordinance No.3274/2003).

4.2. THE AMATRICE CIVIC TOWER

The built heritage of Amatrice, for what concern the historical part, is generally constituted by masonry buildings having not more than three floors, often characterised by the presence of artistic cornices, arches and decorations. The quality of masonry and of its constructive details that can be found in the city is very heterogeneous, as it can vary a lot depending on the functionality of each structure and on its importance. The cultural heritage is very rich in terms of nobiliary palaces, monumental civic buildings such as the town-hall, or the Civic Tower, but particularly of churches.

All these buildings present in the communal territory, have undergone severe damage, or have been destroyed, by the 2016 seismic sequence [84].

4.2.1. HISTORICAL CONTEST

The Civic Tower is one of the most distinctive landmarks of Amatrice and became particularly famous for being one of the few historical buildings to not collapse completely after the 2016-2017 seismic sequence that affected central Italy, even though it reported several damages. The tower is located at the centre of Cacciatori del Tevere square, at the crossing between the two main streets of the town: Via Roma and Corso Umberto I (**Figure 29**).

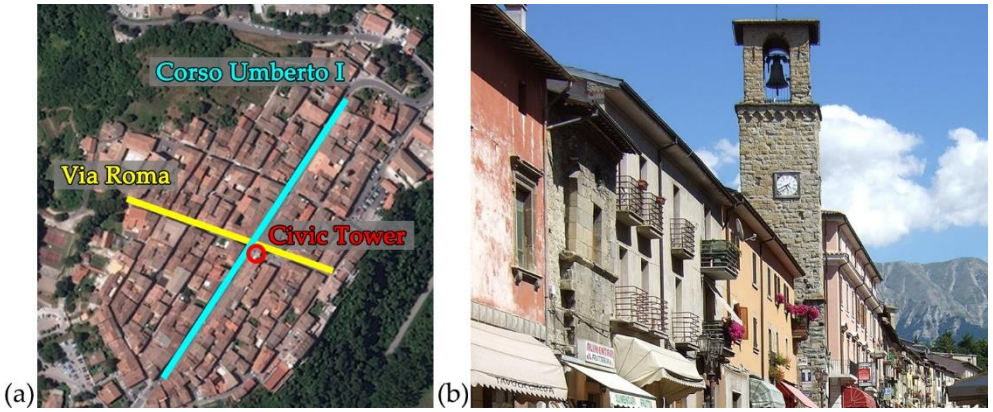

Figure 29 – *Location of the Civic Tower (a) and a photo of the tower before the Central Italy earthquake (b).*

Its origins are placed back to the medieval times, and specifically it was firstly mentioned in a document dated 1293. Originally the clock tower did not have a civic function, in fact the structure was intended as the belltower of the Church of Santa Lucia.

In 1684 the church was demolished by the feudal "lord" Alessandro Maria Orsini to give more space to the adjacent street, so the structure became an isolate tower. On this occasion, the base of the tower was reinforced, and a small annex was added on two sides. For the whole lifetime of the structure its behaviour gave cause for concern, especially due to the high oscillations caused by the bell ring (some documents report 0.20 m of maximum displacement at the top of the tower), and for this reason, starting from the XIX century, a lot of requests of intervention are documented. But probably the only consolidation intervention was carried out on the tower from 1979 to 1985, when, following the earthquake of the Alta Valtiberina (central Italy), significant damage and a vertical crack pattern was noticed to the tower. In 1985 the original bell of 1494 was replaced because it had undergone a crack during the restoration phases: a lighter one has been inserted in the tower to avoid high oscillations as in the past.

4.2.2. STRUCTURAL DESCRIPTION OF THE CIVIC TOWER

The civic tower of Amatrice has a rectangular plan of 4.00x5.30 m and a height of about 25 m. At the base, there is a small overhang leaning only two walls, to east elevation with a depth of 1.50 m, and to north elevation with a depth of 0.60 m. This annex houses the staircase leading to the entrance of upper floors (**Figure 30**).

Figure 30 *– View of the Civic Tower South façade (a), West façade (b), North façade (c) and East façade (d).*

In its vertical development there are three distinct areas marked by the reduction of the wall thickness. The first floor is located at about 9 m in height, and it is composed of smoothed stones on the outer side, falling 0.15 m in the wall thickness, while the second frame is located at the height of about 19 m, and it marks the passageway from the tower to the belfry. In its highest part, there is the bell cell which develops longitudinally for just over 5 m: it consists of four regular piers with dimension 0.90x0.80 m and with same openings on the opposite sides. In the top, Amatrice clock tower has a wooden pavilion roof (**Figure 31**).

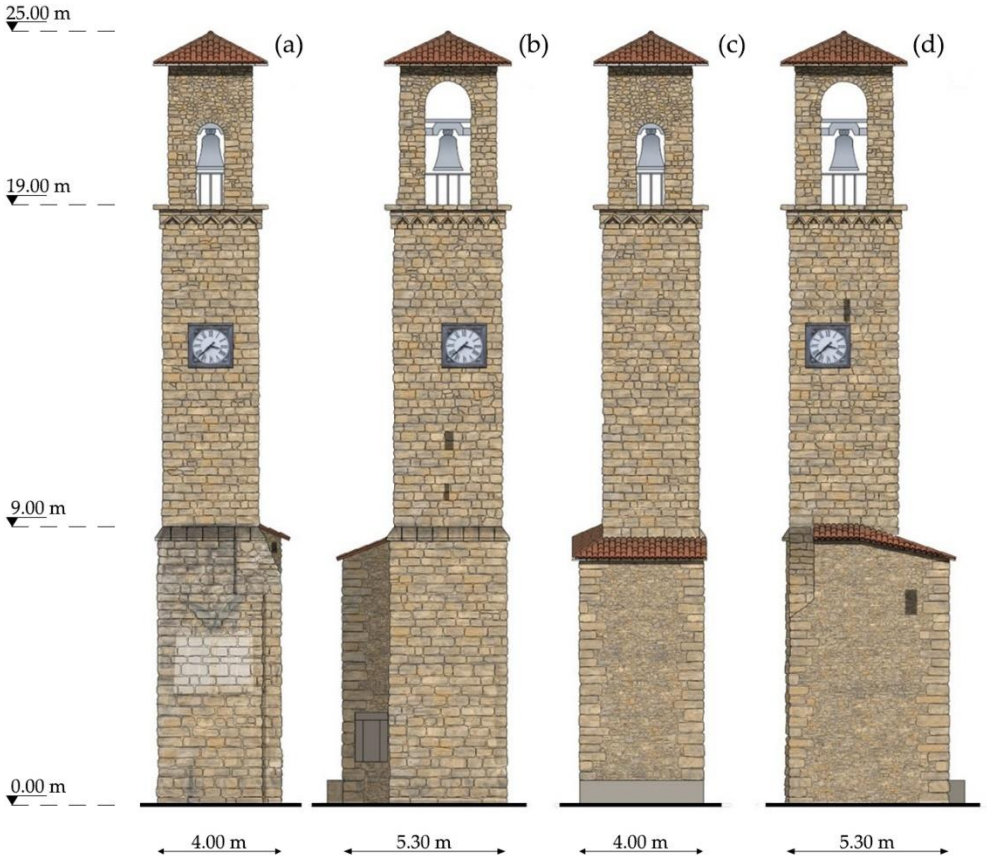

***Figure 31** – Drawing of the North façade (a), East façade (b), South façade (c) and West façade (d)*

The entire tower is made up of roughly squared blocks of local sandstone. These come in different sizes and are arranged on a regular basis for much of the tower, there is therefore a well-organized texture from the base to the piers of the belfry while the masonry above the arches in the terminal part of the tower appears to have a more chaotic and incoherent texture (**Figure 32**).

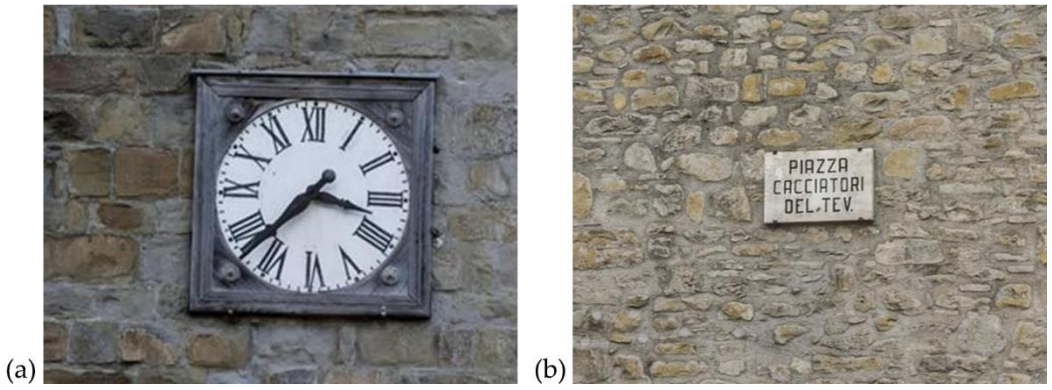

***Figure 32** – Comparison between regular masonry (a) made of square blocks and chaotic masonry present in the central part of the annex wall.*

Same thing in the annex at the base of the tower which presents large and square stones at the corners while internally the masonry has a disordered layout (**Figure 32b**).

The wall thickness at the base of the tower is not constant along the perimeter: the walls overlooking Corso Umberto I and his parallel have a thickness of 1.15 m, while for the other two walls the thickness is 0.95 m. The wall thicknesses are not constant even in height: each wall is 0.15 m thinner in the higher part of the tower, having as result walls with thicknesses of 1.00 m and 0.80 m respectively, up to the cell bell. For what concern the annex, realized in 1684, a small amount of information was available.

Moreover, it was assumed to contain a full masonry wall below the staircase, for its whole thickness. The only confirmed data regarding the annex, obtained from the historical drawings of the tower, suggests that the perimeter walls surrounding the staircase have a thickness of 0.20 meters.

4.2.3. REINFORCING INTERVENTIONS

The tower has been subjected to reinforcing interventions from 1981 until 1988, after a series of requests carried out by the municipality towards the superintendency of cultural heritage. The necessity of realizing some seismic improvement works has

been recognized since the second half of the '900, as testified by the countless reports drawn up between 1964 and 1979, which show the concern that the state of the tower was arousing. The 1964 report assess that: "*The lack of intermediate slabs in the elevation of the tower, the presence of old badly recovered cracks and the consistency of the walls undermined by the weather, with the joints of mortar, in some areas, very deteriorated, are determining factors in the oscillation of the Tower.*". So, it appears clear that the tower state has always given concern, as it is stated in a 1979 report: "*The tower oscillates nearly 20 centimetres to the sound of the "big bell", which weighs many miles of pounds and is remarkable for its size, and its significant oscillation has always aroused great concern in the inhabitants of neighbouring houses.*" The situation became serious after the Comunanza 1972 (Mw 5.48) and particularly the Valnerina 1979 (Mw 5.8) seismic events, that damaged the tower, as stated in a 1979 report: "*The earthquakes of 19/9/1979 caused serious damage to the monument with threats of collapse. Immediate intervention is required for the consolidation of the structure to avoid its collapse*", and again in a technical-scientific-methodological report (after the 1979 earthquake) attached to an expertise of the works: "*rapid investigations revealed the presence of numerous vertical lesions and detachment between the vertical joints of the stone blocks of the Tower; the most serious reason involved the entire belfry which, following the earthquake, underwent a slight rotation on its vertical axis.*"

Finally, in 1981 the consolidation works started, with various objectives (**Figure 33**):

- regenerate the stone masses of the Tower, to increase their bearing capacity,
- restore the continuity of the structure, particularly in areas where it has been compromised by the onset of injuries and detachments,
- Establish a sufficient connection and stiffening of the four faces of the tower.

From the 1981 report: "*At the operational stage, a reinforced framework is being inserted within the thickness of the walls and at various levels, consisting of horizontal stiffening*

frames, made with longitudinal steel bars with improved adhesion, cemented in injection holes and reinforced at the corners from cantonal bars, and from oblique tie rods arranged according to vertical planes to transmit the overall stresses on the reinforced frames. Consequently, the entire face of the Tower will be revised and restored."

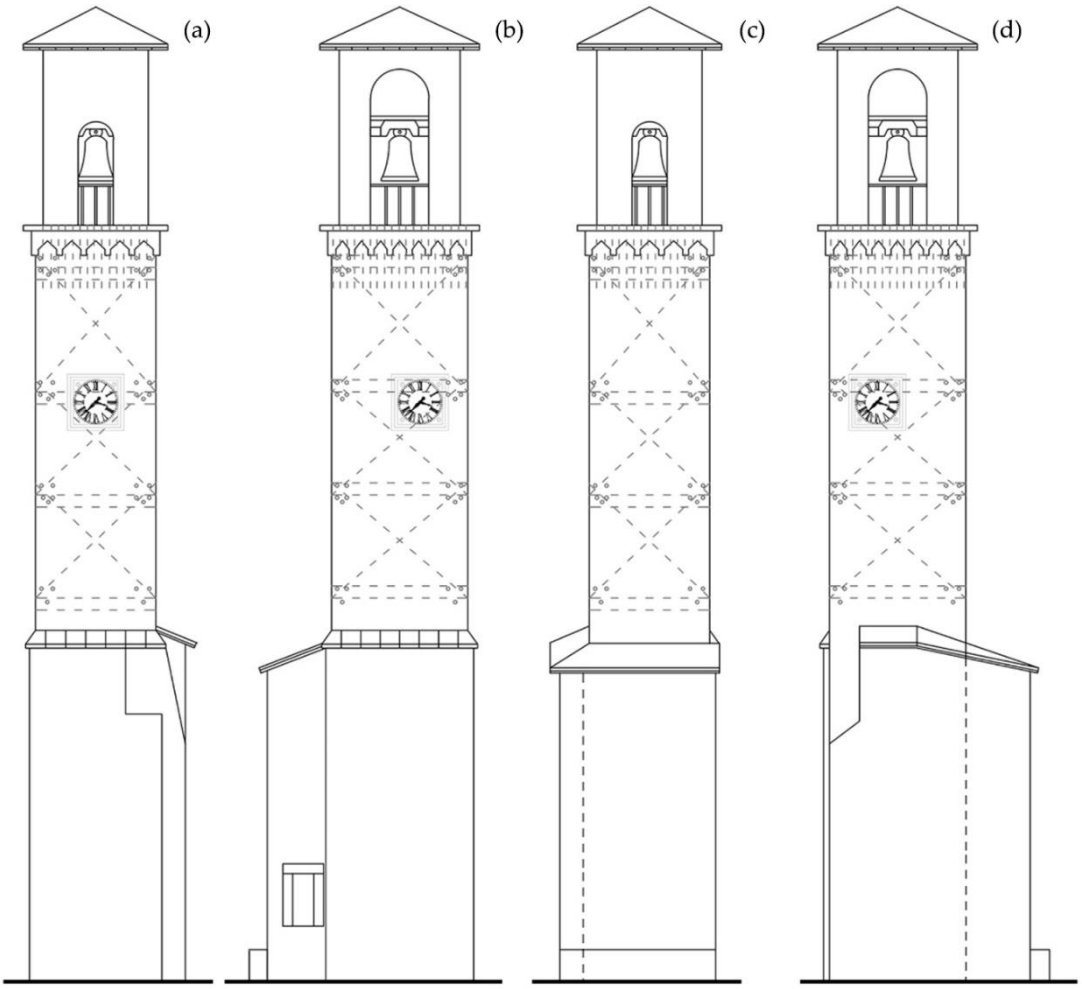

Figure 33 – *Details of the consolidation works carried out in the 1980: the North (a), West(b), South (c) and East (d) façade.*

4.2.4. DAMAGE SURVEY

Following the seismic event of 30th October 2016, the belfry, already partially compromised following the earthquake of 24th August 2016, completely collapsed and the bell did detach from the supports and fell on the closing structure of the tower.

According to the report drawn up by the firefighters for the securing of the tower, on the vertical supporting structure of the building, there were no evident cracking patterns (cracks on the vertical walls and local expulsion of stone material) which denote a state of significant structural stress on the building. This means that the tower responded globally in an adequate manner to the seismic excitation, probably thanks to the reinforcing interventions of the 1980s, that ensured a good connection between orthogonal walls.

But locally the tower has given a sign of vulnerability, precisely in some of the areas typically affected by seismic damage. As already stated the belfry has collapsed (**Figure 34**), as typically happens considering that this peculiar substructure behaves like a small frame, in which four small and not reinforced columns have to bear the horizontal action caused by the inertia force corresponding to the mass of the above four arches made of stones, the wooden roof, and the heavy bell.

(a)  (b) 

***Figure 34** – Details of the belfry after the 24th August 2016 (a) and 30th October 2016 (b) earthquake.*

The other structural element that reported local damage is the annex (**Figure 35**). The body of the building structurally leaning against the tower, made with a different building typology and in a subsequent period, did present important cracking patterns that require an intervention to reduce structural criticalities. Probably its particular vulnerability is given by an insufficient connection with the main body of the tower and to the low thickness and quality of the wall (the most damaged parts were in correspondence of a chaotic portion of masonry, not interested by the 1980s reinforcing works, and part of a very slender wall, with a thickness of just 0.20 m).

Figure 35 – *Details of the crack pattern developed on the annex of the tower after the seismic sequence in 2016.*

After those first securing operations (**Figure 36a**), the tower has completely been incorporated by an external reticular frame consisting of vertical steel elements following the profile of the tower, horizontally hooped by steel cables for the whole height of the building (**Figure 36b**).

In 2021 MiBACT (Ministry of Cultural Heritage and Activities and Tourism) finances the seismic improvement, consolidation, and restoration of the Civic Tower, to allow the iconic structure to be returned to the city in all its beauty and safer than before.

(a)  (b) 

Figure 36 – *View of the tower after the first securing operation (a) and after the interventions carried out after the first securing operations (b).*

4.3. DISCRETE MODELLING OF THE AMATRICE CIVIC TOWER

The geometry of the tower has been represented through a refined three-dimensional discrete model, that has been set up for the purpose. This model has been realized through the MIDAS FEA NX© software, which gives the possibility to represent each unit that composes the real tower, as a separate three-dimensional solid entity. The objective of the simulation was principally to have a realistic representation of the tower under a dynamic excitation and to achieve this goal the profiles of the structure, obtained by photo-survey, have been used as a reference in the modelling, together with all the information collected during the knowledge path of the structure. So, as the major focus was to obtain a model that could correctly represent the local phenomena of disaggregation of masonry, other objectives were proposed in this framework. Particularly, it was meant to also investigate the influence of regularity of the blocks used in the modelling of the tower. This means to understand if modelling the blocks of the towers as irregular extruded polyhedral was necessary to achieve a correct representation of the behaviour of the structure, or if a simplification in the shape of the irregular blocks, represented as cuboids having

dimensions approximately like the original ones, was acceptable. For this purpose, two different models of the towers have been initially realized: a *realistic* one, constituted by irregular extruded polyhedral blocks (**Figure 37a-d**), and an *idealized* one, constituted by regularized blocks (**Figure 37e-h**).

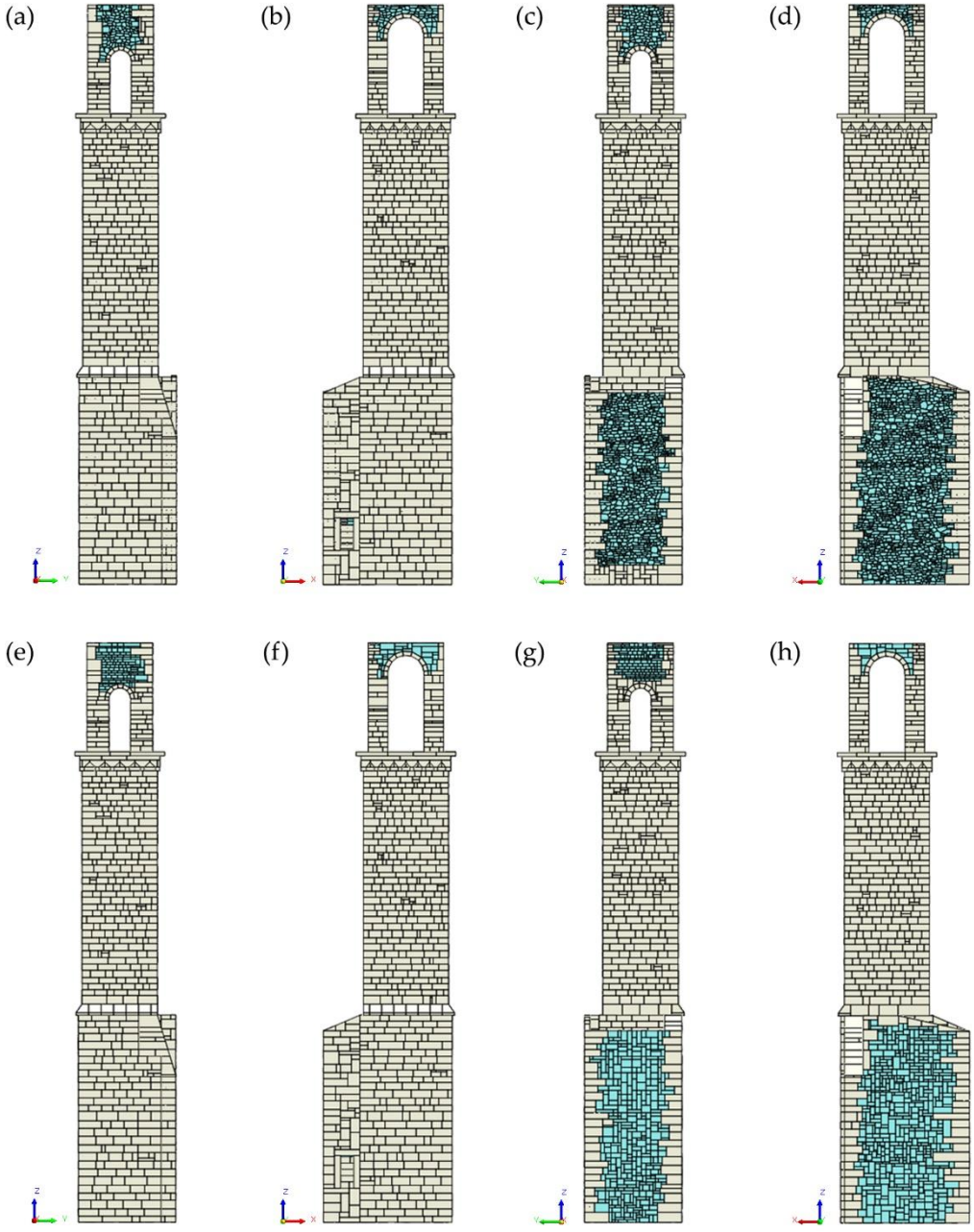

Figure 37 – *North (a), East (b), South (c) and West façade (d) of realistic model and North (e), East (f), South (g) and West façade (h) of idealized model.*

Furthermore, it was introduced even the possibility of modelling the effectiveness of the reinforcing intervention, carried out in the '80s of the last century, modelling the steel rods that were inserted in-depth of the masonry walls of the elevation of the tower, and at the interior of the mini-vaults that constitutes the belfry of the structure. This operation has been carried out for both the two models (realistic and idealized), giving, as a result, the presence of two additional models to be analysed (**Figure 38**).

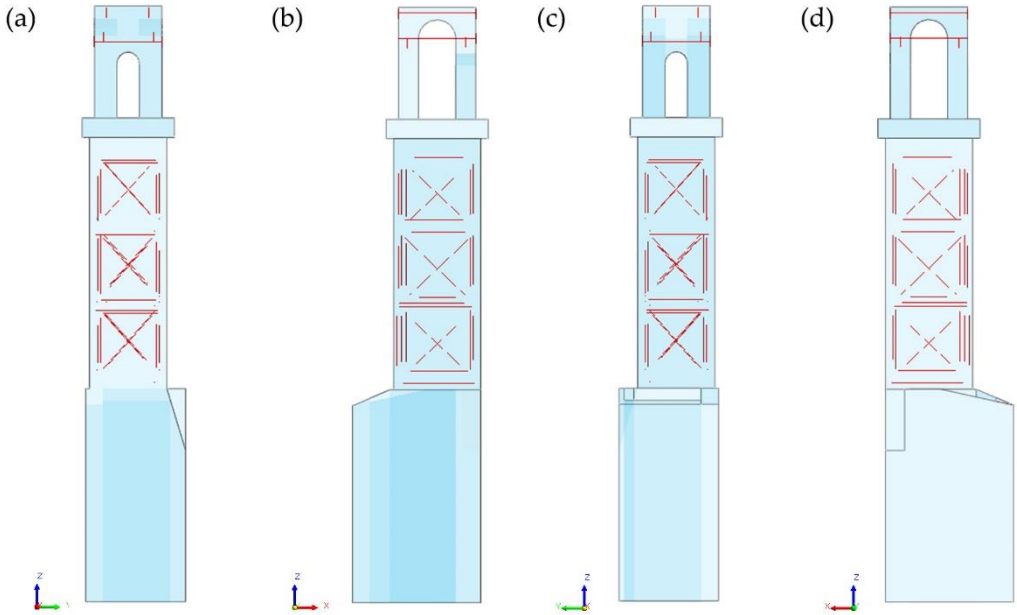

***Figure 38** – Reinforcing intervention in the numerical models: North (a), East (b), South (c) and West façade (e).*

It is worth mentioning that in both the idealized and the realistic model, in each of their versions (with or without steel bars), each element has been represented exclusively through convex 3D solids.

4.3.1. NUMERICAL MODELS

The representation of the *realistic* model has been carried out with the specific objective of obtaining the most realistic and trustable geometric simulation of the real structure, with an approximatively one-to-one correspondence between the blocks of

the model and the original stones (**Figure 39**). In this perspective, a fundamental tool has been the usage of the photo-surveys of the tower's profiles, obtained from the data archived at the Superintendency Archaeology, Fine Arts and Landscape for the provinces of Frosinone, Latina and Rieti. Through those data, it has been possible to understand the external texture of masonry, constituting the main visible walls (**Figure 39**a).

Other information, such as the thickness of walls, the planimetry, the presence of openings, niches, stairs, and slabs, have been obtained from the historical drawings of the tower, collected during the critical survey of the structure.

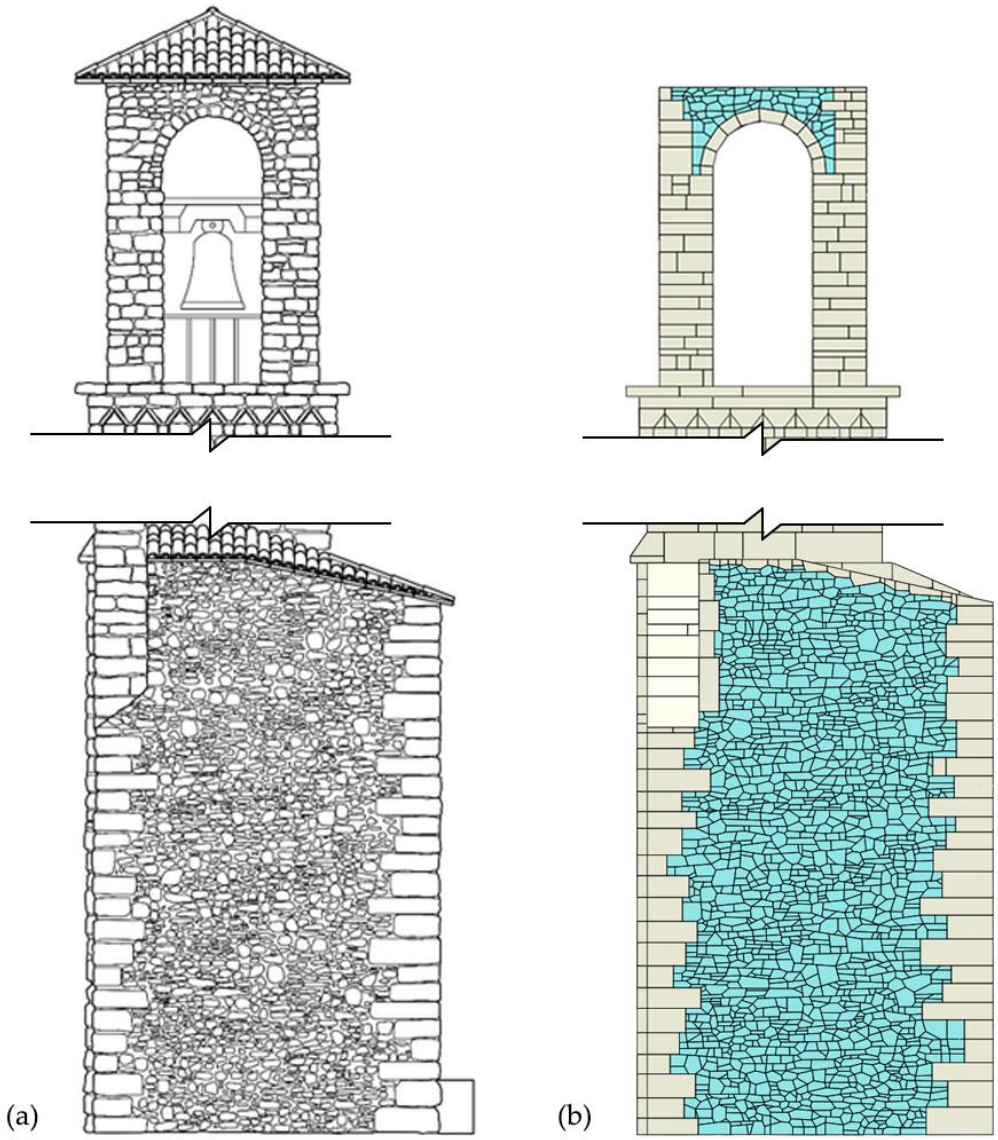

Figure 39 – *East façade: comparison between the photo survey (a) and the realistic model (b).*

As regards the representation of the inner core of the walls, the major assumption has been the presence of a layer of rubble masonry (inner sack). This hypothesis has been considered acceptable in relation to the period of construction of the tower and refers to the traditional methodologies of construction in the area. This assumption has been considered convincing only if referred to the walls having a considerable thickness (the vast majority of walls constituting the tower ranging in between 0.70

m and 1.00 m of thickness), while for the thinner parts (in particular some areas of the annex measuring only 0.20 m of thickness, and the four columns constituting the belfry) this hypothesis wasn't accepted.

For the areas modelled as bag masonry, the presence of three layers (**Figure 40**) was taken into account, so each wall was divided into three uniform parts. The two exterior parts have been modelled looking at the photo survey (the non-visible part has been assumed specular as the visible one). While the inner part has been modelled as constituted by very small irregular blocks, ordered chaotically, having a prevalent dimension of approximatively 0.10 m.

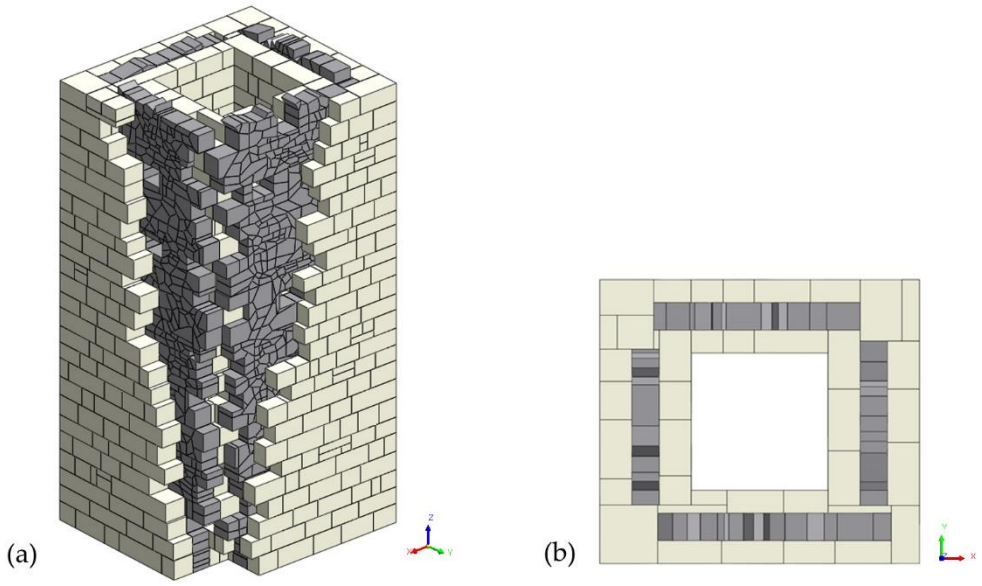

***Figure 40** – The inner rubble masonry (a) and disposition of the three layers (b) in realistic model.*

Another aspect, very important to obtain a realistic behaviour of the structure, has been the interlocking between the orthogonal walls. It has been assumed a good degree of connection between all the four main walls of the original body of the tower, as it was possible to observe, thanks to a photo survey, how regular, and well connected were the original cornerstones. A good interlocking has been represented

in the model superimposing the corner-blocks for a good extent and misaligning the joints (**Figure 41a**).

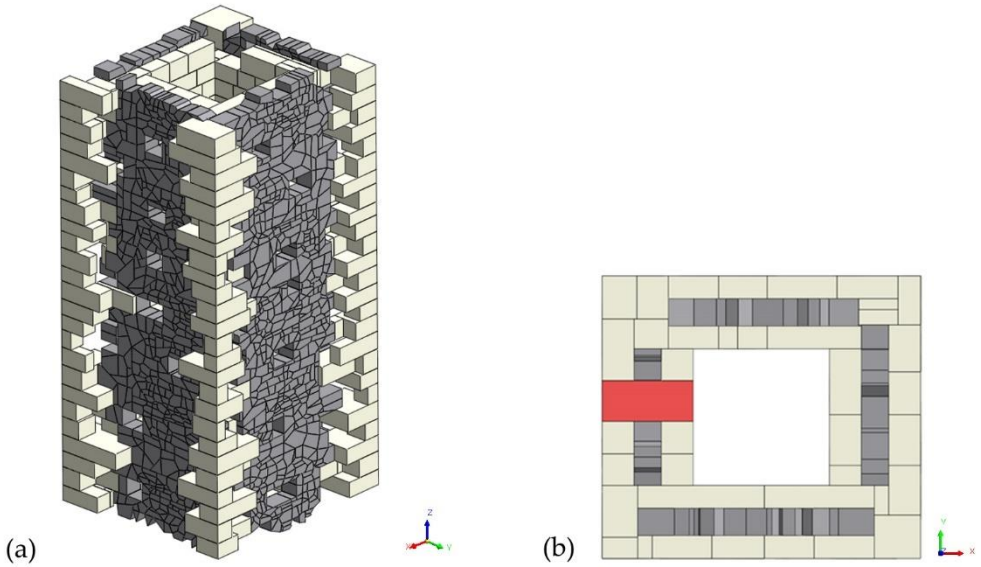

Figure 41 – *Details of the corner-blocks (a) and the diatons element (b) in the realistic model.*

Even the annex presents a good connection between its two main orthogonal walls, but, on the other hand, no apparent attention was made to constraining the annex to the original structure. This is the reason why in the model of the structure no connection has been represented between the annex and the original body of the tower as if they were simply adjacent to each other.

It was important also to model correctly the connection between the different layers constituting each wall, so the interlocking between the two external layers with the inner rubble core. This has been carried out modelling some elements as passing through the different layers of the wall, connecting them in some extent, as diatons elements (**Figure 41b**). Those elements are supposed to be present only in a discrete way in the interior of the walls, so approximately one diaton has been modelled for every square meter of masonry.

As a result of this modelling process a full detailed representation of the tower, constituted by 17472 blocks is obtained (**Figure 42**).

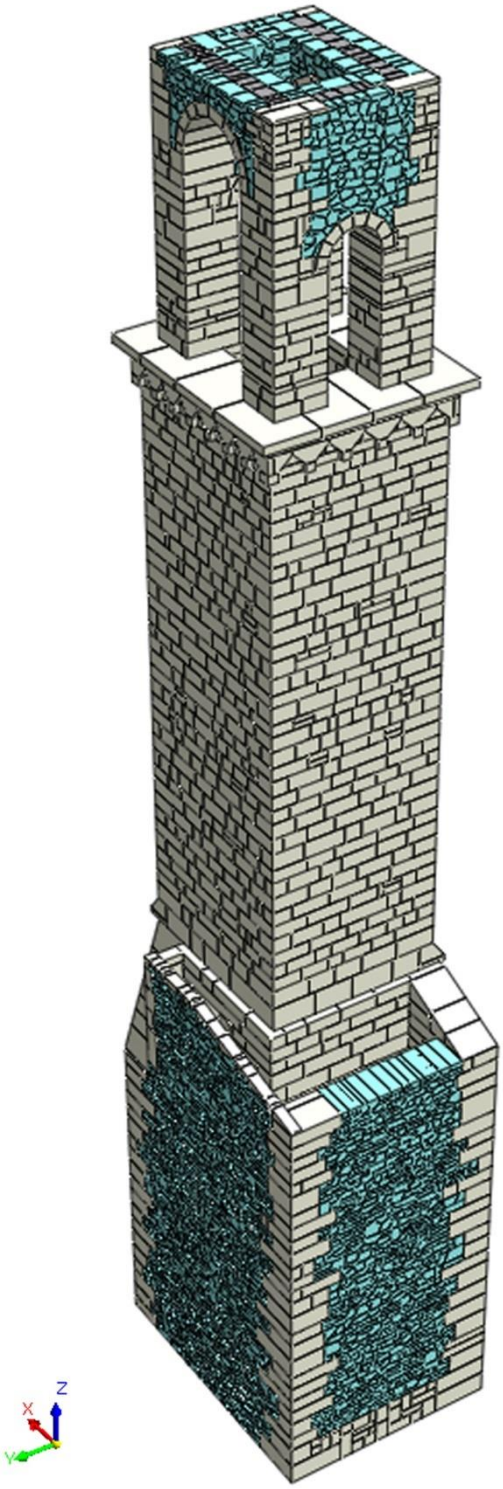

***Figure 42** – Realistic numerical model.*

An *idealized* model has been setup, having the main feature of regularizing the polygons that constitutes the visible side of each block assembling the Tower. In this way, the modelling setup has been carried out more quickly, as it was easier to draw the faces of each unit (**Figure 43**)

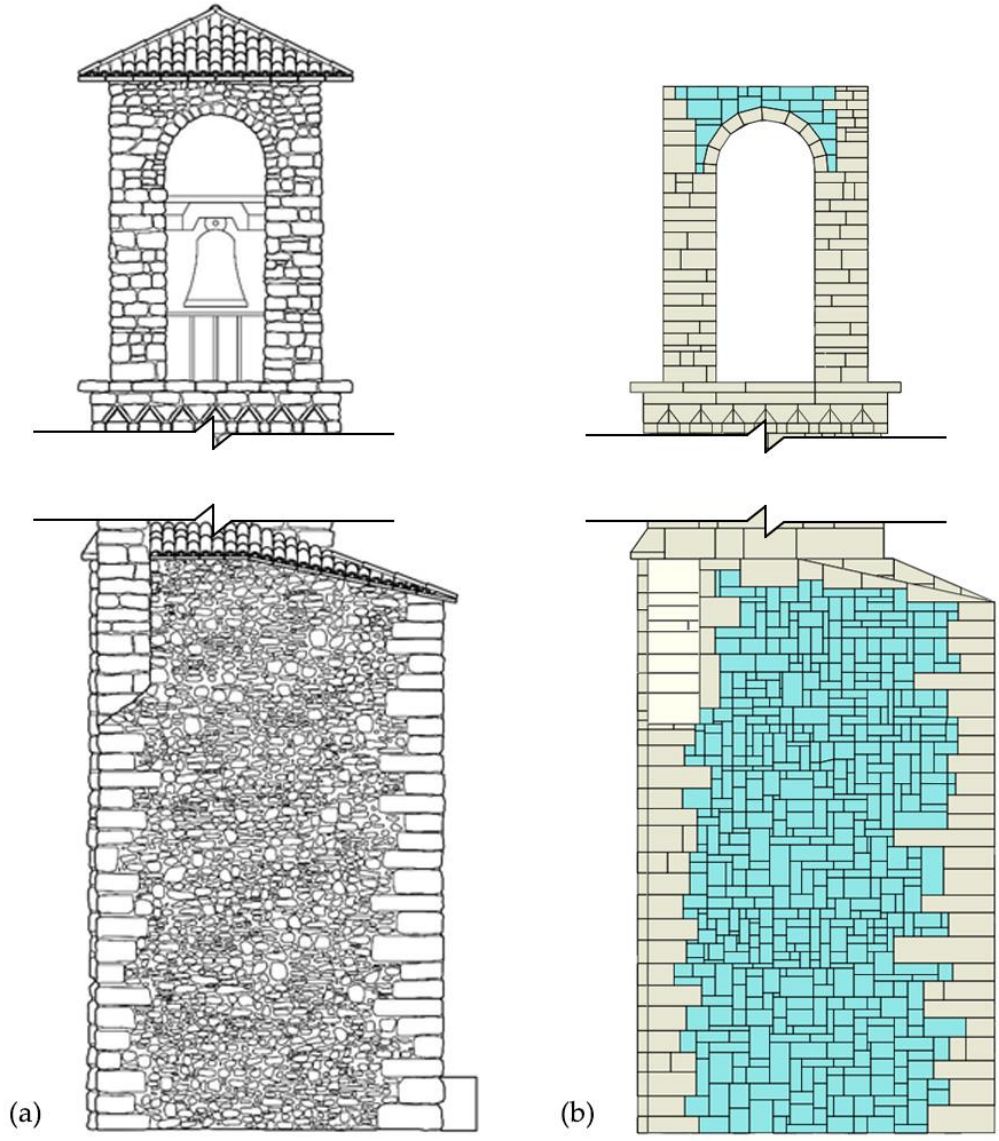

***Figure 43** – East façade: comparison between the photo survey (a) and the idealized model (b).*

Particular attention was given to have blocks having at least a few centimetres of superposition, to avoid contact detection problems from the used software. For what concerns the representation of the inner core, differently from the real model, a series of aligned cuboids has been used, to represent the poor mechanical quality of the material. Inner cores of this kind of structure are often made of rubble masonry, having very limited mechanical characteristics. Aligned blocks create the possibility of having straight discontinuity surfaces, between columns and rows of them, and in this way simulate the vulnerability of the rubble masonry.

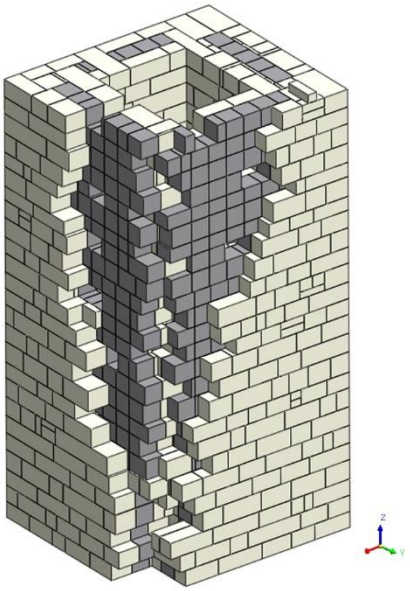

***Figure 44** – Detail of inner rubble masonry in idealized model.*

Due to the presence of a regular texture used to model the inner core, and to the general presence of squared blocks, this model is constituted by a considerably lower number of entities, ending up with 8138 blocks (**Figure 45**). This relative simplicity adopted in the modelling leads to a faster analysis.

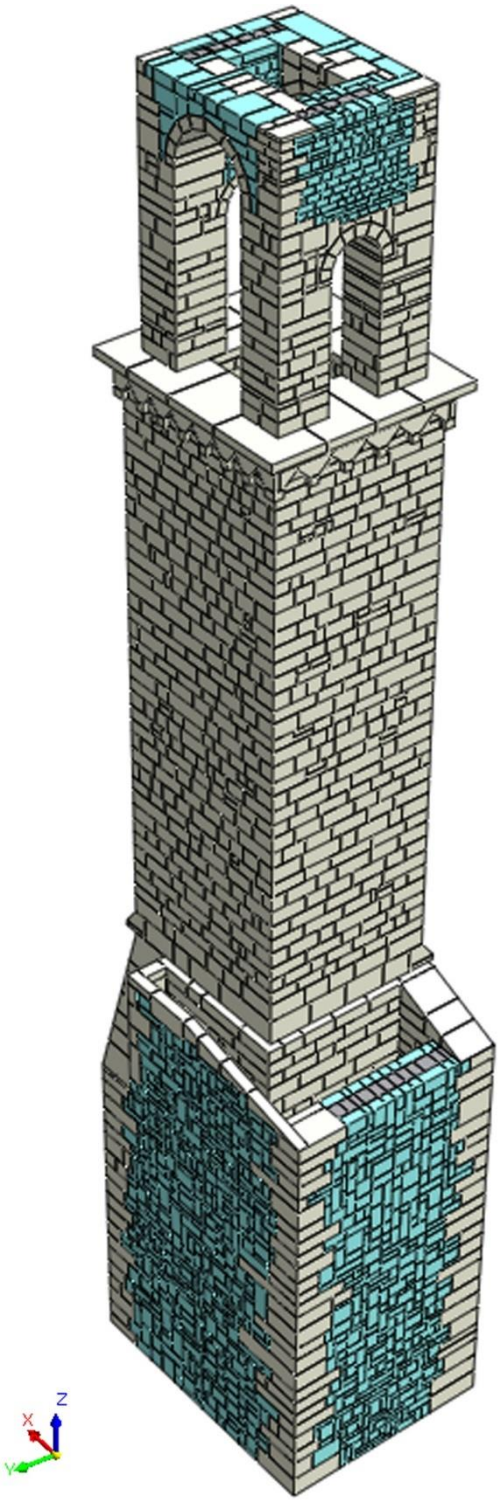

Figure 45 – *Idealized numerical model.*

Finally, the presence of a series of steel rods has been modelled for the *realistic* and *idealized* model as shown in **Figure 38**. Those elements were really included in the original Tower during the reinforcing interventions carried out in the 80s. To obtain the more realistic behaviour possible for the structure, those steel elements had to be placed and modelled as the original ones. So the first issue in this phase has been the collecting of all the information related to the reinforcing intervention carried out on the Civic Tower. To do this reference was made to the documents available from the Superintendency Archaeology, Fine Arts and Landscape for the provinces of Frosinone, Latina and Rieti. In those papers, data are available about the dimensions (average length and diameter) and quantity of those bars, that were inserted in the depth of the walls constituting the medium-upper part of the structure (elevation). Other few bars were also included in the belfry, again according to the available documentation (**Figure 46**).

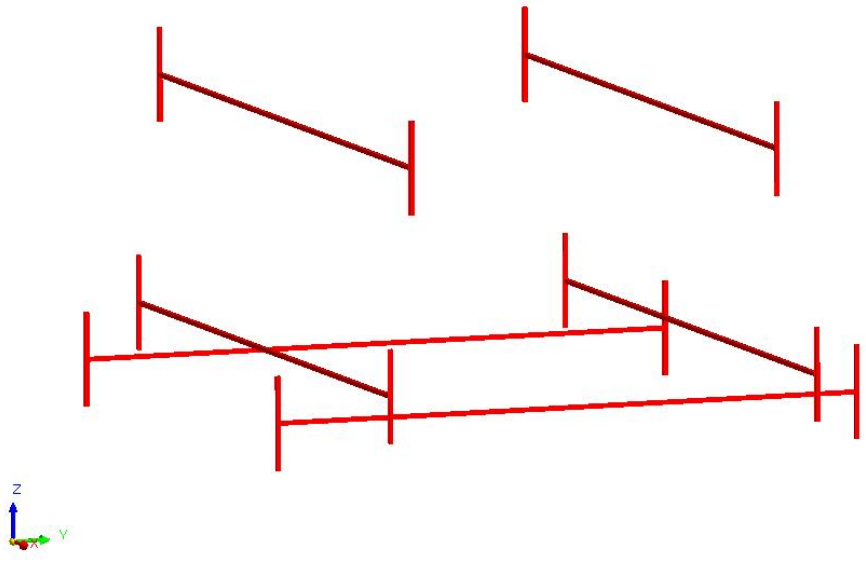

***Figure 46** – Steel bars in the belfry.*

From an operational point of view, the bars were modelled simply as very elongated parallelepiped elements, having a square section of 0.02 m as sides. This was a necessary simplification, due to modelling issues, because the real bars have a circular section of 0.02 m as diameter. For what concern their position, it was possible to obtain qualitative indications from a drawing attached to the request of intervention.

Two models are obtained: a first one representing the *idealized* model of the Civic Tower rearranged to contain the steel bars, constituted by 11502 blocks, and a second one, starting from the *realistic* model and embedding the presence of the reinforcing, constituted by 24372 blocks.

4.3.2. MATERIAL PROPERTIES

For all models described (Section 4.3.1), i.e., realistic (Model R), idealized (Model I), realistic with reinforcing interventions (Model RR) and idealized with reinforcing interventions (Model IR) the parameters have been chosen in line with Italian code.

It should be specified that it was not possible to carry out tests on materials, nor a dynamic identification to identify in a non-invasive way some parameters of the structure such as the elastic modulus. The mechanical parameters used are summarized in **Table 4**.

Table 4 - *Characteristic of the mechanical parameters used for the numerical analyses for all configurations.*

MODEL R, MODEL I, MODEL RR, MODEL IR		*DEM*
Density ρ	*[kg/m³]*	*2200, 1900*
Joint friction μ	*-*	*17°, 27°, 42°*
Joint normal stiffness Jk_n	*[Pa/m]*	*3.83e9, 7.67e9, 2.67e10*
Joint shear stiffness Jk_s	*[Pa/m]*	*1.53e9, 3.07e9, 1.07e10*
Joint cohesion Jcoh	*[Pa]*	*0.1e6*
Joint tensile strength Jten	*[Pa]*	*0.1e6*

The blocks were considered as rigid, a density of 2200 kg/m^3 was assigned to the regular blocks of the Tower, instead, a density value of 1900 kg/m^3 was assigned to the chaotic masonry and the inner bag.

A value of the friction coefficient between the blocks equal to:

- 27° between the contacts of the blocks of the external layers,
- 17° between the contacts of the blocks of the internal layer and between the contacts of the internal layer with the external ones,
- 42° between the blocks in contact with the foundation.

In particular, a coefficient of friction value of 17° was used to characterize the rubble masonry and thus reproduce a mortar of poor quality.

At the values of the coefficient of friction described above must be added other parameters, about the value of joint normal stiffness values equal to:

- 2.67e10 Pa/m between the contacts of the regular blocks of the external layers of the tower and the annex,
- 7.67e9 Pa/m between the contacts of the chaotic blocks of external layers of the tower and the annex,
- 3.83e9 Pa/m between the blocks of the internal layer of the tower and between the contacts of the internal layer with the external ones.

While about joint shear stiffness values equal to:

- 1.07e10 Pa/m between the contacts of the regular blocks of the external layers of the tower and the annex,
- 3.07e9 Pa/m between the contacts of the chaotic blocks of external layers of the tower and the annex,
- 1.53e9 Pa/m between the blocks of the internal layer of the tower and between the contacts of the internal layer with the external ones.

Finally, to the joint cohesion and the joint tensile strength a value of 0.1e6 Pa, although these assume small values, it has been seen that they can influence the displacement capacity.

4.3.3. APPLICATION LOADS

To consider loads of the floors and the roof, load analyses were carried out in line with Italian code and the construction techniques of the time. The loads were inserted in terms of density to the rows of blocks near the floors and the roof.

The structure was first studied under the action of gravitational loads, then the base of the Civic Tower was excited with a set of speeds in the three main directions (two horizontal and one vertical). The speeds were recorded by the Amatrice station (AMT) during the 2016 Central Italy seismic sequence.

The **Table 5** shows the characteristics of the four main events.

Table 5 - *Characteristic of main earthquakes recorded in Amatrice (AMT) stations during the Central Italy earthquake in 2016, where * indicates that site classification is not based on a direct $V_{s,30}$ measurements.*

Seismic Event		M_L	*Depth*	*Station*	*Class EC8*	R_{jb}	R_{rup}	R_{epi}	*Channel NS PGA*	*Channel EW PGA*	*Channel UD PGA*
[-]		*[-]*	*[km]*	*[-]*	*[-]*	*[km]*	*[km]*	*[km]*	*[cm/s²]*	*[cm/s²]*	*[cm/s²]*
1st	***24/08/2016***	*6*	*8.1*	*AMT*	*B**	*1.38*	*4.62*	*8.5*	*368.39*	*-850.8*	*391.37*
2nd	***24/08/2016***	*5.4*	*8*	*AMT*	*B**	*-*	*-*	*20.9*	*-93.28*	*105.58*	*63.77*
2nd	***26/10/2016***	*5.9*	*7.5*	*AMT*	*B**	*25.93*	*26.09*	*33.3*	*-58.55*	*90.74*	*-49.11*
3rd	***30/10/2016***	*6.1*	*9.2*	*AMT*	*B**	*10.12*	*11.49*	*26.4*	*393.63*	*521.62*	*317.82*

where [79–81]:

- R_{jb}, is the Joyner-Boore distance, known as the smallest spacing from the site to the surface projection of the rupture surface,
- R_{rup}, is the shortest distance between the site and the rupture surface,
- R_{epi}, is the distance estimated by the geometric swap.

The velocigram that was obtained is represented in **Figure 47**, has a total duration of 46 seconds and was obtained by considering 10 seconds of strong motion for each event and two seconds of zero velocity between one event and another. The seconds of rest inserted in between each strong motion are necessary to ensure that the inertia forces, depending on the previous event, will not influence the behaviour of the tower in relation to the subsequent event.

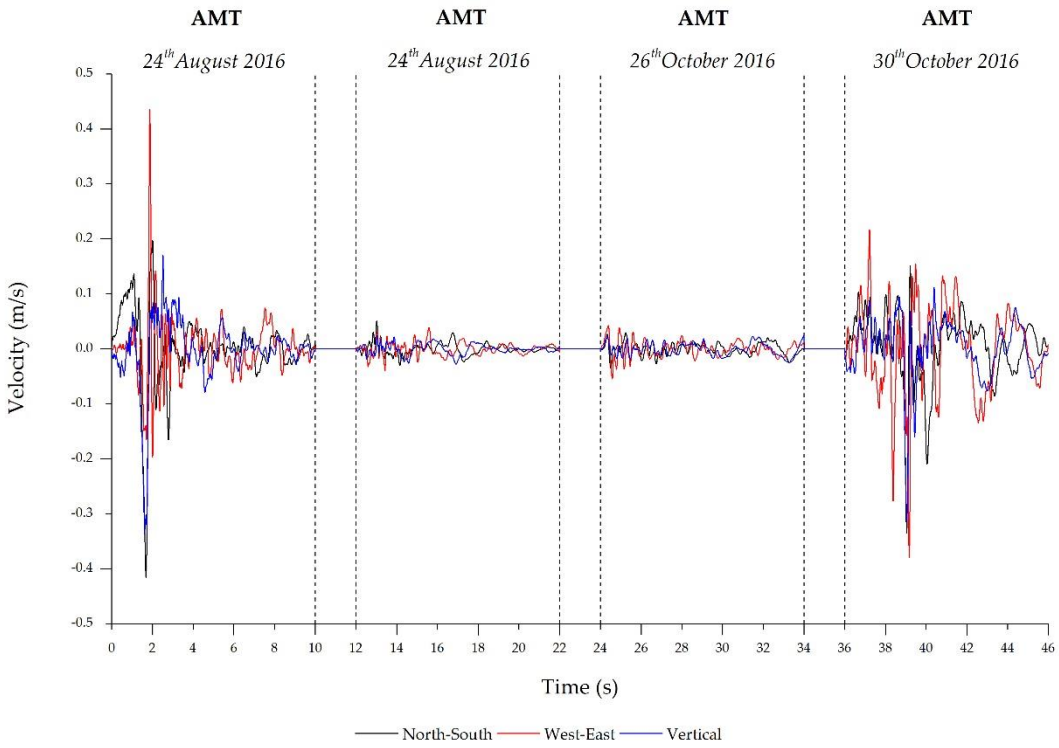

***Figure 47** – Velocity of strong motion recorded by the Amatrice (AMT) station.*

4.4. NUMERICAL RESULTS OF THE AMATRICE CIVIC TOWER

To compare the results of the various models in **Figure 48**, the four control points are shown, two located at the top of the tower, one at the base of the belfry and one at the annex.

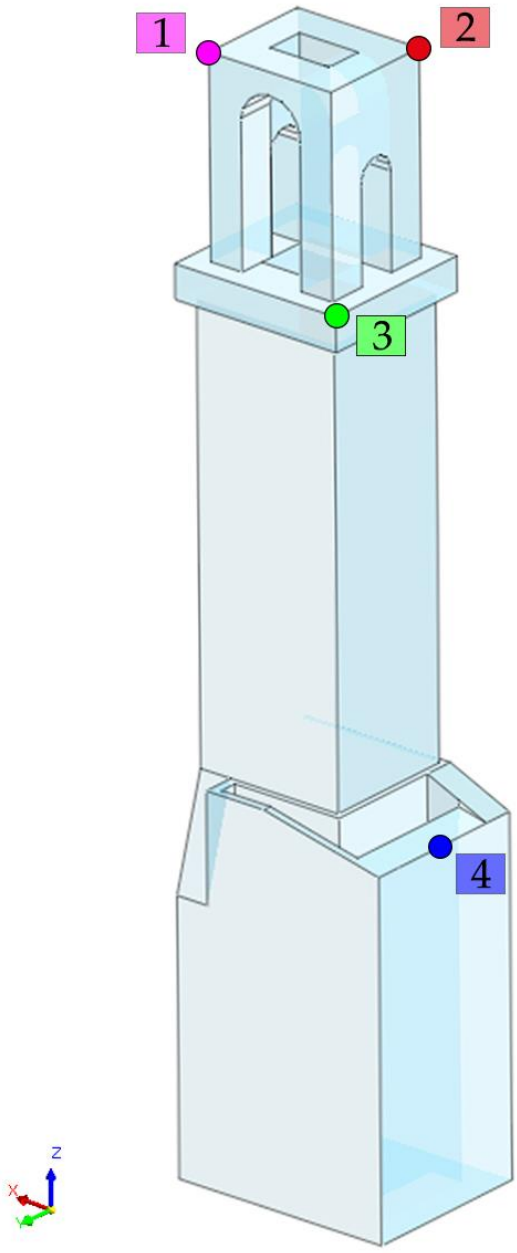

***Figure 48** – Location for the control points used for the nonlinear dynamic analises of the Amatrice Civic Tower (Rieti, Italy).*

The following images show the displacements of the four control points in the different models.

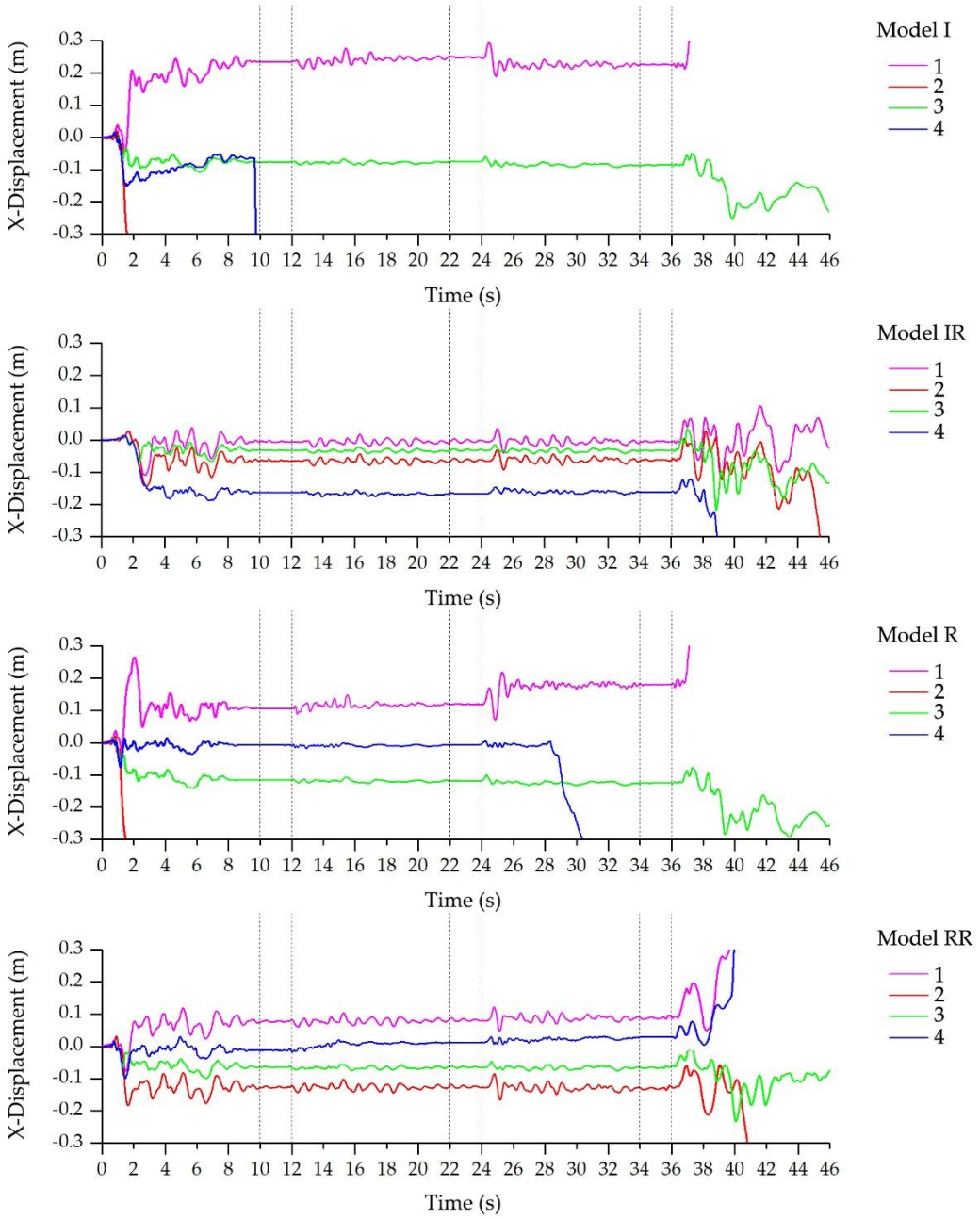

Figure 49 – *X-Displacements time histories of the Amatrice Civic Tower (Rieti province, Italy), under the four main shocks recorded in the Amatrice Station during the Central Italy seismic sequence in 2016 for the four configurations models analysed.*

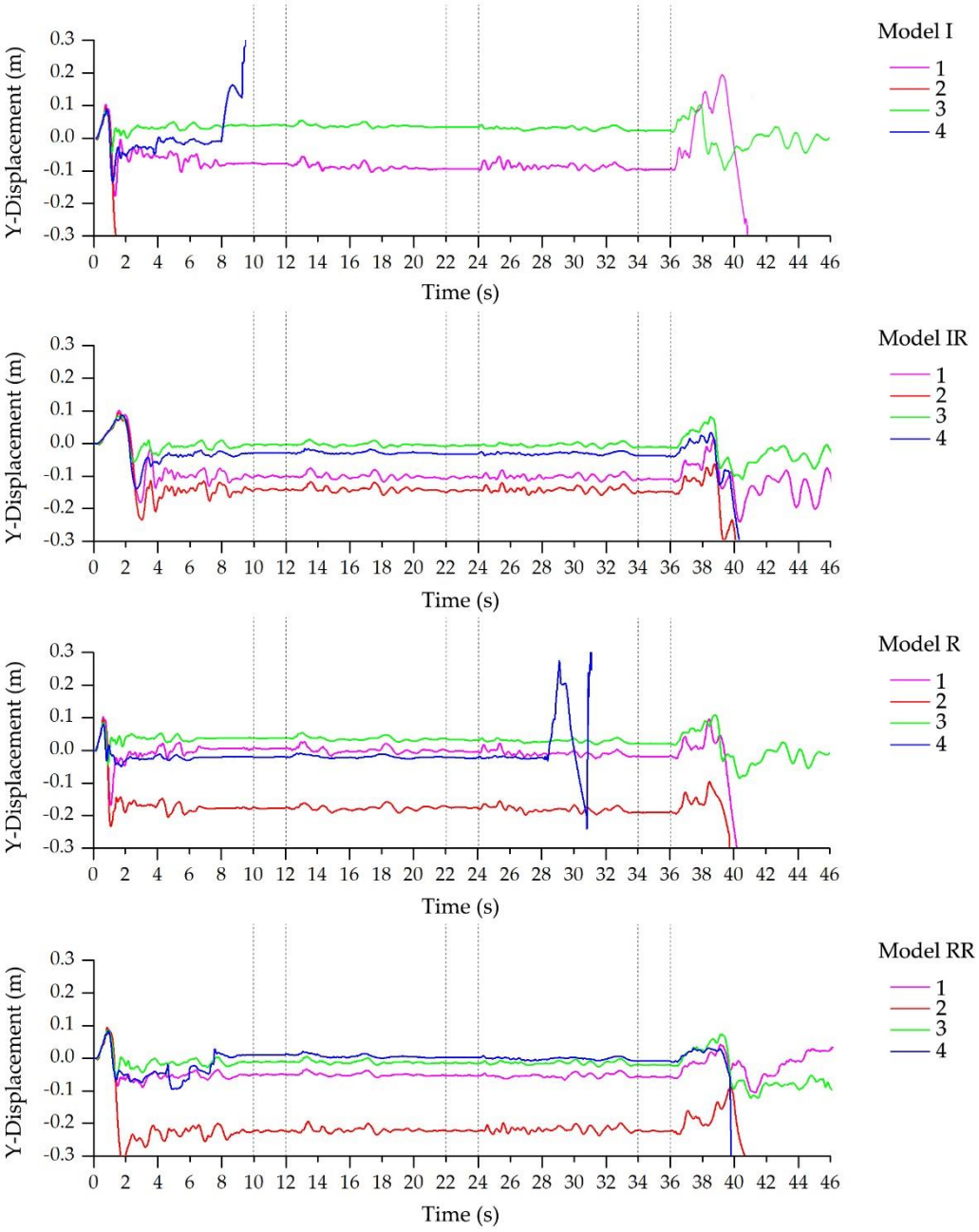

Figure 50 – *Y-Displacements time histories of the Amatrice Civic Tower (Rieti province, Italy), under the four main shocks recorded in the Amatrice Station during the Central Italy seismic sequence in 2016 for the four configurations models analysed.*

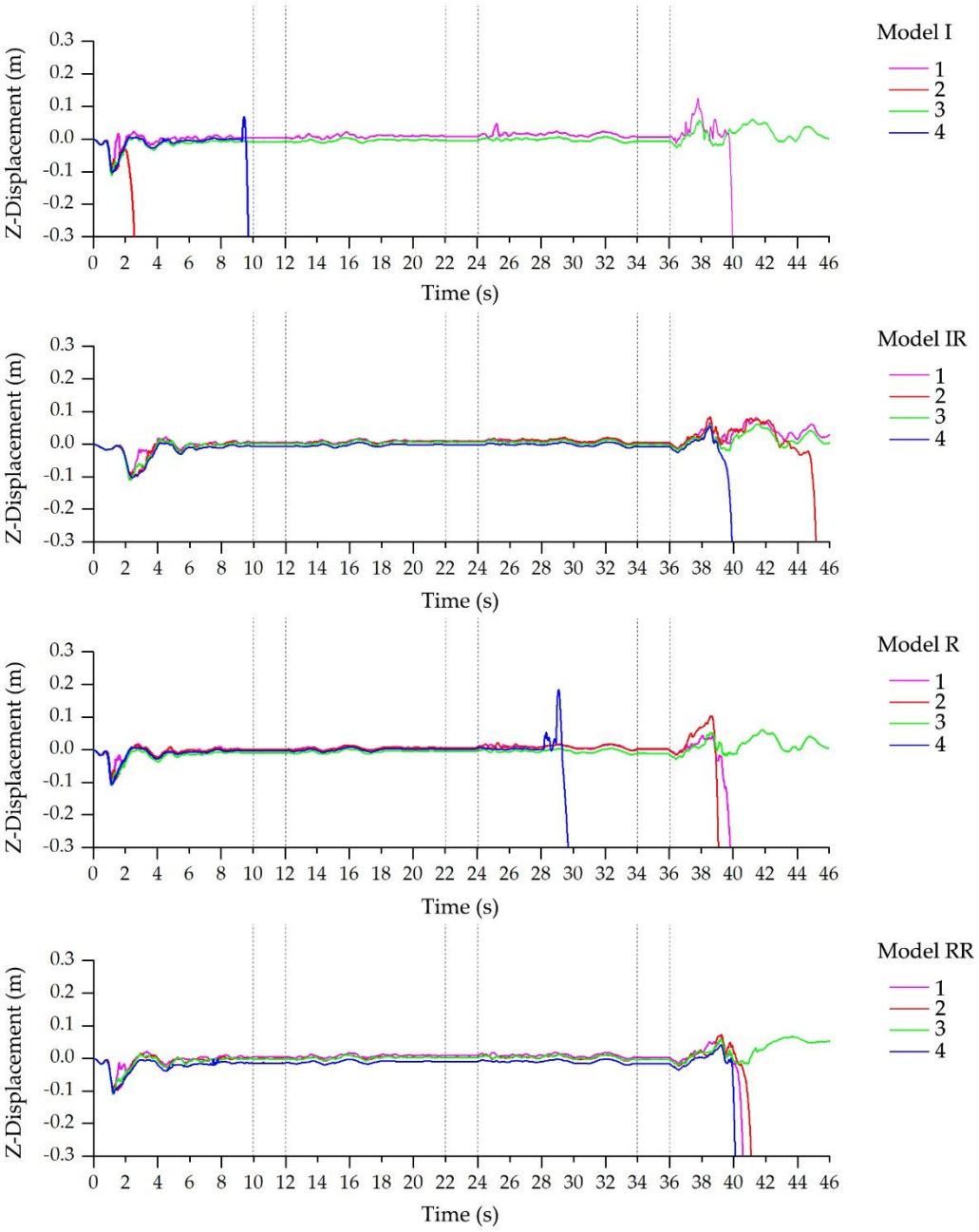

Figure 51 – *Z-Displacements time histories of the Amatrice Civic Tower (Rieti province, Italy), under the four main shocks recorded in the Amatrice Station during the Central Italy seismic sequence in 2016 for the four configurations models analysed.*

Let's start by comparing the realistic model (Model R) with the idealized one (Model I), the control point #1 in Model I shows greater displacements in the x-direction and y-direction than in model R, in the z-direction instead the fall occurs at the same time instant.

Control point #2 in Model I in the initial moments of the simulation immediately collapses, while in Model R it reaches important displacements, of the order of 0.30 m and collapses at the last event.

Control point #3, located at the base of the belfry, unlike the first two points, has an almost identical behaviour in both models it reaches displacements of the order of 0.20 m in the x-direction and 0.06 m in the y-direction without arriving at the collapse at the end of the simulation.

Control point #4, located at the annex in Model I, collapses at the end of the first shock while in Model R the collapse occurs during the third event.

Comparing models with reinforcement interventions, i.e. Model IR and Model RR we can see that the control point #1 in the IR Model arrives at displacements of the order of 0.20 m in the y-direction without arriving at the collapse as a result of the seismic sequence; instead, in the Model RR, it collapses during the last event.

Control point #2, similarly to #1, in the IR Model arrives at displacements of the order of 0.30 in the y-direction and collapses only at the end of the seismic sequence, instead in the Model RR this falls during the last event.

The control point #3 in both Model IR and Model RR during the last event achieves displacements of the order of 0.20 m in the x-direction and 0.10 m in the y-direction without however arriving at the collapse at the end of the simulation.

Control point #4 also shows similar behaviour in both models, i.e., Model IR and Model RR, in fact, following the first event in the y-direction arrives at displacements of the order of 0.10 m and 0.20 m in the x-direction in the Model IR. The collapse in both Model IR and Model RR comes during the last event.

It is also interesting to note the contribution of reinforcement interventions, in Model I and in the IR Model. Comparing the control points , the control point #1 in the Model IR does not collapse, while in Model I it collapses during the last event.

Control point #2 in Model I collapses at the first seconds of the simulation while in Model IR the collapse occurs at the end. Similar speech for the control point #4 where in Model I there is the collapse at the end of the first event while in the Model IR it occurs at the last shock. Control point #3 shows comparable behaviour in both Model I and Model IR.

Finally, comparing the Model R with the Model RR the contribution of the reinforcement interventions is visible in terms of maximum displacements reached in the x and y-directions, in fact except for only control point #4, the collapse in the other control points takes place in comparable moments.

The most vulnerable part of the structure is the belfry; in fact, the arched openings make this part of the structure particularly weak as shown in **Figure 52**. Thanks to the reinforcement interventions and the good connection between the walls, the structure do not highlight mechanisms outside the plane. The part of the structure that shows vulnerabilities is the annex it is a body added later and consequently not well connected with the central body of the Civic Tower.

All models highlight the vulnerabilities described, the anticipated collapse of the belfry in models without intervention (Model I, Model R) is justified by the absence of chains, which allow a boxy behaviour and prevent the arches from opening.

In models with retrofitting interventions (Model IR, Model RR) the contribution of the chains at the belfry stands out. It should be emphasized that the behaviour closest to the real one is the Model RR, where the chaotic representation of the inner rubble masonry and the stones allowed to reproduce the existing damage, something that with an approximate discretization of the inner rubble masonry and the stones was not fully possible. In the IR Model, the belfry is damaged but it has not come to collapse as in the real situation (**Figure 52**).

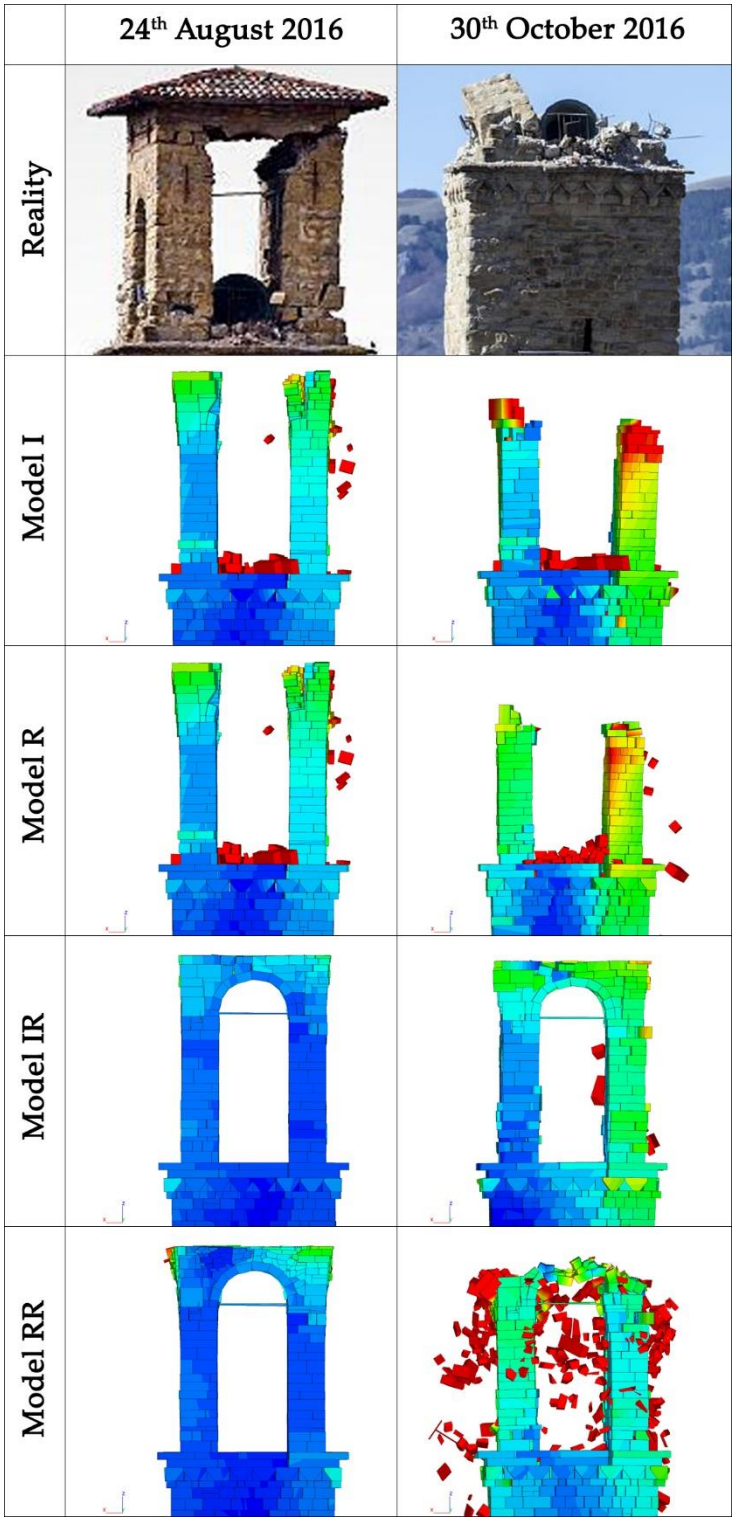

Figure 52 *– Comparison between the reality and the four numerical models of the Amatrice Civic Tower (Rieti province, Italy) under the four main shocks recorded in the Amatrice station during the Central Italy seismic sequence of 2016.*

5 | A FIRST PROOF OF OPERATION MODAL ANALYSIS USING DEM

5.1. INTRODUCTION

The assessment of the state of health of historical structures through dynamic monitoring has been extensively studied and investigated in the FEM world [85–87], even reaching an automatic calibration through genetic algorithms [59,61].

The Operation Modal Analyses (OMA) in the DEM world are not extensively developed, except for simple elements such as arches and vaults [62].

With this work, in this section, we have chosen to apply this methodology to a more articulated case study: the Smeducci Tower.

5.2. THE CASE STUDY

The case study is the Smeducci Tower placed in San Severino Marche, Macerata province, Italy. The historic center is characterized by the northern part, more anthropized, where there is the Piazza del Popolo with its singular oval shape, and by the southernmost part occupied by the Monte Nero hill. It is right on its top that stands the Smeducci Tower, which together with the bell tower of the Dome are the symbols of the city (**Figure 53**).

Figure 53 – *Position of the Smeducci Tower (San Severino Marche, Macerata province, Italy).*

It stands on the top of the hill called Monte Nero or Castello, about 342 m above sea level. It is the only monument of military architecture that has remained intact in San Severino and one of the oldest buildings in the whole city, probably dating back to the twelfth or thirteenth century. It has a square plan and has a total height of 40 m from the ground level.

The first memory in the documents of the tower of San Severino is in a parchment preserved in the municipal historical archive: in it we read that on 1st November 1307 Rainaldo Mercati, consul of the arts, stipulated an agreement with certain Deotesalve said Siqualdo, who undertook to guard the tower, day and night, for the duration of a month for a fee of 30 Ravenna money.

But the tower of Castello had not only defensive functions; it also served to spread sounds to signal moments of danger, for the convocation of the Council and for the scanning of time. On its top were placed in fact the bell of the Municipality and the public clock. Even the placement of the latter in the tower dates back to very ancient times, having news since the fifteenth century when the Municipality already paid the moderator. The bell is remembered since the fourteenth century: on 15th January 1397 there is the contract stipulated with master Fidanza, foundry living in Camerino,

to redo the large bell of the Municipality and place it on the tower, which bell had to weigh no less than 4000 pounds and feel, in quiet time, up to Montecchio (today Treia).

Thanks to its height, which dominated a large stretch of territory, the main destination of the tower, however, was that of sighting and signaling; from the crenellated top the lookouts could wander with their eyes for considerable distances and control what was happening in the valley.

From a purely structural point of view, the first element to consider is the height of the tower itself which was originally 40 m from the ground level. Popular tradition, however, has it that the tower has, over the years, undergone numerous interventions aimed at progressively reducing its height in order to limit the risk of static problems. However, to date there is no supporting documentation of these interventions.

It can be absolved with certainty that the first important intervention dates back to 1560, and consisted in the construction of the current belfry, which housed the bell after a necessary restoration given the previous exposure of the same to atmospheric agents.

The venerable age of the tower has meant that it was the victim of all the seismic events of the last seven hundred years, which have contributed to its deterioration visibly translated into an inclination causing a lead of about 0.85 m along the East-West direction and 0.25 m along the North-South (**Figure 54**).

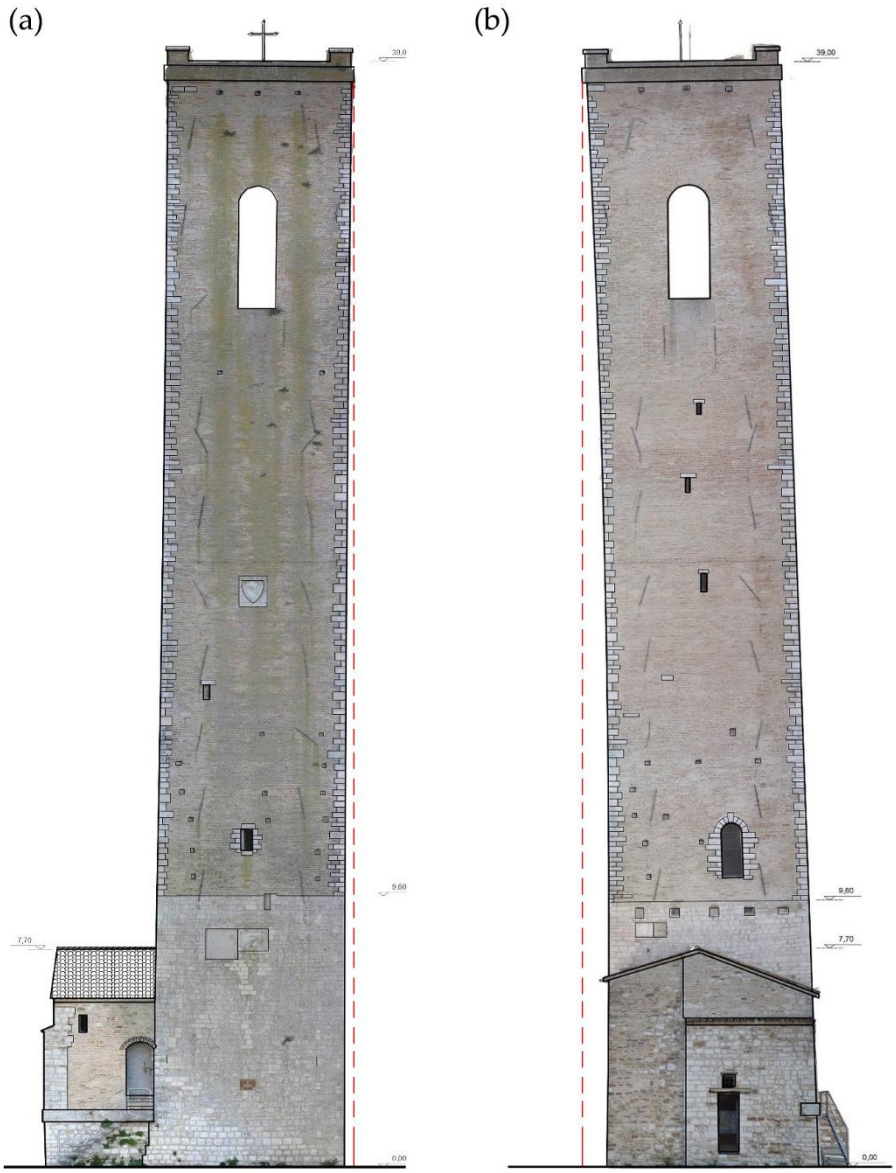

***Figure 54** – East façade (a) and South façade (b).*

Over the years there have been several interventions (**Figure 55**) among the most relevant we can find:

- 1972-1973: construction of a foundation with micropiles 20 m deep. The wooden floors were replaced with reinforced concrete floors and a reinforced seam was made up to the height of the belfry.
- 1979-1980: realization of additional micropiles brought to a depth of 35 m.

- 1997: following the dramatic earthquake of September 1997, it was planned to carry out some renovation works of the Tower including the demolition of the last two reinforced concrete slabs and the replacement of the same with a traditional wooden roof slab, insertion of tie rods in order to make the reinforced concrete floors collaborate with the external facing of the masonry, the emptying and subsequent filling with light material of the two brick vaults of the roof and the belfry, filling the voids inside the inner sack by injections of lime and sand mortar made from inside and outside the facings. The bell placed in the belfry was also removed.

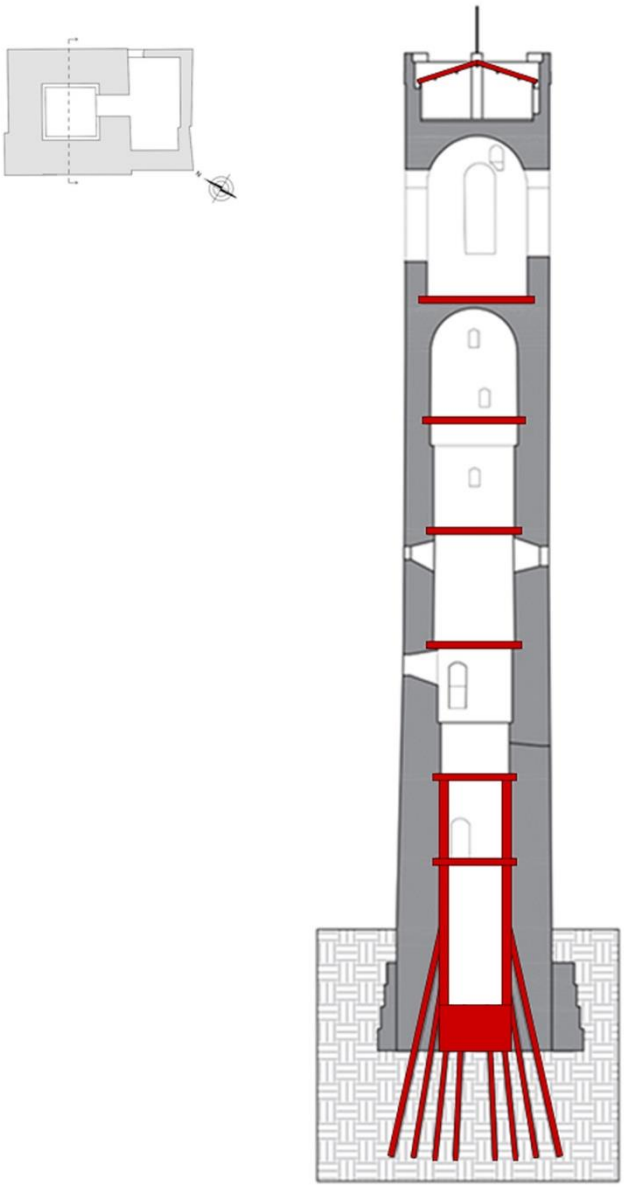

***Figure 55** – Reinforcement interventions on the Smeducci Tower placed in San Severino Marche (Macerata province, Italy).*

From the survey on site it was also possible to identify the three types of masonry that make up the tower. The annex is characterized by stone masonry, the body of the tower and a portion of the annex are characterized by regular stone with internal rubble masonry and the bell cell is characterized by brick masonry (**Figure 56**).

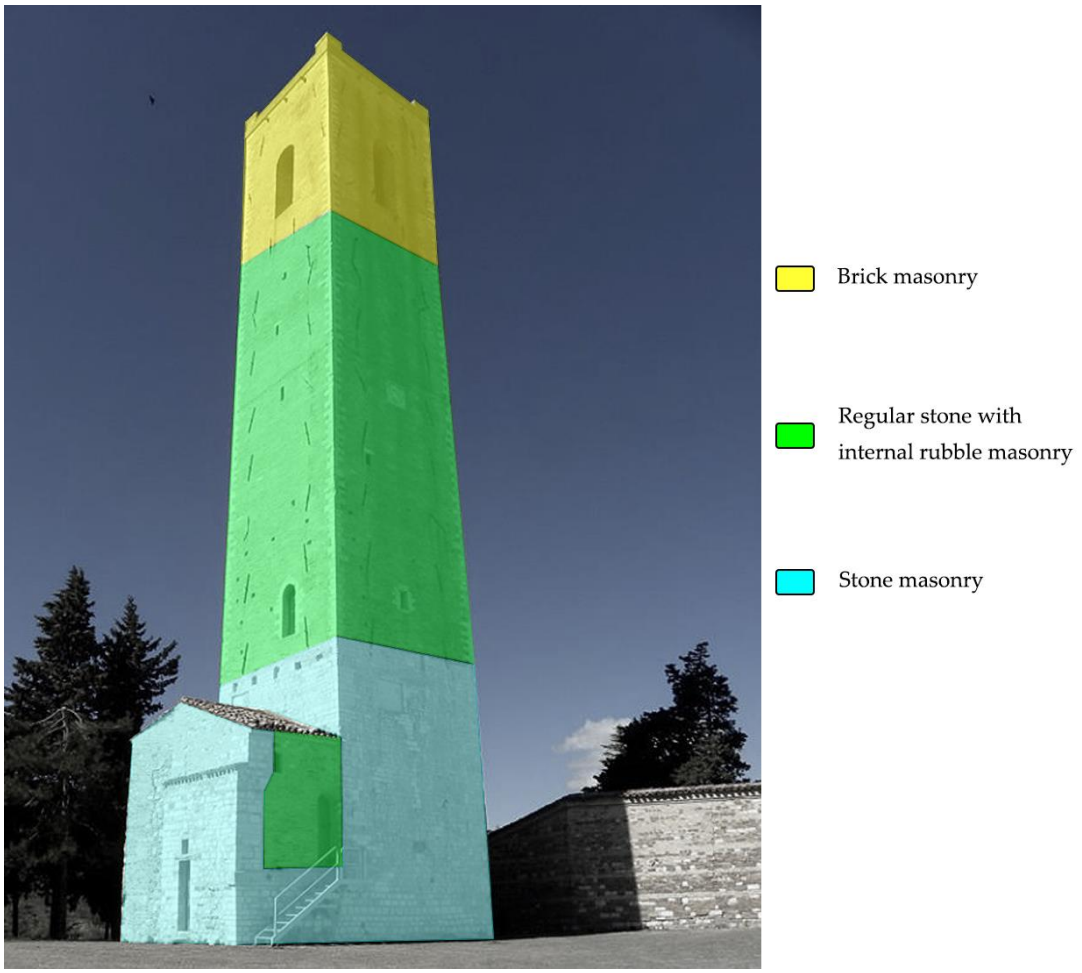

Figure 56 – *Material survey of the Smeducci Tower placed in San Severino Marche (Macerata province, Italy).*

5.3.DYNAMIC IDENTIFICATION

The health state of the Smeducci Tower has been evaluated with the use of the dynamic monitoring and OMA identification procedures.

The monitoring tasks were carried out using a sensor network made up of 4 triaxial GEA II sensors (Sequoia, Moncalieri, Italy). These are hybrid piezo-MEMS sensors with maximum measurable value of 8 g, sensitivity of 1 V/g, high dynamic range of 120 dB due to the 24-bit A/D converter. These sensors are connected using cables up

to 100 m long to a sync Hub (Sequoia, Moncalieri, Italy), which allows them to be synchronized, connected to the acquisition unit. The data were acquired and recorded by using the GEA Lab© software (Sequoia, Moncalieri, Italy).

After a brief pre-process that consists of detrending, filtering, and decimating the signal to the 0-12.5 Hz frequency range, the data are then submitted to further identification processes.

The information is then subjected to identification software analysis to derive the dynamic properties, natural frequencies, and modal shapes of the structure.

The identification software employs the time-domain Stochastic Subspace Identification (SSI) algorithm to compute the system's Frequency Response Function (FRF), from which the modal parameters are extrapolated [88].

The method for choosing the real modes is based on the modal parameter values that were determined for each order of the selected model; it allows for the introduction of comparison parameters, for which a conservatively determined acceptance threshold value can be determined. A criterion for comparing the modes is attached to three newly introduced parameters, frequency (f), modal shape (φ), and damping ratio (ξ), which correspond to the three modal parameters.

$$\Delta f = \frac{|f_1 - f_2|}{f} < 1\% \tag{5.3.1}$$

$$\Delta \xi = \frac{|\xi_1 - \xi_2|}{\xi} < 5\% \tag{5.3.2}$$

$$MAC(\varphi_1, \varphi_2) = \frac{\left|\varphi_1^T \cdot \varphi_2^*\right|^2}{(\varphi_1^T \cdot \varphi_1^*)(\varphi_2^T \cdot \varphi_2^*)} > 95\% \tag{5.3.3}$$

The M.A.C. (Modal Assurance Criterion) is used to compare the modal forms calculated at different model orders.

If all of the selection criteria are satisfied, the pole is deemed as stable. The structural modes are aligned using the stabilisation diagram, removing the purely numerical modes, and this estimate is made for each order of the model.

A modal model was created to visually represent the Tower in question. This model, excluding information on materials and boundary conditions, allows to determine the motion of each observed point at each natural frequency.

To determine how the various sensors move one another reciprocally, each point is linked to details on the modulus and phase of each modal vector (in phase or counterphase)

The following presumptions were made when graphing the modal forms:

- Rigid behavior in the plane of the various decks,
- Modal forms referring only to the x and y axes (plane),

According to the equation of Eq. 5.3.3, M.A.C. was used to verify the validity of the mode forms.

5.3.1. SENSOR LAYOUT, IDENTIFICATION OF FREQUENCIES AND MODAL SHAPE

Each accelerometer, which monitors a spatial direction, is fixed using mounting supports in groups of three orthogonal sensors (X, Y, Z). The position of accelerometers is shown in (**Figure 57**). Six recordings were made, keeping the accelerometers represented in red fixed for each recording.

This capture had a sampling frequency of 100 Hz, and it lasted 40 minutes.

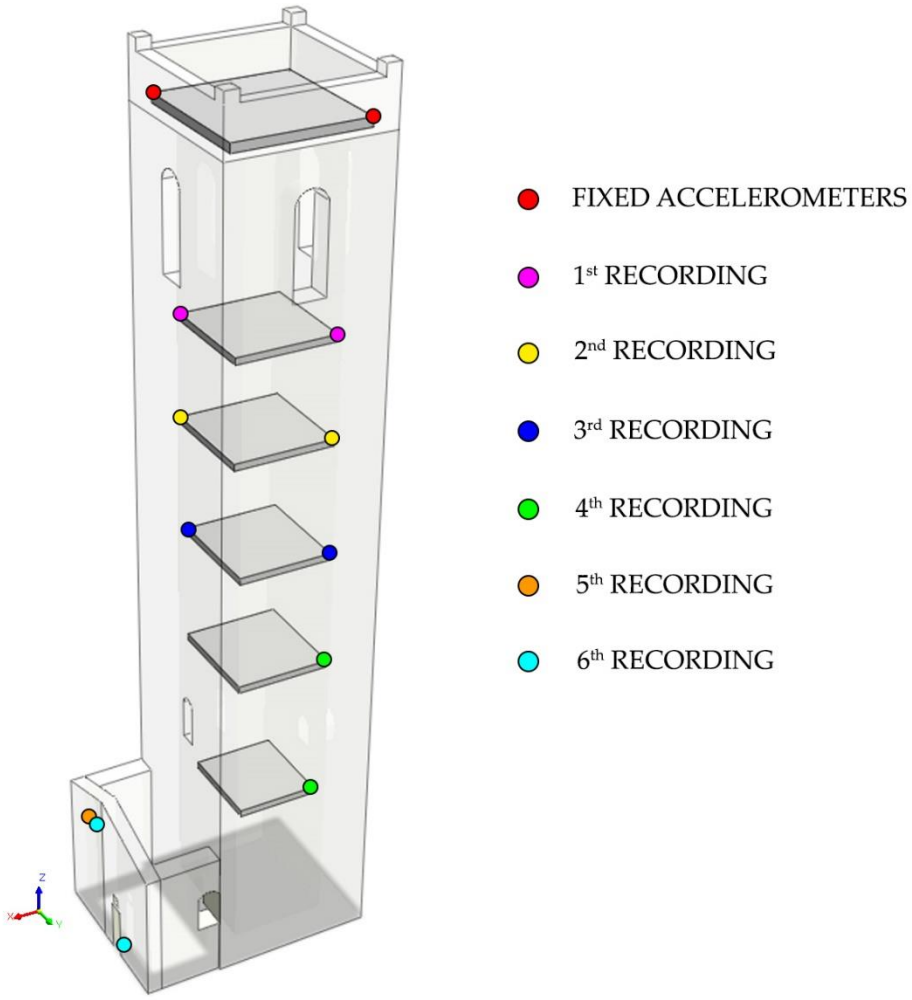

***Figure 57** – Position of the accelerometers at each recording*

Figure 58 shows the three main modal shapes and their rispectively frequencies of the Experimental Model (EM).

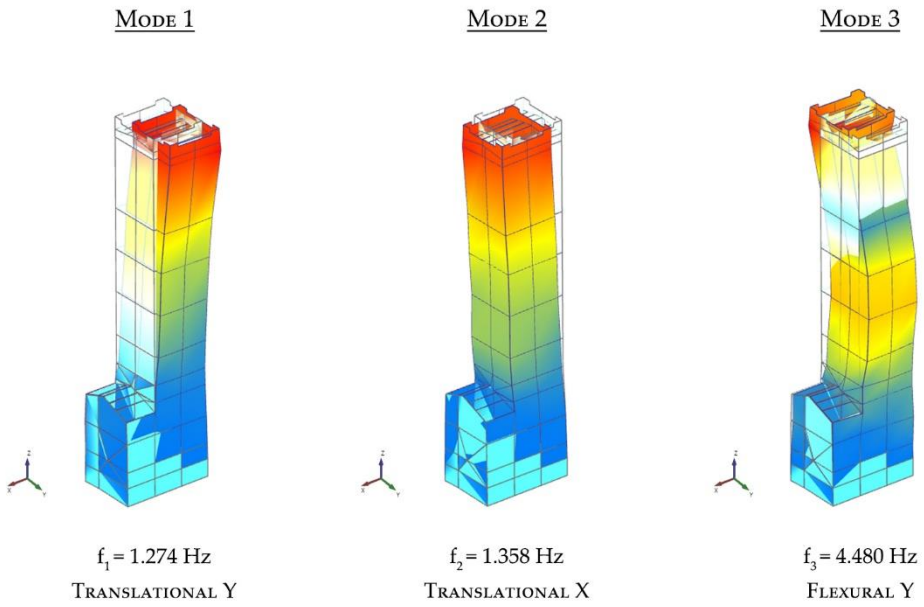

Figure 58 – *Frequencies and mode shape obtained from short time monitoring data analysis for the Smeducci Tower.*

For the purposes of the subsequent calibration process, the estimated natural frequencies (f_{exp}) and damping ratios (ξ) are reported in **Table 6** along with the Mode Complexity Factor (MCF) assigned to each mode. This scalar value, which ranges from 0% to 100%, measures how complex a mode shape is, or how much the modal vector deviates from a real-valued one [89,90]. Mode shapes with predominately imaginary components have complexity values close to 1 (MCF = 100%), whereas real-valued mode shapes have complexity values close to 0 (MCF = 0%).

Table 6 - *Global modal parameters of the EM identified for the Smeducci Tower.*

MODE	f_{EM} ***[Hz]***	ξ ***[%]***	***MCF [%]***
1	*1.274*	*2.71*	*9.09*
2	*1.358*	*2.54*	*4.12*
3	*4.480*	*0.18*	*2.75*

5.4. NUMERICAL MODEL

The main purpose of the Numerical Model (NM) is to reproduce as faithfully as possible the geometry and structural elements that make up the Smeducci Tower.

Thanks to the survey with drone and an accurate survey made in situ it was possible to obtain the 4 main façade of the Tower

To reduce computational burdens, it was considered appropriate to use a large block modelling, the 3D model was made with the Midas FEA NX© software, reproducing the blocks one by one, avoiding complex shapes, and simplifying the shape when deemed necessary.

The masonry is represented by rigid non-convex three-dimensional blocks reproducing a good interlocking between them. The openings, vaults and arches were discretized with regular blocks, and the foundation was represented with a block.

As regards the floors, it was decided to model every floors and the vaulted floors present inside the towers. This was possible thanks to the accurate survey, which made it possible to identify the various floors. In this way, the model counts 1200 blocks (Figure 59).

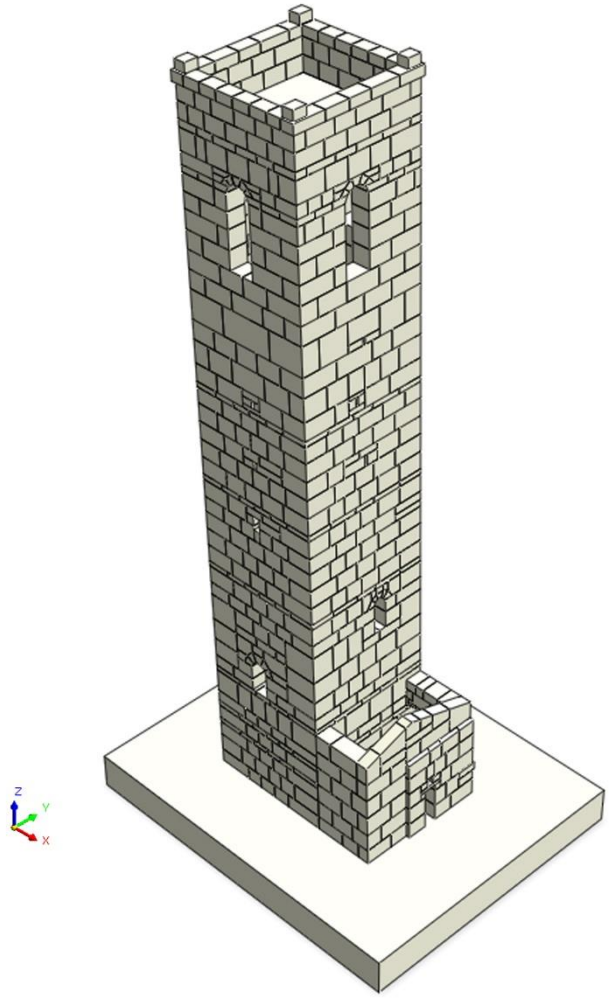

Figure 59 – *The numerical model of the Smeducci Tower placed in San Severino Marche (Macerata province, Italy).*

The structure was fixed at the base, in the initial NM (Step 0) the mechanical parameters are summarized in **Table 7**.

Table 7 – *Mechanical parameters used in the NM at Step 0.*

STEP 0		***Stone masonry***	***Regular stone with internal rubble masonry***	***Brick masonry***
Density ρ	*[kg/m³]*	*2100*	*1900*	*1800*
Joint friction μ	*-*	*27°*	*27°*	*27°*
Joint normal stiffness Jk_n	*[Pa/m]*	*70e9*	*70e9*	*70e9*
Joint shear stiffness Jk_s	*[Pa/m]*	*58e9*	*58e9*	*58e9*
Joint cohesion Jcoh	*[Pa]*	*0.1e6*	*0.1e6*	*0.1e6*
Joint tensile strength Jten	*[Pa]*	*0.1e6*	*0.1e6*	*0.1e6*

Due to the high computational burdens, the first three modal forms have been considered. The first two modal forms from a first quick view appear quite consistent with those obtained in EM (**Figure 60**).

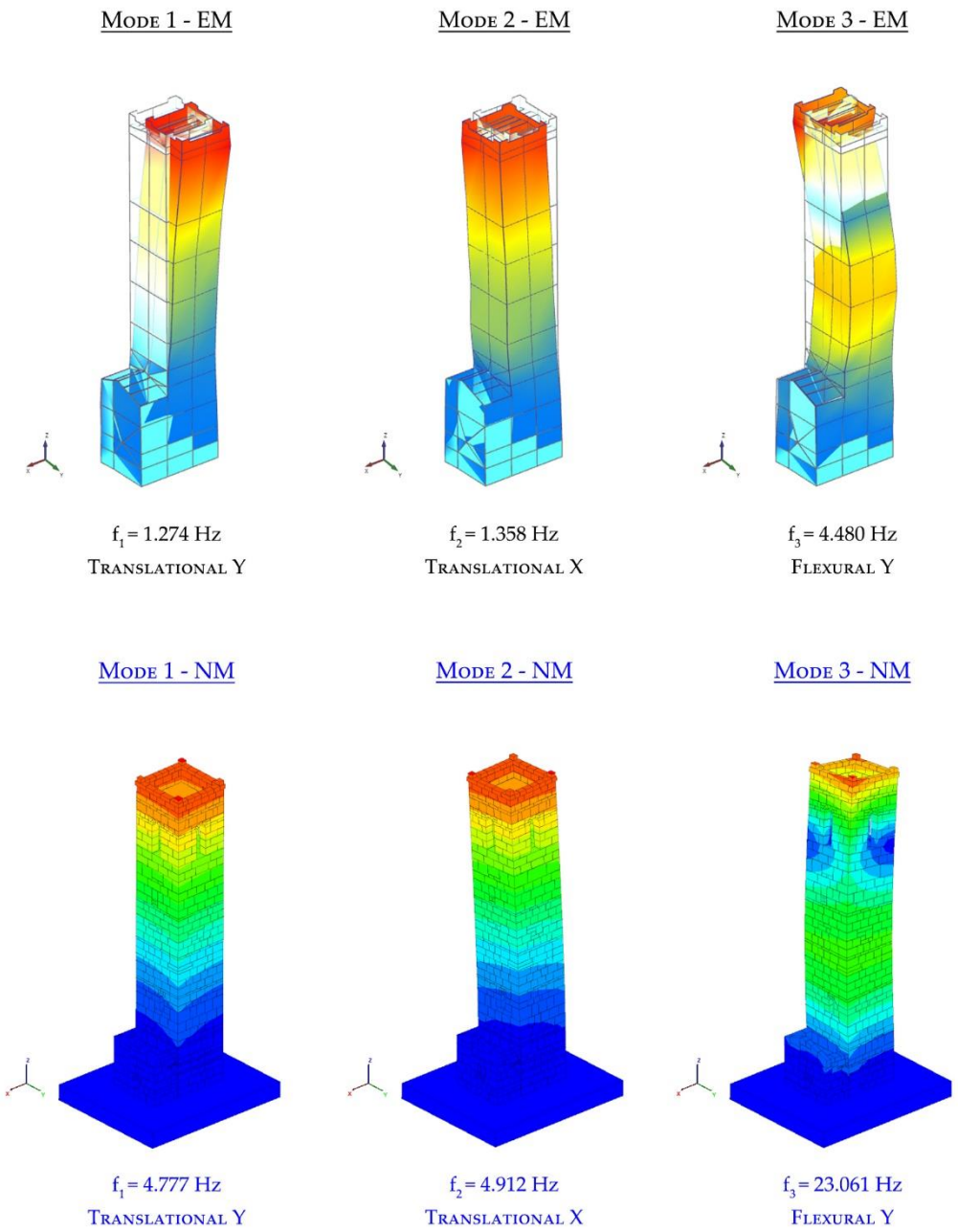

Figure 60 – *Comparison between EM and NM at Step 0.*

Instead, in **Table 8** comparing the frequencies obtained in the NM with those of the EM we note a big difference.

***Table 8** – Comparison between the EM and NM frequencies at Step 0.*

MODE	f_{EM} *[Hz]*	f_{NM} *[Hz]*	Δf_0 *[%]*	**Shape EM** *[-]*	**Shape NM** *[-]*
1	*1.274*	*4.777*	***274.961***	*Trasl. Y*	*Trasl. Y*
2	*1.358*	*4.912*	***261.708***	*Trasl. X*	*Trasl. X*
3	*4.480*	*23.061*	***414.754***	*Flex. Y*	*Flex. Y*

5.5.DEM CALIBRATION

The calibration was obtained with an iterative manual procedure in which joint normal stiffness (Jkn) and joint shear stiffness (Jks) is updated. The aim is to obtain the correspondence of modal shapes and frequencies of the NM with modal shapes and frequencies of EM.

For this purpose, different values of normal and shear stiffness have been assigned to the joints (**Table 9**), one for each type of masonry present in the tower (**Figure 56**). These compared to the values assigned to Step 0 (**Table 7**) have been reduced because the quality of the joints is not in such a condition that they can assume optimal values.

***Table 9** – Mechanical parameters used in the NM at Step 1.*

STEP 1		***Stone masonry***	***Regular stone with internal rubble masonry***	***Brick masonry***
Density ρ	*[kg/m³]*	*2100*	*1900*	*1800*
Joint friction μ	*-*	*27°*	*27°*	*27°*
Joint normal stiffness Jk_n	*[Pa/m]*	*16.7e9*	*3.83e9*	*13.3e9*
Joint shear stiffness Jk_s	*[Pa/m]*	*6.67e9*	*1.53e9*	*5.33e9*
Joint cohesion Jcoh	*[Pa]*	*0.1e6*	*0.1e6*	*0.1e6*
Joint tensile strength Jten	*[Pa]*	*0.1e6*	*0.1e6*	*0.1e6*

From the comparison between EM and NM it is also noticeable at first view that a good correspondence is not obtained in terms of modal shapes (**Figure 61**).

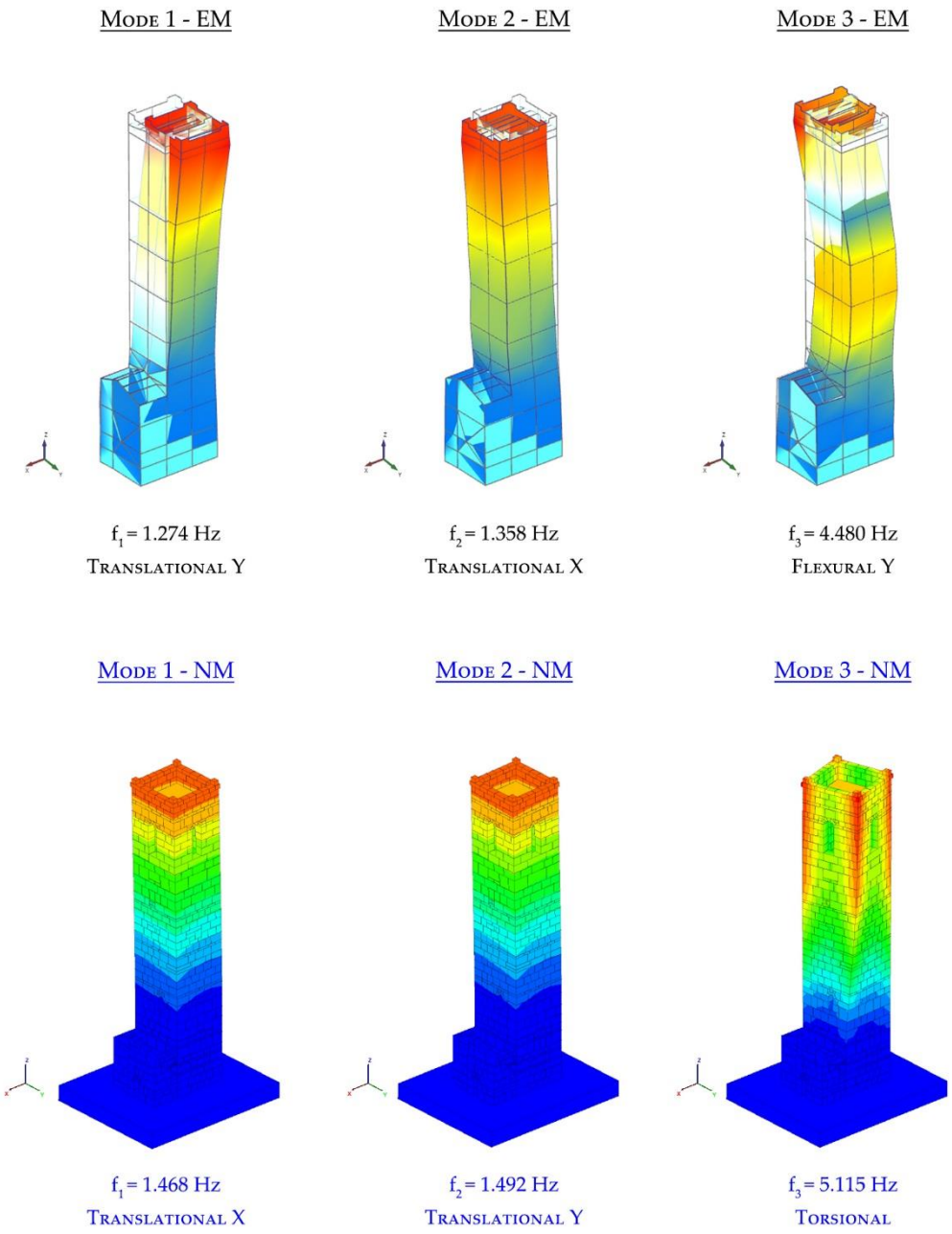

***Figure 61** – Comparison between EM and NM at Step 1.*

Despite this difference in terms of modal shapes, it was noted that the gap in terms of frequency between EM and NM was reduced **Table 10**.

Table 10 *– Comparison between the EM and NM frequencies at Step 1.*

MODE	f_{EM} *[Hz]*	f_{NM} *[Hz]*	Δf_1 *[%]*	**Shape EM** *[-]*	**Shape NM** *[-]*
1	*1.274*	*1.468*	***15.228***	*Trasl. Y*	*Trasl. X*
2	*1.358*	*1.492*	***9.867***	*Trasl. X*	*Trasl. Y*
3	*4.480*	*5.115*	***14.174***	*Flex. Y*	*Tors.*

Finally, in Step 2 it was noted that the central part of the body of the tower (in purple color) compared to the sides is in better condition, therefore, a further distinction was made (**Figure 62**).

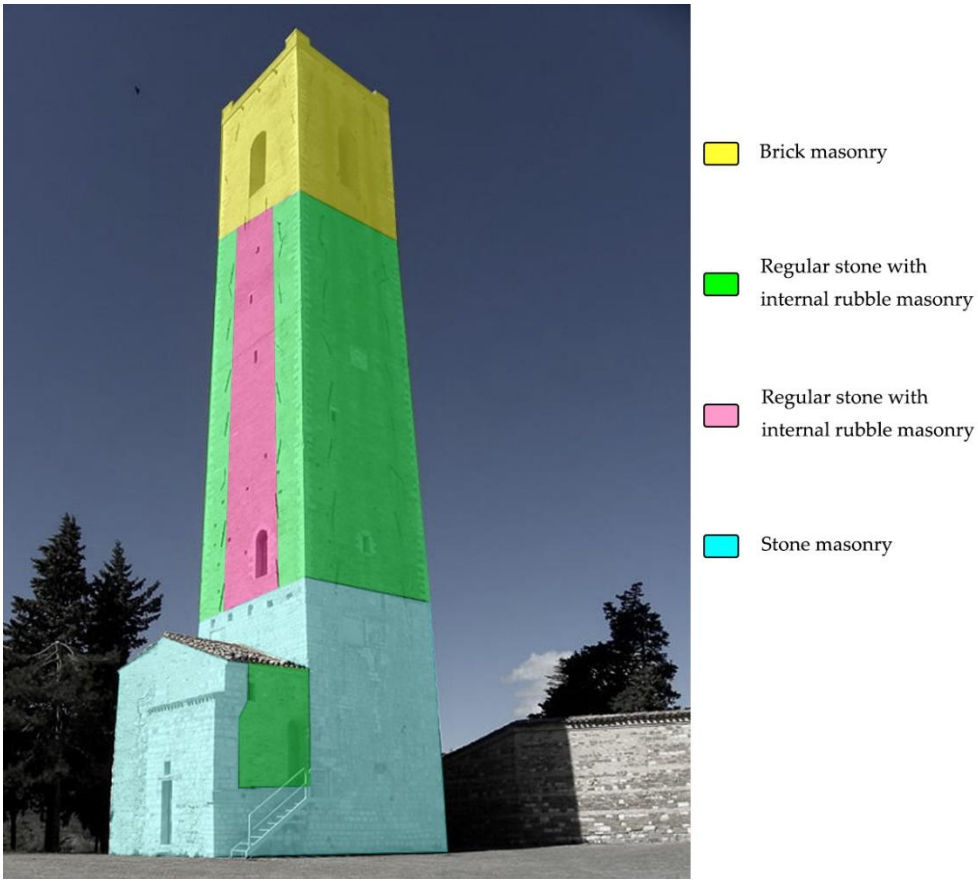

Figure 62 *– Material distinction in Step 2.*

The parameter that most influences the values of the frequencies is the joint normal stiffness (Jkn), at this purpose in Step 2, the values of the joint normal stiffness have been further reduced but at the same time those of the joint shear stiffness (Jkn) have been increased as it has been seen that this parameter affects the modal shape (**Table 11**).

Table 11 – *Comparison between the EM and NM frequencies at Step 2 where (*) indicates the values assigned to masonry in purple color (**Figure 62**).*

STEP 2		***Stone masonry***	***Regular stone with internal rubble masonry***	***Brick masonry***
Density ρ	*[kg/m³]*	*2100*	*1900*	*1800*
Joint friction μ	*-*	*27°*	*27°*	*27°*
Joint normal stiffness Jk_n	*[Pa/m]*	*5.0e9*	*2.5e9 4.5e9**	*0.8e9*
Joint shear stiffness Jk_s	*[Pa/m]*	*42.0e9*	*30.0e9 40.0e9**	*20.0e9*
Joint cohesion Jcoh	*[Pa]*	*0.1e6*	*0.1e6*	*0.1e6*
Joint tensile strength Jten	*[Pa]*	*0.1e6*	*0.1e6*	*0.1e6*

These values allow to obtain, unlike Step 1, modal shapes comparable between EM and NM as shown in **Figure 63**.

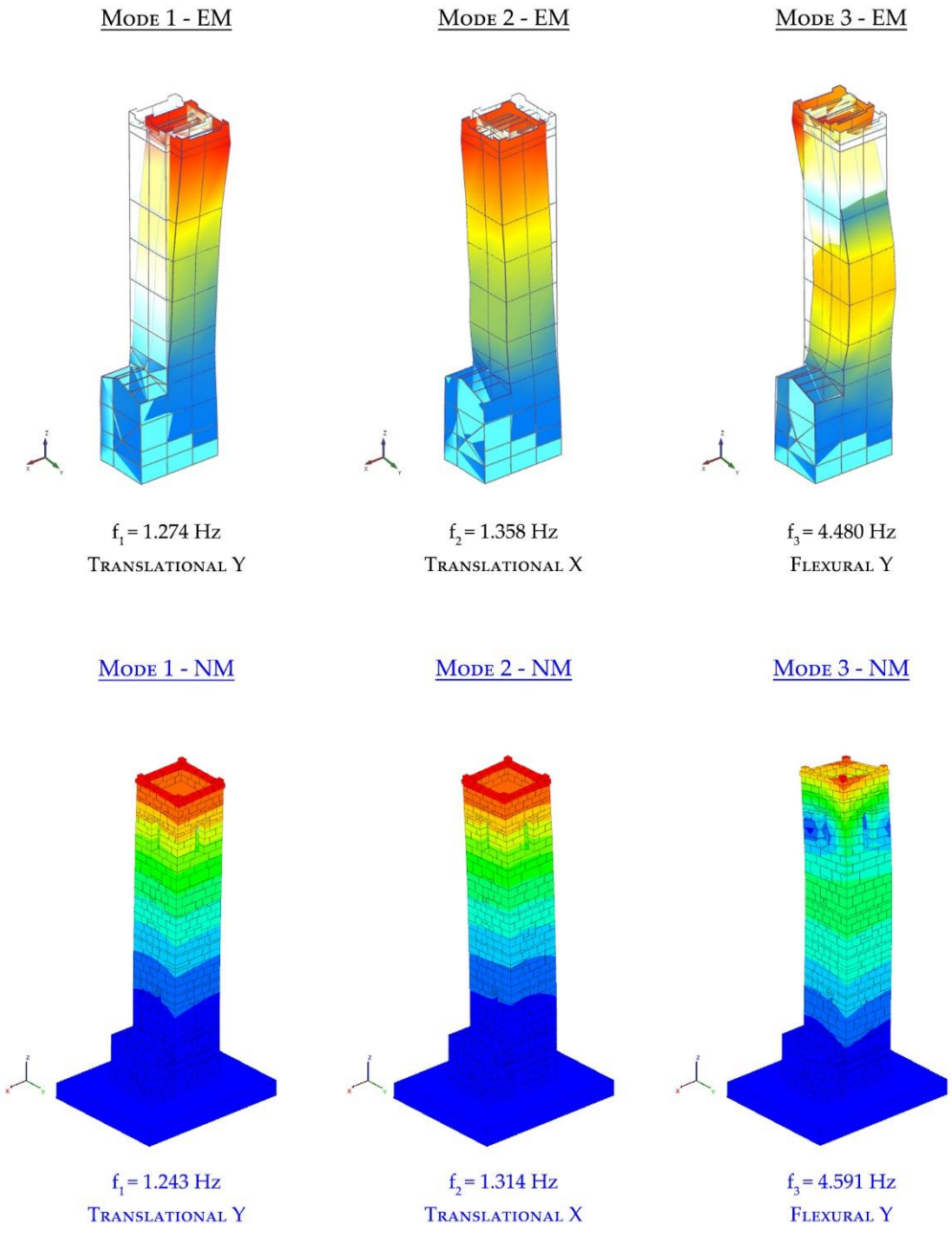

***Figure 63** – Comparison between EM and NM at Step 2.*

Acceptable values are those that show a percentage difference in terms of frequencies lower than 5%, in **Table 12** the values obtained are shown highlighting that all be included in the limits of this threshold.

***Table 12** – Comparison between the EM and NM frequencies at Step 2.*

MODE	f_{EM} *[Hz]*	f_{NM} *[Hz]*	Δf_2 *[%]*	**Shape EM** *[-]*	**Shape NM** *[-]*
1	*1.274*	*1.243*	***2.433***	*Trasl. Y*	*Trasl. Y*
2	*1.358*	*1.314*	***3.240***	*Trasl. X*	*Trasl. X*
3	*4.480*	*4.591*	***2.478***	*Flex. Y*	*Flex. Y*

According to the results obtained, the manual calibration technique produced a good (quantitative) match in terms of frequencies. Using the modal assurance criterion, a further comparison between EM and NM for modal shapes can be conducted in order to obtain a quantitative measurement (MAC).

The optimal result is obtain when the values on the main diagonal are equal to 1, while outside the main diagonal are equal to 0.

In the following figures (**Figure 64**, **Figure 65** and **Figure 66**) the CrossMACs between EM and NM at each calibration step are shown.

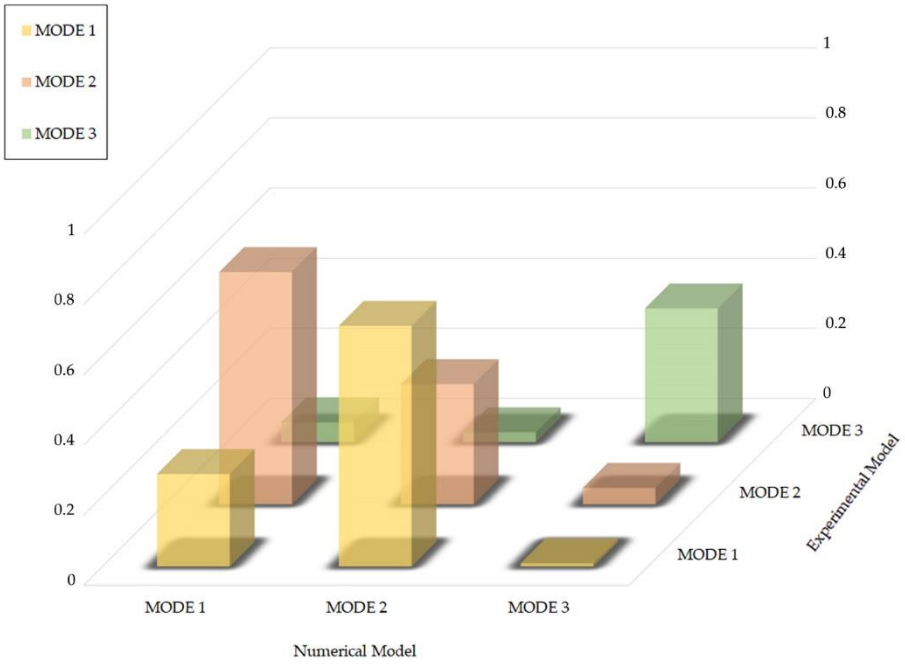

***Figure 64** – Cross Modal Assurance Criterio (CrossMAC) between EM and NM at Step 0.*

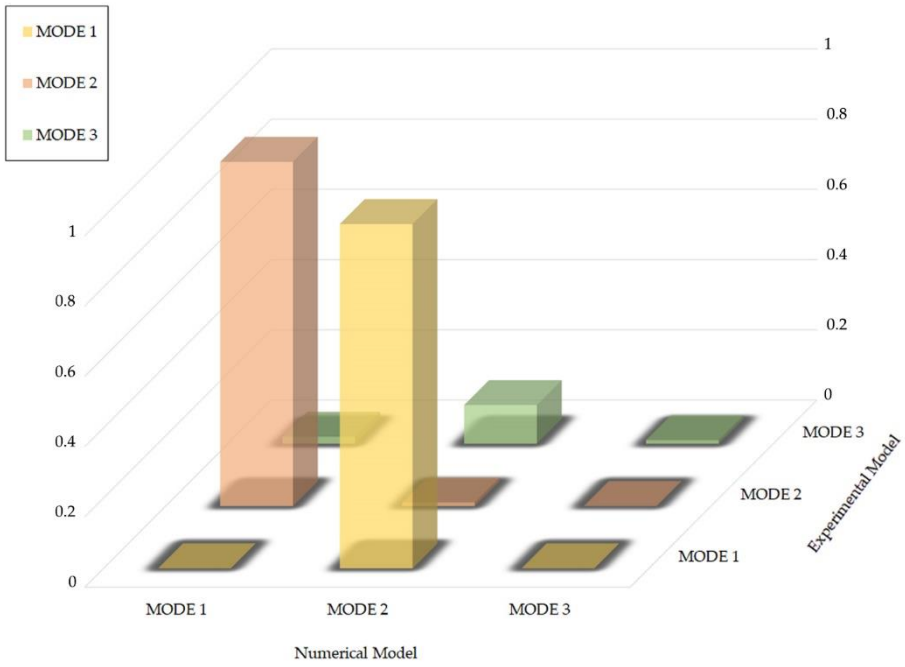

Figure 65 – *Cross Modal Assurance Criterio (CrossMAC) between EM and NM at Step 1.*

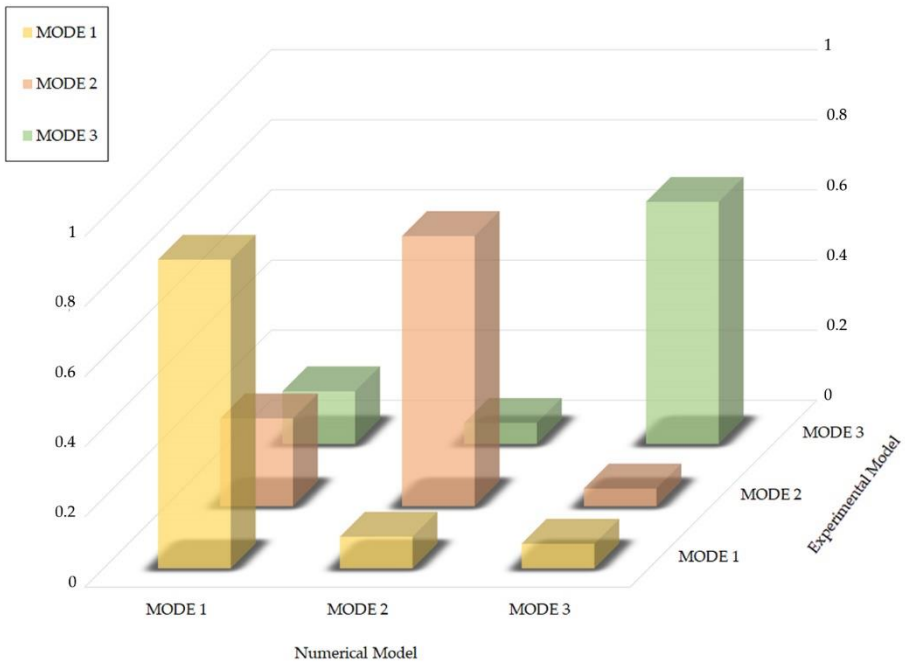

Figure 66 – *Cross Modal Assurance Criterio (CrossMAC) between EM and NM at Step 2.*

The direct cross-validation between EM and NM mode shapes through the MAC further proves the satisfactory agreement between experimental and numerical counterparts.

The results in Step 2 are not to close to the optimal solution with values equal to 1 in the main diagonal, but they show a value higher than 0.75 in all modes. The values decrease from the first to the third mode, in fact, the first mode show a value equal to 0.883, the second one equal to 0.771 and the last equal to 0.754 (**Figure 66**).

It is worth highlighting the relevance of the achieved results, in fact, it is a first proof and the literature in this field is somewhat lacking, if not totally absent.

6| CONCLUSIONS

This thesis work focuses on the conservation of cultural heritage that make up the Italian historical and artistic heritage. The study is done through continuous and discontinuous numerical models.

In the literature there are several works with continuous models for the study of the vulnerability of historical structures, as regards discrete modeling, this initially used for the representation of granular materials, thanks to the progress of computer science, has also been applied on a large scale.

Therefore, two approaches to discontinuous (DMs) and one to continuous (CM) have been compared in **Chapter 3**|. In the CM approach masonry was represented as a continuous medium and the nonlinearity was assigned different constitutive laws in tension and compression. In the DMs approaches, two methods wer used: one smooth and the other non-smooth. Masonry was modeled as an assembly of discrete blocks, and the non-linearity was assigned to their interactions.

The structural response during the Central Italy seismic sequence in 2016 was simulated by considering the whole structure (real configuration) and the tower alone in order to understand how much the palace's presence affected the tower's damage.

Comparing the two DMs approaches the results are comparable for all the analyses performed. Both CM and DMs approaches showed that in the real structural configuration, the points that suffered more damage were those on the upper part of the tower, having measured the largest plastic deformation. Another vulnerable point identified by both of them was the palace section close to the tower that showed vertical cracks between the openings and in the connection palace-tower.

The numerical models' damage showed that the DMs were able to retrace the real cracks present in the tower compared to the CM. Indeed, the cracks that occurred

highlighted the activation of the out-of-plane mechanism of the tower's corners that can be identified only with DMs. It must be underlined that this behavior is commonly observed on old towers excited by quakes. Both CM and DMs, on the other hand, accurately simulated the cracks caused by in-plane mechanisms that were visible in the building between the entrance openings and at the tower connection.

The study of the isolated tower led to additional considerations. CM and DMs react differently. The tower in the CM exhibited the typical behavior of a cantilever beam cracking only near the base. This meant that the top plastic displacements were less than in the previous condition. Instead, both DMs, particularly the one that used the non-smooth contact law, displayed higher irreversible displacement whereas the type of damage remained constant. In other words, as in the whole model, the DMs of the isolated tower were characterized by the activation of the corners overturning, which began at a lower height in this case.

This demonstrated the importance of using the correct masonry modeling technique when analyzing old masonry towers, particularly isolated ones. Indeed, due to their constant exposure to atmospheric agents and poor state of conservation, they frequently exhibit out-of-plane mechanisms that are unrepeatable using continuous FEM.

In **Chapter 4**| the role of irregular stones was investigated. The behaviour of the Amatrice Civic Tower was studied with the discontinuous approach implemented in the 3DEC© code.

Two discontinuous models were compared using two different stereotomies: in one, the irregular stones were approximated to regular one (Model I) and in the other, the irregularity of these stones is faithfully reproduced (Model R). The contribution of the interventions (real configuration) present in the tower was also evaluated both in the numerical model with regular stones (Model IR) and in that with irregular one (Model RR).

To investigate these aspects, non-linear dynamic analyses were carried out by applying the seismic sequence of Central Italy to the four numerical models, considering the events recorded near the Civic Tower.

Comparing the state of the damage of the numerical models without intervention with the real state of the structure does not obtain comparable results. Both models identify the belfry as the most vulnerable part, the collapse, however, unlike reality, occurs following the first event. On the other hand, models (Model I and Model R) show comparable behavior both in terms of damage and displacement.

A clearer picture is obtained by comparing the models with the reinforcement interventions. In fact, comparing the models, we note how the Model IR shows a better behaviour following the horizontal load of the earthquake, while in the Model RR there are vulnerabilities in the correspondence of the belfry already following the first event and then to the collapse following the last event of the seismic sequence of Central Italy. The behaviour of the Model RR is close to reality and it is confirmed by the real state of the Tower, which suffered damage following the first event coming to the collapse with the last shock.This demonstrates the importance of a correct evaluation in the modeling phase, where the approximation of stereotomy can lead to untrue and misleading results. Precisely for this reason, using simplified modeling in favor of lower computational burdens can compromise the reliability of the results, it is therefore correct, in the case of erratic and chaotic masonry, to take into account their stereotomy in order to obtain results faithful to reality.

Chapter 5| started from the direct observation of the dynamic characteristics of Smeducci Tower through OMA with the aim of obtain a DEM calibration.

The calibration was carried out considering a large blocks model, without neglecting the inclination of the tower and the main structural components that characterize it.

The Smeducci Tower is characterized by three different types of masonry, these have been considered by assigning different values to the masonry. The calibration was performed by changing the parameters of normal and shear stiffness, as regards

the values of cohesion and tensile strength, these remained unchanged as they do not significantly affect the modal shapes.

In detail, analyzing the results obtained with manual calibration, it was seen that there is a valid match between the numerical frequencies and the experimental ones, in fact, a percentage difference of less than 5% is obtained. CrossMAC, on the other shows acceptable but not extremely accurate values.

To achieve more accurate values in terms of CrossMAC, numerical model with a high degree of detail should be used. This aspect is not negligible, as it would further increase the already high computational burdens.

Moreover, with the computer available (Intel Core Processor 2.40 GHz with 20 processors, and 224 GB of RAM) it is not possible to perform modal analysis with a number of blocks greater than those used in this thesis work.

This is an aspect that will be investigated in the future with more performing computers.

Other discrete approaches application of large-scale structures are now being developed in order to improve the current knowledge in this area of research.

All this was done to obtain a digital twin, i.e., starting from the survey and experimental investigations, realising a numerical model as realistic as possible using the DEM approach, monitoring the structure, and applying the events recorded during the monitoring to the numerical model. In this way, it is possible to observe the update of the damage on the structure, thus going to work on the quantification and localization of the damage. On models that use FEM approaches, this could be a harbinger of some approximations since damage is treated as a parameter of damage and it is not possible to consider borderline situations such as collapses.

Finally, an aspect to be taken into consideration for future research is the soil-structure iteration in precise conditions of the site, an aspect that does not concern this thesis work, the soil has been represented in a rough way without taking into account the mechanical properties of the soil.

BIBLIOGRAPHY

[1] A. Rovida, M. Locati, R. Camassi, B. Lolli, P. Gasperini, The Italian earthquake catalogue CPTI15, Bull. Earthq. Eng. 18 (2020) 2953–2984. https://doi.org/10.1007/s10518-020-00818-y.

[2] F. Monni, F. Clementi, E. Quagliarini, E. Giordano, S. Lenci, Seismic Assessment of Cultural Heritage: Nonlinear 3d Analyses of "Santa Maria Della Carità" in Ascoli Piceno, in: Proc. 6th Int. Conf. Comput. Methods Struct. Dyn. Earthq. Eng. (COMPDYN 2015), Institute of Structural Analysis and Antiseismic Research School of Civil Engineering National Technical University of Athens (NTUA) Greece, Athens, 2017: pp. 2533–2541. https://doi.org/10.7712/120117.5586.18082.

[3] M. Acito, M. Bocciarelli, C. Chesi, G. Milani, Collapse of the clock tower in Finale Emilia after the May 2012 Emilia Romagna earthquake sequence: Numerical insight, Eng. Struct. 72 (2014) 70–91. https://doi.org/10.1016/j.engstruct.2014.04.026.

[4] G. Milani, Lesson learned after the Emilia-Romagna, Italy, 20–29 May 2012 earthquakes: A limit analysis insight on three masonry churches, Eng. Fail. Anal. 34 (2013) 761–778. https://doi.org/10.1016/j.engfailanal.2013.01.001.

[5] F. Clementi, A. Ferrante, E. Giordano, F. Dubois, S. Lenci, Damage assessment of ancient masonry churches stroked by the Central Italy earthquakes of 2016 by the non-smooth contact dynamics method, Bull. Earthq. Eng. (2019). https://doi.org/10.1007/s10518-019-00613-4.

[6] G. De Matteis, M. Zizi, Preliminary Analysis on the Effects of 2016 Central Italy Earthquake on One-Nave Churches, in: 2019: pp. 1268–1279. https://doi.org/10.1007/978-3-319-99441-3_136.

[7] F. Clementi, A. Ferrante, E. Ribilotta, G. Milani, S. Lenci, On the dynamics of the civic clock tower of Rotella (Ascoli Piceno) severly damaged by the Central Italy seismic sequence of 2016, in: Atti Del XVIII Convegno ANIDIS L'ingegneria Sismica Ital. Ascoli Piceno, 15-19 Settembre 2019, Pisa University Press, Pisa, 2019. https://doi.org/10.1400/271235.

[8] F. Clementi, E. Giordano, A. Ferrante, S. Lenci, Damage survey and advanced seismic analyses of different masonry churches after the central Italy earthquake of 2016, in: COMPDYN Proc., Institute of Structural Analysis and Antiseismic Research School of Civil Engineering National Technical University of Athens (NTUA) Greece, Athens, 2019: pp. 1321–1328. https://doi.org/10.7712/120119.7000.19094.

[9] R. Pluijm, van der, Shear behaviour of bed joints, 6th North Am. Mason. Conf. 6-9 June 1993, Philadelphia, Pennsylvania, USA. (1993) 125–136.

[10] M. Mosoarca, I. Onescu, E. Onescu, A. Anastasiadis, Seismic vulnerability assessment methodology for historic masonry buildings in the near-field areas, Eng. Fail. Anal. 115 (2020) 104662. https://doi.org/10.1016/j.engfailanal.2020.104662.

[11] M. Mosoarca, V. Gioncu, Failure mechanisms for historical religious buildings in Romanian seismic areas, J. Cult. Herit. 14 (2013) e65–e72. https://doi.org/10.1016/j.culher.2012.11.018.

[12] A. Formisano, G. Vaiano, F. Fabbrocino, G. Milani, Seismic vulnerability of Italian masonry churches: The case of the Nativity of Blessed Virgin Mary in Stellata of Bondeno, J. Build. Eng. 20 (2018) 179–200. https://doi.org/10.1016/j.jobe.2018.07.017.

[13] G. Lancioni, S. Lenci, Q. Piattoni, E. Quagliarini, Dynamics and failure mechanisms of ancient masonry churches subjected to seismic actions by using the NSCD method: The case of the medieval church of S. Maria in Portuno, Eng. Struct. 56 (2013) 1527–1546. https://doi.org/10.1016/j.engstruct.2013.07.027.

[14] B. Pulatsu, E. Erdogmus, P.B. Lourenço, Comparison of in-plane and out-of-plane failure modes of masonry arch bridges using discontinuum analysis, Eng. Struct. 178 (2019) 24–36. https://doi.org/10.1016/j.engstruct.2018.10.016.

[15] D. V. Oliveira, P.B. Lourenço, P. Roca, Cyclic behaviour of stone and brick masonry under uniaxial compressive loading, Mater. Struct. 39 (2007) 247–257. https://doi.org/10.1617/s11527-005-9050-3.

[16] P.B. Lourenço, Recent advances in masonry modelling: micromodelling and homogenisation, in: Multiscale Model. Solid Mech. Comput. Approaches, 2009: pp. 251–294. https://doi.org/10.1142/9781848163089_0006.

[17] P. Taforel, F. Dubois, S. Pagano, Evaluation of numerical uncertainties on the modeling of dry masonry structures submitted to out-of-plane loading, using the NSCD method in comparison with experimental test, in: ECCOMAS 2012 - Eur. Congr. Comput. Methods Appl. Sci. Eng. E-b. Full Pap., European Congress on Computational Methods in Applied Sciences and Engineering, 2012: pp. 7698–7716. https://hal.archives-ouvertes.fr/hal-00806832.

[18] B. Pantò, F. Cannizzaro, S. Caddemi, I. Caliò, 3D macro-element modelling approach for seismic assessment of historical masonry churches, Adv. Eng. Softw. 97 (2016) 40–59. https://doi.org/10.1016/J.ADVENGSOFT.2016.02.009.

[19] P.B. Lourenco, Computational strategies for masonry structures, 1996. https://doi.org/ISBN 90-407-1221-2.

[20] M. Valente, G. Milani, Seismic response and damage patterns of masonry churches: Seven case studies in Ferrara, Italy, Eng. Struct. 177 (2018) 809–835. https://doi.org/10.1016/j.engstruct.2018.08.071.

[21] J. Ortega, G. Vasconcelos, H. Rodrigues, M. Correia, P.B. Lourenço, Traditional earthquake resistant techniques for vernacular architecture and local seismic cultures: A literature review, J. Cult. Herit. 27 (2017) 181–196. https://doi.org/10.1016/j.culher.2017.02.015.

[22] A. Formisano, G. Milani, Seismic Vulnerability Analysis and Retrofitting of the SS. Rosario Church Bell Tower in Finale Emilia (Modena, Italy), Front. Built

Environ. 5 (2019) 70. https://doi.org/10.3389/fbuil.2019.00070.

[23] T.M. Ferreira, N. Mendes, R. Silva, Multiscale Seismic Vulnerability Assessment and Retrofit of Existing Masonry Buildings, Buildings. 9 (2019) 91. https://doi.org/10.3390/buildings9040091.

[24] D. V. Oliveira, I. Basilio, P.B. Lourenço, Experimental Behavior of FRP Strengthened Masonry Arches, J. Compos. Constr. 14 (2010) 312–322. https://doi.org/10.1061/(ASCE)CC.1943-5614.0000086.

[25] D. V. Oliveira, R.A. Silva, E. Garbin, P.B. Lourenço, Strengthening of three-leaf stone masonry walls: an experimental research, Mater. Struct. 45 (2012) 1259–1276. https://doi.org/10.1617/s11527-012-9832-3.

[26] M. Mosoarca, I. Apostol, A. Keller, A. Formisano, Consolidation Methods of Romanian Historical Building with Composite Materials, Key Eng. Mater. 747 (2017) 406–413. https://doi.org/10.4028/www.scientific.net/KEM.747.406.

[27] L. Jing, A review of techniques, advances and outstanding issues in numerical modelling for rock mechanics and rock engineering, Int. J. Rock Mech. Min. Sci. 40 (2003) 283–353. https://doi.org/10.1016/S1365-1609(03)00013-3.

[28] R.W. Clough, Original formulation of the finite element method, Finite Elem. Anal. Des. 7 (1990) 89–101. https://doi.org/10.1016/0168-874X(90)90001-U.

[29] P.A. Cundall, A computer model for simulating progressive large-scale movements in blocky rock systems, in: Proocedings Symp. Int. Soc. Rock Mech. Nancy 2, 1971.

[30] P.A. Cundall, O.D.L. Strack, A discrete numerical model for granular assemblies, Geotechnique. 29 (1979) 47–65. https://doi.org/10.1680/geot.1979.29.1.47.

[31] V. Sarhosis, G. Milani, A. Formisano, F. Fabbrocino, Evaluation of different approaches for the estimation of the seismic vulnerability of masonry towers, Bull. Earthq. Eng. 16 (2018) 1511–1545. https://doi.org/10.1007/s10518-017-0258-8.

[32] P.B. Lourenço, N. Mendes, L.F. Ramos, D. V. Oliveira, Analysis of Masonry

Structures Without Box Behavior, Int. J. Archit. Herit. 5 (2011) 369–382. https://doi.org/10.1080/15583058.2010.528824.

[33] V. Sarhosis, J. V Lemos, A detailed micro-modelling approach for the structural analysis of masonry assemblages, Comput. Struct. 206 (2018) 66–81. https://doi.org/10.1016/j.compstruc.2018.06.003.

[34] A. Ferrante, E. Giordano, F. Clementi, G. Milani, A. Formisano, FE vs. DE Modeling for the Nonlinear Dynamics of a Historic Church in Central Italy, Geosciences. 11 (2021) 189. https://doi.org/10.3390/geosciences11050189.

[35] F. Clementi, E. Quagliarini, F. Monni, E. Giordano, S. Lenci, Cultural Heritage and Earthquake: The Case Study of "Santa Maria Della Carità" in Ascoli Piceno, Open Civ. Eng. J. 11 (2017) 1079–1105. https://doi.org/10.2174/1874149501711011079.

[36] G. Bartoli, M. Betti, S. Monchetti, Seismic Risk Assessment of Historic Masonry Towers: Comparison of Four Case Studies, J. Perform. Constr. Facil. 31 (2017) 4017039. https://doi.org/10.1061/(ASCE)CF.1943-5509.0001039.

[37] A. Rafiee, M. Vinches, Mechanical behaviour of a stone masonry bridge assessed using an implicit discrete element method, Eng. Struct. 48 (2013) 739–749. https://doi.org/10.1016/j.engstruct.2012.11.035.

[38] D. Baraldi, C.B. de Carvalho Bello, A. Cecchi, E. Meroi, E. Reccia, NONLINEAR BEHAVIOR OF MASONRY WALLS: FE, DE, AND FE/DE MODELS, Compos. Mech. Comput. Appl. An Int. J. 10 (2019) 253–272. https://doi.org/10.1615/CompMechComputApplIntJ.2019026998.

[39] D. Baraldi, E. Reccia, A. Cecchi, In plane loaded masonry walls: DEM and FEM/DEM models. A critical review, Meccanica. 53 (2018) 1613–1628. https://doi.org/10.1007/s11012-017-0704-3.

[40] T.T. Bui, A. Limam, V. Sarhosis, M. Hjiaj, Discrete element modelling of the in-plane and out-of-plane behaviour of dry-joint masonry wall constructions, Eng. Struct. 136 (2017) 277–294. https://doi.org/10.1016/j.engstruct.2017.01.020.

[41] B. Pulatsu, E.M. Bretas, P.B. Lourenco, Discrete element modeling of masonry

structures: Validation and application, Earthquakes Struct. 11 (2016) 563–582. https://doi.org/10.12989/eas.2016.11.4.563.

[42] N. Bianchini, N. Mendes, P. Candeias, M. Rossi, C. Calderini, P. Lourenço, A. Costa, Seismic Performance of Masonry Cross Vaults through Shaking Table Testing on a Scaled Model, in: 12th Int. Conf. Struct. Anal. Hist. Constr., CIMNE, 2021. https://doi.org/10.23967/sahc.2021.230.

[43] N. Mendes, S. Zanotti, J. V. Lemos, Seismic Performance of Historical Buildings Based on Discrete Element Method: An Adobe Church, J. Earthq. Eng. 24 (2020) 1270–1289. https://doi.org/10.1080/13632469.2018.1463879.

[44] A. Ferrante, D. Loverdos, F. Clementi, G. Milani, A. Formisano, S. Lenci, V. Sarhosis, Discontinuous approaches for nonlinear dynamic analyses of an ancient masonry tower, Eng. Struct. 230 (2021) 111626. https://doi.org/10.1016/j.engstruct.2020.111626.

[45] B. Pulatsu, F. Gencer, E. Erdogmus, Study of the effect of construction techniques on the seismic capacity of ancient dry-joint masonry towers through DEM, Eur. J. Environ. Civ. Eng. 26 (2022) 3913–3930. https://doi.org/10.1080/19648189.2020.1824823.

[46] E. Çaktı, Ö. Saygılı, J. V. Lemos, C.S. Oliveira, Nonlinear dynamic response of stone masonry minarets under harmonic excitation, Bull. Earthq. Eng. 18 (2020) 4813–4838. https://doi.org/10.1007/s10518-020-00888-y.

[47] J. Lemos, Discrete Element Modeling of the Seismic Behavior of Masonry Construction, Buildings. 9 (2019) 43. https://doi.org/10.3390/buildings9020043.

[48] J. V Lemos, Discrete Element Modeling of Masonry Structures, Int. J. Archit. Herit. 1 (2007) 190–213. https://doi.org/10.1080/15583050601176868.

[49] F. Dubois, V. Acary, M. Jean, The Contact Dynamics method: A nonsmooth story, Comptes Rendus Mécanique. 346 (2018) 247–262. https://doi.org/10.1016/j.crme.2017.12.009.

[50] V. Acary, Energy conservation and dissipation properties of time-integration methods for nonsmooth elastodynamics with contact, ZAMM - J. Appl. Math.

Mech. / Zeitschrift Für Angew. Math. Und Mech. 96 (2016) 585–603. https://doi.org/10.1002/zamm.201400231.

[51] V. Beatini, G. Royer-Carfagni, A. Tasora, A non-smooth-contact-dynamics analysis of Brunelleschi's cupola: an octagonal vault or a circular dome?, Meccanica. 54 (2019) 525–547. https://doi.org/10.1007/s11012-018-00934-9.

[52] M. Schiavoni, A. Ferrante, G.P. Salachoris, C. Mariotti, F. Clementi, Out-of-plane seismic response of a masonry facade using distinct element methods, Int. J. Mason. Res. Innov. 1 (2022) 1. https://doi.org/10.1504/IJMRI.2022.10051745.

[53] A. Ferrante, M. Schiavoni, F. Bianconi, G. Milani, F. Clementi, Influence of Stereotomy on Discrete Approaches Applied to an Ancient Church in Muccia, Italy, J. Eng. Mech. 147 (2021) 04021103. https://doi.org/10.1061/(ASCE)EM.1943-7889.0002000.

[54] G. Bartoli, M. Betti, A. Vignoli, A numerical study on seismic risk assessment of historic masonry towers: a case study in San Gimignano, Bull. Earthq. Eng. 14 (2016) 1475–1518. https://doi.org/10.1007/s10518-016-9892-9.

[55] E. Magrinelli, M. Acito, M. Bocciarelli, Numerical insight on the interaction effects of a confined masonry tower, Eng. Struct. 237 (2021) 112195. https://doi.org/10.1016/j.engstruct.2021.112195.

[56] S. Degli Abbati, A.M. D'Altri, D. Ottonelli, G. Castellazzi, S. Cattari, S. de Miranda, S. Lagomarsino, Seismic assessment of interacting structural units in complex historic masonry constructions by nonlinear static analyses, Comput. Struct. 213 (2019) 51–71. https://doi.org/10.1016/j.compstruc.2018.12.001.

[57] A. Pierdicca, F. Clementi, P. Mezzapelle, A. Fortunati, S. Lenci, One-year monitoring of a reinforced concrete school building: Evolution of dynamic behavior during retrofitting works, Procedia Eng. 199 (2017) 2238–2243. https://doi.org/10.1016/j.proeng.2017.09.206.

[58] G. Standoli, E. Giordano, G. Milani, F. Clementi, Model Updating of Historical Belfries Based on Oma Identification Techniques, Int. J. Archit. Herit. (2020) 1–

25. https://doi.org/10.1080/15583058.2020.1723735.

[59] F. Bianconi, G.P. Salachoris, F. Clementi, S. Lenci, A Genetic Algorithm Procedure for the Automatic Updating of FEM Based on Ambient Vibration Tests, Sensors. 20 (2020) 3315. https://doi.org/10.3390/s20113315.

[60] L.F. Ramos, L. Marques, P.B. Lourenço, G. De Roeck, A. Campos-Costa, J. Roque, Monitoring historical masonry structures with operational modal analysis: Two case studies, Mech. Syst. Signal Process. 24 (2010) 1291–1305. https://doi.org/10.1016/j.ymssp.2010.01.011.

[61] G. Standoli, G.P. Salachoris, M.G. Masciotta, F. Clementi, Modal-based FE model updating via genetic algorithms: Exploiting artificial intelligence to build realistic numerical models of historical structures, Constr. Build. Mater. 303 (2021) 124393. https://doi.org/10.1016/j.conbuildmat.2021.124393.

[62] J. Kim, F. Lorenzoni, M. Salvalaggio, M.R. Valluzzi, Seismic vulnerability assessment of free-standing massive masonry columns by the 3D Discrete Element Method, Eng. Struct. 246 (2021) 113004. https://doi.org/10.1016/j.engstruct.2021.113004.

[63] J. Azevedo, G. Sincraian, J. V. Lemos, Seismic Behavior of Blocky Masonry Structures, Earthq. Spectra. 16 (2000) 337–365. https://doi.org/10.1193/1.1586116.

[64] Itasca Consulting Group Inc., 3DEC- 3D Distinct Element Code, Version 5.0, User's Manual, 2013. https://doi.org/10.1017/CBO9781107415324.004.

[65] B. Chetouane, F. Dubois, M. Vinches, C. Bohatier, NSCD discrete element method for modelling masonry structures, Int. J. Numer. Methods Eng. 64 (2005) 65–94. https://doi.org/10.1002/nme.1358.

[66] J. Lubliner, J. Oliver, S. Oller, E. Oñate, A plastic-damage model for concrete, Int. J. Solids Struct. 25 (1989) 299–326. https://doi.org/10.1016/0020-7683(89)90050-4.

[67] J. Lee, G.L. Fenves, Plastic-Damage Model for Cyclic Loading of Concrete Structures, J. Eng. Mech. 124 (1998) 892–900.

https://doi.org/10.1061/(ASCE)0733-9399(1998)124:8(892).

[68] M. Valente, G. Milani, Damage assessment and collapse investigation of three historical masonry palaces under seismic actions, Eng. Fail. Anal. 98 (2019) 10–37. https://doi.org/10.1016/j.engfailanal.2019.01.066.

[69] M. Jean, The non-smooth contact dynamics method, Comput. Methods Appl. Mech. Eng. 177 (1999) 235–257. https://doi.org/10.1016/S0045-7825(98)00383-1.

[70] J.J. Moreau, Unilateral Contact and Dry Friction in Finite Freedom Dynamics, in: Nonsmooth Mech. Appl., Springer Vienna, Vienna, 1988: pp. 1–82. https://doi.org/10.1007/978-3-7091-2624-0_1.

[71] P.A. Cundall, ADAPTIVE DENSITY-SCALING FOR TIME-EXPLICIT CALCULATIONS., in: A. A. Balkema, 1982: pp. 23–26.

[72] F. Galvez, L. Sorrentino, D. Dizhur, J.M. Ingham, Damping considerations for rocking block dynamics using the discrete element method, Earthq. Eng. Struct. Dyn. 51 (2022) 935–957. https://doi.org/10.1002/eqe.3598.

[73] A. Formisano, A. Marzo, Simplified and refined methods for seismic vulnerability assessment and retrofitting of an Italian cultural heritage masonry building, Comput. Struct. 180 (2017) 13–26. https://doi.org/10.1016/j.compstruc.2016.07.005.

[74] G. Fiorentino, A. Forte, E. Pagano, F. Sabetta, C. Baggio, D. Lavorato, C. Nuti, S. Santini, Damage patterns in the town of Amatrice after August 24th 2016 Central Italy earthquakes, Bull. Earthq. Eng. 16 (2018) 1399–1423. https://doi.org/10.1007/s10518-017-0254-z.

[75] A.M. D'Altri, G. Castellazzi, S. de Miranda, Collapse investigation of the Arquata del Tronto medieval fortress after the 2016 Central Italy seismic sequence, J. Build. Eng. 18 (2018) 245–251. https://doi.org/10.1016/j.jobe.2018.03.021.

[76] F. Clementi, A. Ferrante, S. Lenci, The Non-smooth Dynamics of Multiple Leaf Masonry Walls of the Arquata Del Tronto Fortress, in: 2020: pp. 1798–1807. https://doi.org/10.1007/978-3-030-41057-5_145.

[77] Ministero delle Infrastrutture e dei Trasporti, Aggiornamento delle "Norme Tecniche per le Costruzioni" - NTC 2018 (in italian), (2018) 1–198.

[78] M. delle infrastrutture e dei trasporti, Circolare 21 gennaio 2019 n. 7 C.S.LL.PP. Istruzioni per l'applicazione dell'aggiornamento delle "Norme Tecniche per le Costruzioni" di cui al D.M. 17/01/2018 (in Italian), Suppl. Ord. Alla G.U. n. 35 Del 11/2/19. (2019).

[79] L. Luzi, S. Hailemikael, D. Bindi, F. Pacor, F. Mele, F. Sabetta, ITACA (ITalian ACcelerometric Archive): A Web Portal for the Dissemination of Italian Strong-motion Data, Seismol. Res. Lett. 79 (2008) 716–722. https://doi.org/10.1785/gssrl.79.5.716.

[80] F. Pacor, R. Paolucci, L. Luzi, F. Sabetta, A. Spinelli, A. Gorini, M. Nicoletti, S. Marcucci, L. Filippi, M. Dolce, Overview of the Italian strong motion database ITACA 1.0, Bull. Earthq. Eng. 9 (2011) 1723–1739. https://doi.org/10.1007/s10518-011-9327-6.

[81] L. Luzi, F. Pacor, R. Puglia, Italian Accelerometric Archive v 2.3, Rome, 2017. https://doi.org/10.13127/ITACA.2.3.

[82] F. Clementi, A. Ferrante, E. Giordano, S. Lenci, The non-smooth story of different masonry towers damaged by the central Italy seismic sequence of 2016, in: COMPDYN Proc., Institute of Structural Analysis and Antiseismic Research School of Civil Engineering National Technical University of Athens (NTUA) Greece, Athens, 2019: pp. 1312–1320. https://doi.org/10.7712/120119.6999.19092.

[83] A. Ferrante, F. Clementi, G. Milani, Advanced numerical analyses by the Non-Smooth Contact Dynamics method of an ancient masonry bell tower, Math. Methods Appl. Sci. (2020) mma.6113. https://doi.org/10.1002/mma.6113.

[84] E. Moriconi, La Storia di Amatrice. Dalla preistoria ai giorni nostri, (2020).

[85] A. Preciado, Seismic vulnerability and failure modes simulation of ancient masonry towers by validated virtual finite element models, Eng. Fail. Anal. 57 (2015) 72–87. https://doi.org/10.1016/j.engfailanal.2015.07.030.

[86] S. Invernizzi, G. Lacidogna, N.E. Lozano-Ramírez, A. Carpinteri, Structural monitoring and assessment of an ancient masonry tower, Eng. Fract. Mech. 210 (2019) 429–443. https://doi.org/10.1016/j.engfracmech.2018.05.011.

[87] A. Cabboi, C. Gentile, A. Saisi, From continuous vibration monitoring to FEM-based damage assessment: Application on a stone-masonry tower, Constr. Build. Mater. 156 (2017) 252–265. https://doi.org/10.1016/j.conbuildmat.2017.08.160.

[88] P.A. R. Brincker, C.E. Ventura, Damping estimation by Frequency Domain Decomposition, IMAC2001 A Conf. Struct. Dyn. (2001).

[89] Z.L. A.P. Brincker R, Modal identification from ambient responses using frequency domain decomposition, 18th Int. Modal Anal. Conf. San Antonio, TX, Febr., San Antonio, Texas. (2000) 625–630.

[90] A. Bajrić, J. Høgsberg, Identification of damping and complex modes in structural vibrations, J. Sound Vib. 431 (2018) 367–389. https://doi.org/10.1016/j.jsv.2018.05.048.